# **International Ocean Discovery Program Expedition 353 Scientific Prospectus**

# iMonsoon

# Indian monsoon rainfall in the core convective region

#### Steven C. Clemens

Co-Chief Scientist
Geological Sciences
Brown University
324 Brook Street
Providence Rhode Island 02912
USA

#### **Wolfgang Kuhnt**

Co-Chief Scientist
Institute of Geosciences
Christian-Albrechts-Universität zu Kiel
Ludewig-Meyn-Strasse 10-14
D-24118 Kiel
Germany

#### Leah J. LeVay

Expedition Project Manager/Staff Scientist International Ocean Discovery Program 1000 Discovery Drive College Station Texas 77845 USA



Published by International Ocean Discovery Program

#### Publisher's notes

This publication was prepared by the International Ocean Discovery Program U.S. Implementing Organization (IODP-USIO): Consortium for Ocean Leadership, Lamont-Doherty Earth Observatory of Columbia University, and Texas A&M University, as an account of work performed under the International Ocean Discovery Program. Funding for the program is provided by the following agencies:

National Science Foundation (NSF), United States

Ministry of Education, Culture, Sports, Science and Technology (MEXT), Japan

European Consortium for Ocean Research Drilling (ECORD)

Ministry of Science and Technology (MOST), People's Republic of China

Korea Institute of Geoscience and Mineral Resources (KIGAM)

Australian Research Council (ARC) and GNS Science (New Zealand), Australian/New Zealand Consortium

Ministry of Earth Sciences (MoES), India

Coordination for Improvement of Higher Education Personnel, Brazil

#### Disclaimer

Any opinions, findings, and conclusions or recommendations expressed in this publication are those of the author(s) and do not necessarily reflect the views of the participating agencies, Consortium for Ocean Leadership, Lamont-Doherty Earth Observatory of Columbia University, Texas A&M University, or Texas A&M Research Foundation.

Portions of this work may have been published in whole or in part in other International Ocean Discovery Program documents or publications.

This IODP *Scientific Prospectus* is based on precruise Science Advisory Structure panel discussions and scientific input from the designated Co-Chief Scientists on behalf of the drilling proponents. During the course of the cruise, actual site operations may indicate to the Co-Chief Scientists, the Staff Scientist/Expedition Project Manager, and the Operations Superintendent that it would be scientifically or operationally advantageous to amend the plan detailed in this prospectus. It should be understood that any proposed changes to the science deliverables outlined in the plan presented here are contingent upon the approval of the IODP JR Science Operator Director.

## Copyright

Except where otherwise noted, this work is licensed under a Creative Commons Attribution License. Unrestricted use, distribution, and reproduction is permitted, provided the original author and source are credited.

#### Citation:

Clemens, S.C., Kuhnt, W., and LeVay, L.J., 2014. iMonsoon: Indian monsoon rainfall in the core convective region. *International Ocean Discovery Program Scientific Prospectus*, 353. http://dx.doi.org/10.14379/iodp.sp.353.2014

# **Abstract**

Scientific ocean drilling (Deep Sea Drilling Project [DSDP], Ocean Drilling Program [ODP], and Integrated Ocean Drilling Program) has never taken place in the Bay of Bengal north of 9°N. Thus, the core region of summer monsoon precipitation has never been investigated. DSDP Leg 22 (1974) and ODP Leg 121 (1989) drilled the southernmost region (5°-9°N), capturing the distal end of the summer monsoon influence. India's partnership in the International Ocean Discovery Program (IODP) provides an opportunity to investigate this key northern region. IODP Expedition 353 seeks to recover Upper Cretaceous-Holocene sediment sections that record erosion and runoff signals from river input to the Bay of Bengal as well as the resulting northsouth surface water salinity gradient. Analysis of sediment sections from the Mahanadi Basin (northeast Indian margin), the Nicobar-Andaman Basin (Andaman Sea), and the northern Ninetyeast Ridge (southern Bay of Bengal) will be used to understand the physical mechanisms underlying changes in monsoonal precipitation, erosion, and run-off across timescales from millennial through tectonic. These sites will provide crucial new information within which to interpret differences among existing results from previous monsoon-themed drilling expeditions in the Arabian Sea (ODP Leg 117), the South China Sea (ODP Leg 184), and the Sea of Japan (Integrated Ocean Drilling Program Expedition 346). These goals directly address challenges in the "Climate and Ocean Change" theme of the IODP Science Plan.

# Schedule for Expedition 353

International Ocean Discovery Program (IODP) Expedition 353 is based on IODP drilling proposal Number 795-Full2 (available at iodp.tamu.edu/scienceops/expeditions/indian\_monsoon.html). Following ranking by the IODP Scientific Advisory Structure, the expedition was scheduled for the R/V JOIDES Resolution. At the time of publication of this Scientific Prospectus, the expedition is scheduled to start in Singapore on 29 November 2014 and to end in Singapore on 29 January 2015. A total of 61 days will be available for the transit, drilling, coring, and downhole measurements described in this report (for the current detailed schedule, see iodp.tamu.edu/scienceops/). Further details about the facilities aboard the JOIDES Resolution and the USIO can be found at www.iodp-usio.org/.

# **Background**

# Motivation for drilling in the Bay of Bengal

### Pliocene-Pleistocene

A threefold motivation exists for targeting the precipitation/salinity signal recorded in sediments at the Expedition 353 drilling locations (Fig. F1). First, the Bay of Bengal/ Andaman Sea and surrounding catchments are within the Earth's strongest hydrological regime, impacting billions of people (Fig. F2); a solid understanding of the physics behind monsoonal climate change is of significant societal relevance (Nicholls et al., 2007). The net annual surface water exchange (precipitation plus runoff minus evaporation) within the Bay of Bengal and Andaman Sea during the summer monsoon is  $184 \times 10^{10}$  m<sup>3</sup>, dominating the winter signal of  $-32 \times 10^{10}$  m<sup>3</sup> for an annual average of  $152 \times 10^{10}$  m<sup>3</sup> (Varkey et al., 1996). The effects of this budget are clearly evident in the surface salinity climatology (Fig. F3) (Antonov et al., 2010), indicating a well-defined strong signal that can be used to monitor changes in monsoonal precipitation via chemical, physical, and isotopic indicators for changes in precipitation, salinity, and terrestrial erosion/runoff. The strength of this runoff signal is sufficient to mute (via stratification) what would otherwise result in strong summer season productivity in response to wind-driven upwelling along the eastern Indian margin, similar to that seen in the Arabian Sea (Guptha et al., 1997; Kumar et al., 2002). Compared to other monsoon regions, the Bay of Bengal is optimal for isolating and recording the summer monsoon precipitation signal (Fig. F4).

Second, recent studies have called into question the extent to which basin-scale monsoon winds and continental precipitation are coupled over a range of timescales and space scales (Clemens et al., 2010; Clemens and Prell, 2007; Liu et al., 2006; Molnar, 2005; Ruddiman, 2006; Wang et al., 2008; Ziegler et al., 2010). Nearly all proxy records indicate strong coupling between summer monsoon winds and precipitation across the Indo-Asian monsoon subsystems at the millennial scale (Altabet et al., 2002; Cai et al., 2006; Clemens, 2005; Schulz et al., 1998; Sun et al., 2011; Wang et al., 2001); this tight coupling is likely attributed to the strong role of the winter westerlies in linking high- and low-latitude climate change. However, the all-important physical mechanisms behind these links are not fully understood; this was a primary goal of recent Integrated Ocean Drilling Program Expedition 346. Progress is also being made in understanding winter monsoon and summer monsoon linkages at the millennial timescale. For example, recent work offshore Goa, western India, shows synchronous breakdown in summer and winter monsoon airflow over the Arabian

Sea during Heinrich events (Singh et al., 2011), which is in contrast to the East Asian Monsoon system that shows an asynchronous relationship between summer and winter monsoon strength at the millennial scale (Yancheva et al., 2007). Consensus does not yet exist on the extent of the coupling or the ultimate forcing of monsoon winds and precipitation at the orbital and longer timescales (An et al., 2011; Caley et al., 2011a, 2011b, 2011c; Cheng et al., 2009; Clemens and Prell, 2007; Clemens et al., 1996, 1991, 2008; Clift et al., 2008; Ruddiman, 2006; Wang et al., 2008; Ziegler et al., 2010). Some argue for a close coupling between changes in Indian and East Asian summer monsoon winds and precipitation across the entire region spanning the Arabian Sea (Ocean Drilling Program [ODP] Leg 117), the South China Sea (ODP Leg 184), and terrestrial records from the Loess Plateau. In this case, changes in the strength of summer monsoon circulation across these regions are thought to be sensitive to Northern Hemisphere sensible heating (insolation), the timing of energy release from the Southern Hemisphere Indian Ocean, and the timing of global ice volume minima (An et al., 2011; Caley et al., 2011b, 2011c; Clemens and Prell, 2003, 2007; Clemens et al., 1996, 2008). In contrast, others interpret the timing of summer monsoon circulation, on the basis of speleothem records from southeast China, as forced entirely and directly by external insolation with little or no influence from internal boundary conditions such as ice volume or Southern Hemisphere ocean atmosphere latent heat exchange (Cheng et al., 2009; Ruddiman, 2006; Wang et al., 2008). Caballero-Gill et al. (2012) demonstrate that these contrasting interpretations are not attributable to differences in terrestrial and marine chronologies. Therefore, this lack of consensus points either to a strong deficit in our understanding of monsoon sensitivity to changes in the most basic of boundary conditions including insolation, ocean/atmosphere energy exchange, ice volume, and atmospheric greenhouse gas concentrations or to the misinterpretation of the influence of seasonality on proxy records (e.g., Fig. **F4**).

Lack of consensus also extends to the tectonic scale, where the timing of monsoon intensification to modern strength is also debated. Some proxy records suggest initial intensification occurred at ~7–8 Ma (e.g., Kroon et al., 1991; Prell et al., 1992), whereas others suggest a considerably earlier intensification, perhaps as early as ~22 Ma (Clift et al., 2008; Guo et al., 2002; Sun and Wang, 2005). Emergence and expansion of arid-adapted C<sub>4</sub> flora in South Asia argues for reduced precipitation since ~8 Ma (e.g., Cerling et al., 1997; Huang et al., 2007; Quade and Cerling, 1995), whereas proxies dedicated to reconstructing seasonality suggest, instead, little variability in the monsoon over the last 10 m.y. (Dettman et al., 2001). Clift and Plumb (2008), Molnar et al. (2010), and the report from the Detailed Planning Group "Asian

Monsoon and Cenozoic Tectonic History" (www.iodp.org/doc\_download/2336-mmdpgreport) provide comprehensive overviews of these issues. More recently, Rodriguez et al. (2014) suggested that the ~8 Ma intensification inferred on the basis of increased *Globigerina bulloides* concentrations is an artifact of increased preservation related to uplift of the Owen Ridge at this time, resulting in enhanced preservation.

Third, recent work suggests that interpretation of the oxygen minimum zone (OMZ) signal in the northern Arabian Sea (Leg 117) may be complicated by changing oxygen content of southern-source intermediate waters (Anand et al., 2008; Caley et al., 2011c; Schmittner et al., 2007; Ziegler et al., 2010). This presents a potential complication in the interpretation of the OMZ signal as a direct response to atmospheric circulation in the core region of summer monsoon winds (i.e., oxygen drawdown in response to decay of upwelling-produced organic carbon). A multibasin, multiproxy approach is required to resolve these outstanding issues. Precipitation, salinity, and runoff indicators are not influenced by the chemistry of externally sourced intermediate and deepwater masses, offering the potential to disentangle the influences of these factors in interpreting monsoon proxy records.

The iMonsoon drilling effort, targeting the core of the monsoon precipitation signal in the Bay of Bengal (Figs. F2, F4), will directly address these outstanding issues regarding large-scale monsoonal circulation through a meridional transect approach targeting the northeast Indian margin, the Andaman Sea, and the southern Bay of Bengal (Fig. F1A-F1C). Specifically, new material from this critical region will allow us to assess (1) the relative sensitivity of the monsoon to external insolation forcing and internal climate boundary conditions, including the export of latent heat from the southern hemisphere, the extent of global ice volume, and greenhouse gas concentrations; (2) the timing and conditions under which monsoonal circulation initiated and evolved; and (3) the extent to which Indian and East Asian monsoon winds and precipitation are coupled and at what temporal and geographic scales. Finally, a detailed record of monsoon evolution is also central to testing models that link the climatic evolution of South Asia to the tectonic development of the Himalaya and rising of the Tibetan Plateau. If climatically modulated surface processes really do control the structural evolution, then well-dated climate records are needed to correlate with the increasingly well constrained ages of faulting and exhumation on shore.

Resolving these outstanding questions using the geological record is critical to providing verification targets for climate models, especially given the critical point that the vast majority of current Atmosphere-Ocean General Circulation Models (AOGCMs)

used in the Intergovernmental Panel on Climate Change (IPCC) reports do not accurately simulate the spatial or intraseasonal variability of monsoon precipitation (Randall et al., 2007).

## Deep time

Benthic foraminiferal diversity and assemblage composition, in conjunction with geochemical proxies indicate a stepwise increase in primary production and carbon export and an expansion of the intermediate water OMZ in the northeastern Indian Ocean since the late Oligocene (Gupta et al., 2013). The main increases in productivity started at 14 (Gupta et al., 2013) or 10 (Gupta et al., 2004) Ma and reached levels associated with present Indian monsoon conditions around 2.3 Ma. This late Miocene to Pliocene "biogenic bloom" (Farrell et al., 1995) implies important changes in nutrient cycling in the Indian Ocean and probably on a global scale, which in particular affected the silica and phosphate cycles (Dickens and Owen, 1999). The productivity increase between 10 and 8 Ma in the eastern equatorial Indian Ocean (onset of the biogenic bloom) may have been linked either to global cooling and the expansion of Antarctic ice sheets leading to a major change in deep ocean circulation and nutrient cycling, to the initiation of the Indian monsoons, or a combination of both (Gupta et al., 2004). Deep-sea benthic foraminiferal diversity in the Indian Ocean further decreased between 8 and 6 Ma and is associated with a negative  $\delta^{13}$ C shift at 3.2–2.3 and 1.6–0.9 Ma, coinciding with an increased abundance of species indicative of enhanced organic carbon flux (Singh and Gupta, 2005). Since ~2.8 Ma, roughly coeval with the onset of Northern Hemisphere glaciation, benthic foraminiferal species that are well adapted to strong seasonal fluctuations in carbon flux dominate the assemblages. This has been related to increased duration and strength of the northeast (winter) monsoon, which is accompanied by relatively low primary production in the eastern equatorial Indian Ocean (Gupta and Thomas, 2003). iMonsoon will provide new Neogene intermediate water benthic foraminiferal assemblage and  $\delta^{18}O$  and  $\delta^{13}C$ records along a meridional transect to better understand the relative contribution of monsoon-related productivity-carbon flux changes and changes in intermediate water circulation linked to high-latitude climatic events such as fluctuations in the extension of the East Antarctic Ice Sheet.

The meridional transect of iMonsoon provides a unique opportunity to investigate the nature and timing of variations in deepwater radiogenic isotope composition in response to restriction of the deepwater connection between the Pacific and Indian Oceans through the Indonesian Gateway since the mid-Miocene and to evaluate the influence of enhanced Himalayan weathering since the late Oligocene. The broad

passage between the Indian and Pacific Oceans during the Paleogene must have enabled significant surface and intermediate water exchange and the possibility of deepwater flow from the Indian Ocean to the Pacific Ocean (Thomas et al., 2003). The progressive closure of the Indonesian Gateway because of the northward movement of Australia (Hall, 2002; Hall et al., 2011; Kuhnt et al., 2004) induced changes in deep and intermediate water circulation through the Indonesian Gateway, which may have resulted in a significant change in the eastern Indian Ocean Nd isotope composition during the middle Miocene (Frank et al., 2006; Gourlan et al., 2008). A second shift in eastern Indian Ocean Nd isotopes may have been related to a shift in the source area of the Indonesian Throughflow toward the North Pacific around 3.5 Ma (Cane and Molnar, 2001; Gourlan et al., 2008).

## **Geological setting**

The eastern continental margin of India is the result of the separation of India and the Australia/Antarctica portion of Gondwanaland during the Early Cretaceous at ~130 Ma (Scotese et al., 1988; Powell et al., 1988). All the major Indian rivers draining into the Bay of Bengal are thought to be associated with graben features resulting from the rifting of India from Antarctica as well as subsequent Indian plate motion. The Mahanadi Graben appears to have a continuation in Prydz Bay, Antarctica, known as the Lambert Graben (Federov et al., 1982). The 2000 m isobaths of the northeast Indian continental margin and the Lambert Graben of East Antarctica (Prydz Bay) are closely matched, supporting the inferred alignment of India and Antarctica prior to rifting (Subrahmanyam et al., 2008). The Mananadi Basin includes both onshore and offshore regions of northeast India. The offshore portion extends from ~170 to 240 km off the coast. Sediments are dominated by input from the Mahanadi River drainage basin, which occupies 141,589 km<sup>2</sup> of catchment (extending from  $\sim 80^{\circ}$  to  $85^{\circ}$ E and  $\sim 19^{\circ}$  to  $24^{\circ}$ N) and currently supplies  $\sim 7.1 \times 10^{9}$  kg of sediments per year to the offshore basin (Fig. F5) (Subrahmanyam et al., 2008). Analysis of Bay of Bengal surface sediments indicates that the foraminiferal lysocline, the depth delimiting well preserved from noticeably dissolved assemblages, shoals significantly from south to north. The foraminiferal lysocline rises from 3800 to 3300 m between 0° and 7°N (about Site N90E-2C) then systematically shoals to ~2000 m at ~20°N (Indian margin sites) (Cullen and Prell, 1984).

The Ninetyeast Ridge (NER) is an aseismic volcanic ridge spanning from ~31°S to ~10°N, where it is buried beneath Bengal Fan sediments. The NER is thought to have formed by age-progressive hotspot volcanism from plume sources currently beneath

the Kerguelen Plateau (Royer et al., 1991; Sager et al., 2010). The ridge top rises to a height of ~3.5 km above the surrounding abyssal plain with depths as shallow as ~2000 meters below sea level (mbsl). Site N90E-2C is located at ~5°N at 2963 mbsl. This location provides for good preservation of carbonate microfossils, given that the foraminiferal lysocline in this region is close to 3300 m (Cullen and Prell, 1984).

The Andaman Sea is situated between the Andaman Islands and the Malaya Peninsula (Fig. F1A). The Andaman-Sumatra island arc system results from the oblique subduction of the Indo-Australian plate beneath the Eurasian plate (Singh et al., 2013). Stretching and rifting of the overriding plate in the early Miocene (~25 Ma) has resulted in two distinct plates (Sunda and Burma) separated by an active spreading center (Curray, 1991, 2005) located in the deepest portion of the Andaman Sea. An accretionary wedge complex scraped off the subducting slab lies west of the spreading center, forming a series of shallower basins associated with back-thrust faulting within the accreted sediments (Fig. F6). The Andaman Sea drilling sites are within the Nicobar-Andaman Basin, bounded on either side by the Diligent and Eastern Margin Faults. Terrigenous sediment supply to the Andaman Sea is dominantly from the Irrawaddy and Salween Rivers (Colin et al., 1999, 2006). Analysis of Andaman Sea surface sediments indicates that foraminifers are abundant and well preserved shallower than ~1800 mbsl (>100,000 individuals/gram) and decrease to <100 individuals/gram deeper than 3000 mbsl (Frerichs, 1971).

# Atmospheric and oceanographic circulation

The Indian summer monsoon is characterized by low atmospheric pressure over the Indo-Asian continent (Indo-Asian Low) relative to high atmospheric pressure over the southern subtropical Indian Ocean (Mascarene High). The resulting pressure gradient leads to large-scale displacement of the Intertropical Convergence Zone (ITCZ) and the cross-equatorial flow of low-level winds carrying moisture that is ultimately released over South Asia, the Bay of Bengal, and southeast China (Hastenrath and Greischar, 1993; Liu et al., 1994; Loschnigg and Webster, 2000; Webster, 1987a, 1987b, 1994; Webster et al., 1998). Modern meteorological observations and moisture transport budgets (Fig. F7) quantitatively show that the Southern Hemisphere Indian Ocean is the dominant source of moisture (latent heat) to the Indian and East Asian summer monsoons during June, July, and August (JJA) (Bosilovich and Schubert, 2002; Ding and Chan, 2005; Ding et al., 2004; Emile-Geay et al., 2003; Liu and Tang, 2004, 2005; Park et al., 2007; Simmonds et al., 1999; Wajsowicz and Schopf, 2001; Xie and Arkin, 1997; Zhu and Newell, 1998). The Arabian Sea is a very minor moisture

source (evaporation > precipitation), whereas the Bay of Bengal/Andaman Sea, India, the South China Sea, and southeast China are all moisture sinks (precipitation > evaporation).

A total of 12 major rivers (Fig. F5, F8) feed the Bay of Bengal/Andaman Sea (Ganga, Brahmaputra, Meghna, Damodar, Mahanadi, Godavari, Krishna, Irrawaddy, Salween, Penner, Kavery, and Mahaweli Rivers), discharging in total 943 × 10<sup>9</sup> m³ of water during the summer monsoon months (JJA) (Varkey et al., 1996). Annual rainfall within and surrounding the Bay of Bengal is dominated by precipitation during the summer monsoon months (JJA) with the exception of the Madras Basin in the southernmost peninsular India, where rainfall peaks in November (Fig. F9). The dominance of the summer (JJA) precipitation signal is reflected in the Bay of Bengal surface salinity patterns (Fig. F3), which reach their lowest values in August and September, spanning salinities of 20–34 over both seasonal (summer–winter) and spatial (north–south) dimensions.

Primary surface ocean currents (Schott and McCreary, 2001; Schott et al., 2009) reflect the seasonal wind forcing in both the eastern Arabian Sea and the Bay of Bengal (Fig. **F10**). The West Indian Coastal Current (WICC) flows south during the summer monsoon, connecting with the Southwest Monsoon Current (SMC) that carries high-salinity waters eastward around the tip of India and Sri Lanka into the southern Bay of Bengal at a rate of 8.4 Sverdrup (Sv; 10<sup>6</sup> m³/s). This influx of high-salinity water is reflected in the July, August, and September salinity patterns of the southern Bay of Bengal (Fig. **F3**) and is successfully modeled as a passive tracer in mixed-layer ocean models (Jensen, 2001, 2003). Southwest summer monsoon winds in the Bay of Bengal also drive the northward-flowing East Indian Coastal Current (EICC). During the winter monsoon, northeast winds drive all these surface currents in the opposite directions, transporting 11 Sv of water toward the eastern Arabian Sea.

The proposed drilling plan is designed to take advantage of these strongly seasonal patterns to reconstruct changes in summer monsoon circulation by reconstructing the meridional precipitation/salinity gradients as well as erosion and runoff from proximal drainage basins. An array of drilling locations is proposed, including the Mahanadi Basin, off the northeast Indian margin (BB sites), the Andaman Sea (AA sites), and the southernmost Bay of Bengal (Site N90E-2C) (Fig. F1A–F1C). Salinity on the Indian margin, northwest Bay of Bengal, reaches a minimum of ~22 in September (Fig. F3); this is a lagged response to JJA rainfall over the Bay of Bengal and the surrounding drainage basins. Salinity at this location reaches a maximum of ~34 during

the spring months. The Andaman Sea sites, situated between the modern 32 and 33 isohalines, monitor drainage from the Irrawaddy and Salween Rivers. Site N90E-2C (ODP Site 758) is closely pinned to the 34 isohaline year round, anchoring the southern end of the modern salinity gradient at near open-ocean values. Although this site does not currently experience significant seasonal salinity variability, it does record large-scale changes in precipitation and runoff at the millennial, orbital, glacial-interglacial, and tectonic scales as discussed below. The full meridional transect (spanning the Indian margin, Andaman Sea, and northern NER) has a modern salinity range of 12, equivalent to an ~2‰ surface water  $\delta^{18}$ O signal.

Changes in the meridional salinity gradient will provide robust means of tracking changes in summer monsoon precipitation. Furthermore, the signal should not be influenced to a large degree by temperature gradients, which are small compared to the salinity gradients. Maximum temperature seasonality is ~3°C on the northwest Indian margin (equivalent to <0.8‰ surface water  $\delta^{18}$ O signal) and considerably less at the other sites (Fig. **F10**) (Locarnini et al., 2010). This is largely because of the cooling influence of cloud cover and precipitation during the summer, limiting the amount of sensible surface heating.

Terrestrial runoff products are also of great utility in assessing linkages between monsoon circulation, chemical weathering, and transport at timescales from millennial to tectonic. These topics are recognized by the community as being of considerable importance (Clift and Plumb, 2008; Wang et al., 2005). Changes in monsoon strength are well documented at ~23, 15, 8–7, and 2.75 Ma (Clift and Plumb, 2008). The iMonsoon targets will allow measurement of the consequent impact on weathering rates and transport of particulate materials to the ocean basins in a variety of settings both proximal and distal relative to river inputs.

#### Water masses and circulation

Comprehensive descriptions of eastern Indian Ocean regional oceanography are provided in Wyrtki (1971), Mantyla and Reid (1995), Tomczak and Godfrey (2003), and Schott et al. (2009), from which we briefly summarize descriptions of water masses and circulation patterns relevant for Bay of Bengal drilling in the depth range between 1100 and 3000 m targeted for Expedition 353.

Indian Deep Water (IDW) occupies the depth range from 3800 to ~1500 m within the equatorial and northern Indian Ocean (Fig. F11). IDW in the eastern Indian Ocean is

characterized by high salinities reaching salinity maxima of 34.8 in the southwestern Indian Ocean and 34.75 in the southeastern Indian Ocean, where the IDW upper limit rises to 500 m (Tomczak and Godfrey, 2003). IDW temperature, salinity, and oxygen properties in the high-salinity core are virtually identical with those of North Atlantic Deep Water (NADW) in the Atlantic sector of the Southern Ocean, indicating that IDW is mainly of NADW origin and not originally formed in the Southern Ocean, as is the Antarctic Bottom Water (AABW) that occupies the Indian Ocean deeper than 3800 m (Tomczak and Godfrey, 2003). The flow of IDW is northward and concentrated along western boundaries of the African margin and NER as indicated by the World Ocean Circulation Experiment (WOCE) I08I09 oxygen, silicate, and temperature profiles (Fig. F12). IDW further penetrates northward into the Northern Hemisphere, is modified by mixing with thermocline water from above and upwelling of AABW from below, and spreads into the Arabian Sea and the Bay of Bengal.

Two water masses occupy the thermocline of the Indian Ocean: Indian Central Water (ICW) and Indonesian Throughflow Water (ITW) or Australasian Mediterranean Water (Fig. F13). ICW originates from downwelling in the subtropical convergence south of 30°S and ITW is derived from North Pacific Intermediate Water, strongly modified during its passage through the Indonesian archipelago. There is no formation of thermocline water in the Bay of Bengal, and its thermocline water masses to 1500 m water depth are derived from ICW and ITW. Transfer of ICW to the northern Indian Ocean is accompanied by a rapid decrease in oxygen content, indicating aging along the path. The lowest oxygen values occur in the Bay of Bengal, which contains the oldest ICW. The strong oxygen decrease in the northern Indian Ocean can be explained by restriction of the transfer of ICW to the southwest monsoon season, resulting in a small annual net transfer rate. ITW also contributes to the renewal of thermocline water in the northern Indian Ocean, resulting in significant freshening of the ICW along its path into the Bay of Bengal. Further freshening is observed in the Bay of Bengal near 90°E, resulting from ITW advection directly from its outflow area into the tropical eastern Indian Ocean. The variability and evolution of thermocline circulation in the Bay of Bengal are strongly dependent on monsoonal forcing; however, the present extremely low oxygen levels indicate a very low renewal rate for the thermocline waters of the Bay of Bengal.

The uppermost 100 m of the eastern Indian Ocean in the Bay of Bengal consists of a low-salinity water mass derived from river runoff from India and Indochina, the Bay of Bengal Water (BBW), with surface salinity strongly fluctuating with seasons but remaining below 33 throughout the year. The lower boundary to the ICW is characterized by

a strong halocline. Its southward extension is highest during October–December when it reaches the area along the western Indian coast and is lowest during April–June before the summer monsoon leads to a new expansion of the BBW surface water mass.

## Site survey data

Supporting site survey data for Expedition 353 are archived at the IODP Site Survey Data Bank.

# Scientific objectives

The three drilling regions will recover sediment sections variously spanning Late Cretaceous through Holocene (Fig. F1A), depending on the location.

## Pliocene-Pleistocene objectives

Pliocene–Pleistocene objectives include reconstructing salinity changes as well as the erosion and runoff signals in the Bay of Bengal and Andaman Sea in order to

- Establish the sensitivity and timing of changes in monsoon circulation relative to insolation forcing, latent heat export from the Southern Hemisphere, global ice volume extent, and greenhouse gas concentrations;
- Determine the extent to which Indian and East Asian monsoon winds and precipitation are coupled and at what temporal and geographic scales;
- Better separate the effects of climate change and tectonics on erosion and runoff;
   and
- Provide verification targets for climate models: the majority of current atmosphere—ocean general circulation models do not accurately simulate the spatial or intraseasonal variability of monsoon precipitation.

# Deep-time objectives

Deep-time objectives include the following:

• To understand the timing and conditions under which monsoonal circulation initiated and reconstruct the variability of the Indian monsoon at orbital timescales;

- To unravel the relationship between Indian monsoon variability and major past global climatic events such as the Oligocene/Miocene cooling (Zachos et al., 1997), the onset of the mid-Miocene Climatic Optimum (Holbourn et al., 2007; Zachos et al., 2001), mid-Miocene cooling and Antarctic cryosphere expansion (Holbourn et al., 2013), and the Pliocene–Pleistocene enhancement of Northern Hemisphere glaciation (Lisiecki and Raymo, 2005, 2007);
- To establish a complete Oligocene–present astronomically tuned timescale based on high-resolution benthic and planktonic isotope reference curves for the Indian Ocean; and
- To incorporate high-resolution distribution studies of well-preserved Oligocenerecent calcareous and siliceous microfossils from the Indian Ocean into global compilation studies of paleoclimatic and biotic evolution.

## Chronology, proxies, and tracers

The initial chronostratigraphic reference frame will consist of geomagnetic polarity reversal stratigraphy and nannofossil and foraminiferal biostratigraphy in combination with siliceous microfossil zonation. Using this stratigraphic framework and composite sections from double or triple coring at each site, high-resolution benthic  $\delta^{18}$ O records will be created and correlated to the global marine benthic  $\delta^{18}$ O chronology of the past 5 m.y. (Lisiecki and Raymo, 2005) and to orbitally tuned Pacific records for deeper-time intervals (e.g., Holbourn et al., 2013).

An array of physical, biological, chemical, and isotopic proxies is available to assess changes in runoff and weathering signals associated with monsoonal precipitation and changes in monsoon-related paleoceanographic parameters such as changes in surface productivity, water column stratification and vertical mixing, ventilation, and the presence of externally sourced intermediate waters. The following proxy indicators are essential for these reconstructions.

## Salinity indicators

The composition of core-top planktonic foraminiferal assemblages in the Arabian Sea and the Bay of Bengal are related to surface salinity. In particular, high percentages of *Neogloboquadrina dutertrei* are associated with low surface salinities (Cullen, 1981). Similarly, morphological variations of *Emiliania huxleyi* provide constraints on seawater salinity for the Late Pleistocene record (Bollmann and Herrle, 2007), whereas

the process length of the dinoflagellate cysts of *Lingulodinium machaerophorum* provides salinity information back to the Oligocene (Mertens et al., 2009).

A number of investigators have employed various combinations of sea-surface temperature (SST), planktonic  $\delta^{18}$ O, and sea level reconstructions to derive  $\delta^{18}$ O of seawater ( $\delta^{18}O_{sw}$ ) as a proxy for salinity (Ahmad et al., 2008; Bahr et al., 2011; Billups et al., 2002; Govil and Naidu, 2011; Holbourn et al., 2010; Lea et al., 2000; Rashid et al., 2007, 2010; Steinke et al., 2010). These proxies have been utilized to derive records of changing sea-surface salinity across timescales ranging from millennial to orbital and tectonic. In most applications, Mg/Ca ratios in planktonic foraminifer shells (or alkenone  $U^{k'}_{37}$ ) have been used to derive SSTs independent of  $\delta^{18}O$  (e.g., Dekens et al., 2008; Elderfield and Ganssen, 2000; Nürnberg et al., 1996). Application to Bay of Bengal and Andaman Sea cores demonstrates the utility of this proxy in the northern Bay of Bengal (Govil and Naidu, 2011; Kudrass et al., 2001; Rashid et al., 2007, 2010). The paired SST-planktonic  $\delta^{18}$ O approach is also being applied to individual shells (Haarmann et al., 2011; Khider et al., 2011). Although resource intensive (~50 analyses per sample to achieve reliable statistics), this approach ensures capture of a robust seasonal signal that is associated closely with foraminifers calcifying during the summer monsoon salinity minima. This could play a key role in untangling the debate surrounding the divergent interpretation of summer monsoon proxies (e.g., Clemens et al., 2010; Clemens and Prell, 2007; Ruddiman, 2006; Wang et al., 2008). Local or regional  $\delta^{18}O_{sw}$ -salinity relationships for the Bay of Bengal (Delaygue et al., 2001; Singh et al., 2010) are available to derive even more direct salinity estimates at appropriate timescales (e.g., Fig. F14).

#### Runoff and erosion indicators

The impact of monsoonal precipitation on chemical weathering and transport is recorded in the physical, chemical, and isotopic composition of clastic sediments in the Bay of Bengal and the Arabian Sea. The delivery of terrigenous material to the Bay of Bengal is recorded even at distal locations (Site N90E-2C), where delivery increased in the middle Miocene with two subsequent pulses at ~7.0–5.6 and ~3.9–2.0 Ma (Hovan and Rea, 1992). These increases were interpreted to represent variations in the fluvial flux resulting from the uplift and erosion of the Himalaya, although they could equally represent intensifying erosion driven by strengthening monsoonal precipitation. An independent climate record of rainfall is needed to determine the trigger for changes in erosion patterns and rates. Indeed, it is noteworthy that the timings of these erosional pulses are broadly coincident with large-scale hydrological changes observed in the Himalayan foreland basin and Arabian Peninsula (Huang et al., 2007).

Strong north–south elemental and isotopic gradients in the surface waters also reflect continental erosion and fluvial transport processes that are similarly recorded in underlying sediments.

Carroll et al. (1993) and Moore (1997) recognized the Ganga-Brahmaputra River system as a significant source of Ba to the global ocean. Figure **F15** illustrates this strong Ba-salinity relationship in the Bay of Bengal. More recent studies have established the Ba/Ca ratio of foraminifer CaCO<sub>3</sub> as a proxy for river runoff. Ba/Ca ratios in planktonic foraminifer shells have been utilized to monitor river input to marine sections in the Arctic and Atlantic Oceans (Hall and Chan, 2004; Weldeab et al., 2007a, 2007b) as well as the Mediterranean (Sprovieri et al., 2008). This approach assumes that the Ba/Ca ratio in planktonic foraminifer shells is dominated by the Ba/Ca concentration of seawater rather than other factors. The results of Hönisch et al. (2011) strongly support this assumption; environmental parameters including pH, temperature, salinity, and symbiont photosynthesis do not appear to affect Ba substitution into planktonic foraminiferal calcite.

The utility of Sr and εNd proxies for monitoring the weathering signal from rivers in the Bay of Bengal, the Arabian Sea, and other locations has been well documented (e.g., Burton and Vance, 2000; Clift and Plumb, 2008; Colin et al., 1999; Goswami et al., 2012; Osborne et al., 2008; Padmakumari et al., 2006; Rahaman et al., 2009; Stoll et al., 2007; Tripathy et al., 2011). The Nd isotope composition of the carbonate component of Bay of Bengal sediments has been used to investigate variations in the relative contribution of discharge from the Ganga-Brahmaputra, Irrawaddy, and Arakan Rivers (Burton and Vance, 2000; Gourlan et al., 2008, 2010; Stoll et al., 2007). These studies agree that input from the Ganga-Brahmaputra River decreased during glacial periods, which is consistent with decreased Indian summer monsoon strength. The Nd isotope ratio of surface seawater near the proposed Andaman Sea sites reveals the influence of nonradiogenic inputs from the Ganga-Brahmaputra and Irrawaddy Rivers; ENd ranges from -11.4 in the Andaman Sea to -9.9 near Site N90E-2C (Amakawa et al., 2000). At the Indian margin, the influence of the Deccan and Indian craton should also be important (Goswami et al., 2012). The Sr-Nd isotope composition of the silicate fraction will provide information on temporal variations in provenance and temporal variations in weathering and runoff (Colin et al., 1999; Goswami et al., 2012; Rahaman et al., 2009; Tripathy et al., 2011).

The very narrow east Indian margin is an excellent environment for the application of elemental and mineralogical analysis of terrigenous sediments in order to

constrain variations in the intensity of chemical weathering as well as provenance changes. The combination of high river flow and narrow margins promotes the rapid movement of materials across the shelf to the slope, reducing issues associated with prolonged storage (Ponton et al., 2012; Sridhar et al., 2008) and simplifying the source-to-sink process and interpretation of the marine geochemical record.

The use of nondestructive X-ray fluorescence (XRF) core scanning measurements enables rapid, high-resolution elemental analyses of core sections (e.g., Mulitza et al., 2008). Calibration studies of core-top sediments have shown that different elemental ratios can be reliably applied to trace different weathering regimes or soil types (Govin et al., 2012). Ratios of mobile versus immobile elements have been used for many years to trace the intensity of chemical weathering in river source areas; high-resolution studies have shown that these ratios are responsive to environmental forcing on a number of timescales within the Asian monsoon system (Liu et al., 2007; Wan et al., 2009). Such proxies are even more effective when combined with traditional clay mineralogy, providing additional information on weathering regimes in support of Nd isotopes and elemental XRF analyses. Variations in clay mineralogy have provided a wealth of information on monsoon strength for the past 280 k.y. in the Bay of Bengal (Colin et al., 2006) and have also been used over longer time periods in the South China Sea (Wan et al., 2006, 2007) as well as on short timescales during the Quaternary in the Indus Basin (Alizai et al., 2012). High-resolution clay mineral records can be derived from spectral analysis of the core as well as through traditional XRF methods, and these have been effective in reconstructing weathering intensities from earlier core records (Clift et al., 2008; Giosan et al., 2002).

#### **Environmental water indicators**

Compound-specific leaf-wax D/H ( $\delta D_{wax}$ ) has been applied as a proxy for the D/H of precipitation ( $\delta D_{ppt}$ ) in marine sediments (Huang et al., 2007; Pagani et al., 2006; Schefuß et al., 2011; Sluijs et al., 2006), lake sediments (Hou et al., 2007a, 2007b; Huang et al., 2002; Jacob et al., 2007; Sauer et al., 2001; Shuman et al., 2006; Tierney et al., 2008), and loess sediments (Hou et al., 2008; Liu and Huang, 2005). Sachse et al. (2004) and Hou et al. (2008) defined quantitative links between lake surface sediment  $\delta D_{wax}$  and  $\delta D_{ppt}$  across continental-scale precipitation gradients in Europe and North America, whereas Rao et al. (2009) established the same link between soil  $\delta D_{wax}$  and  $\delta D_{ppt}$  for eastern China. The North American, European, and Chinese data sets are very consistent with one another, demonstrating the broad applicability of this proxy to monitoring changes in the hydrological cycle.  $\delta D$  of alkenones (Schouten et al., 2006; Vasiliev et al., 2013) offers another possible means of salinity reconstruction

through the effect on isotopic fractionation; hydrogen isotopic fractionation of alkenones relative to source water decreases as salinity increases.

The carbon isotopic composition of terrestrial plant biomass is primarily a function of the plant's specific photosynthetic pathway and the isotopic composition of atmospheric  $CO_2$ . Leaf wax  $\delta^{13}C$  records have been used extensively to reconstruct past changes in the balance of  $C_3$  versus arid-adapted  $C_4$  vegetation (see Feakins et al., 2005, and Ponton et al., 2012, for examples in the monsoon domain). Analysis of both leaf-wax  $\delta D$  and  $\delta^{13}C$  can be used to distinguish between changes in moisture source (LeGrande and Schmidt, 2010) and/or availability.

# Deep biosphere linkages

Specific to Indian Ocean sediments, a number of deep biosphere–related scientific problems can be addressed at the proposed drilling locations as put forth in the final report of *Scientific Drilling* in the Indian Ocean workshop (iodp.org/workshopreports/) including:

- How has uplift of the Himalayans influenced monsoon and input of terrestrial matter into the Bay of Bengal and the Arabian Sea and impacted the development of the deep biosphere since the Oligocene?
- How has the drainage from the Himalayan rivers influenced the development of subseafloor community structures and diversity?
- How has the subseafloor biosphere been inoculated with terrestrial microorganisms (biogeography)? Are there regional differences between the Bay of Bengal and the Arabian Sea?

# Operations plan/Drilling strategy

The Expedition 353 coring program prioritizes six primary sites and seven alternate sites in 1091–2925 m water depth (Tables T1, T2). This includes two primary sites in the Andaman Sea, three primary sites in the Mahanadi Basin, and one primary site in the southern Bay of Bengal.

The order in which the sites are planned for drilling has been chosen to minimize transit times between locations and maximize the potential utility of alternate sites, should they be necessary. The Andaman Sea sites will be cored first, followed by the

Mahanadi Basin sites on the Indian margin, and then the southern Bay of Bengal site (Fig. AF1).

The first two sites cored will be Andaman Sea Site AA-4B followed by Site AA-2B. Site AA-4B will have three holes (A, B, and C). Each hole will be cored first using the advanced piston corer (APC) to refusal and then cored to a target depth of 422 meters below seafloor (mbsf) using the extended core barrel (XCB). Site AA-2B will utilize a similar strategy; however, only two holes (A and B) will be cored and Hole B will be wireline logged. Target depth for Site AA-2B is 738 mbsf.

Mahanadi Basin Site BB-7 will be drilled first; it will consist of three holes APC cored to refusal followed by XCB coring to a total depth of 184 mbsf. It is possible that the APC can be pushed to the total depth at this site by using the half-length APC. Site BB-5 will be drilled next and will consist of two holes APC cored to refusal then XCB cored to a total depth of 680 mbsf. Following the comparison of the age models and carbonate preservation between Sites BB-7 and BB-5, the decision will be made to either continue with additional deep holes at Site BB-5 (and not drill Site BB-2B at all) or to terminate Site BB-5 and drill Site BB-2B. This decision tree is designed to account for the observation that Site BB-2B (a shallow ridge-top site offering good carbonate preservation and reduced turbidite input) does not have the same seismic units as found at Sites BB-1B, BB-4, BB-7, and BB-8B. Compared to these sites, Site BB-2B seismics indicate two possibilities. One interpretation is that part of the Pleistocene may be missing from the top of Site BB-2B but it has a section below the light reflectors (i.e., 2.0–2.1 s two-way traveltime at Site BB-7) that is not present in the other sites (Fig. AF12). The other interpretation is that Site BB-2B has an expanded upper section but is missing the light reflector interval.

The final site (N90E-2C) will consist of three holes APC cored to refusal then advanced to the target depth using the XCB. Hole C will be logged using the triple combination and Formation MicroScanner (FMS)-sonic tool strings.

For planning purposes, APC refusal depth is estimated at 100 mbsf, although we anticipate that this may be exceeded at some sites. APC refusal is defined in two ways: (1) a complete stroke is not achieved because the formation is too hard or (2) excess force (>100,000 lb) is required to pull the core barrel out of the formation because the sediment is too cohesive or "sticky." When APC refusal occurs in a hole before target depth is reached, the half-length APC can be employed to advance the hole. When refusal occurs with this system, the XCB technique may be used to advance the hole.

According to the current operations plan, Expedition 353 will core ~6190 m of sediment. Core recovery is often 100% with the APC system but is typically more variable with the XCB system, depending on lithology.

# Logging/Downhole measurements strategy

## Formation temperature measurements

We plan on using the advanced piston corer temperature tool (APCT-3) to measure formation temperature in the first hole of each site. The APCT-3 can only be used with the APC system.

## **Core orientation**

We plan to orient all APC cores with the FlexIT orientation tool and will make use of nonmagnetic coring hardware to the maximum extent possible.

# Downhole wireline logging

Downhole wireline logging using the triple combo and the FMS-sonic tool strings is planned at Sites AA-4B, BB-5, and N90E-2C. The logging tools will be run in the final hole at each site. However, coring is the top priority at each site, and the scheduled logging program may be modified if the coring objectives are not met in the allotted time.

# Risks and contingency

Several potential risks have been identified:

- Unstable hole conditions.
- The presence of chert and/or turbidites that can impact core recovery.
- Weather: although the expedition is scheduled to take place in the winter to avoid cyclone season, severe weather may still occur.
- Sediments with high gas concentrations are expected to be recovered. This can lead to core expansion on deck. The cores may require degassing on the catwalk.

All of these factors may impact drilling and coring operations.

# Sampling and data sharing strategy

Shipboard and shore-based researchers should refer to the IODP Sample, Data, and Obligations Policy (www.iodp.org/program-policies/). This document outlines the policy for distributing IODP samples and data. It also defines the obligations incurred by sample and data recipients. All requests for data and core samples must be approved by the Sample Allocation Committee (SAC). The SAC is composed of the Co-Chief Scientists, the Staff Scientist, and the IODP Curator on shore (on board the ship, the curatorial representative serves in place of the Curator).

Every member of the science party is obligated to carry out scientific research for the expedition and publish the results. For this purpose, shipboard and shore-based scientists are expected to submit sample requests (at web.iodp.tamu.edu/sdrm/) detailing their science plan 3 months before the beginning of the expedition. Based on sample requests (shore-based and shipboard) and input from the scientific party, the SAC will prepare a tentative sampling plan, which will be revised on the ship as dictated by recovery and cruise objectives. The sampling plan will be subject to modification depending upon the actual material recovered and collaborations that may evolve between scientists during the expedition. Given the specific objectives of Expedition 353, great care will be taken to maximize shared sampling to promote integration of data sets and enhance scientific collaboration among members of the scientific party. This planning process is necessary to coordinate the research to be conducted and to ensure that the scientific objectives are achieved. Modifications to sample requests and access to samples and data during the expedition and the one year postexpedition moratorium period require approval of the SAC.

All sampling frequencies and sample sizes must be justified on a scientific basis and will depend on core recovery, the full spectrum of other requests, and the expedition objectives. Some redundancy of measurement is unavoidable, but minimizing the duplication of measurements among the shipboard party and identified shore-based collaborators will be a factor in evaluating sample requests. Success will require collaboration, integration of complementary data sets, and consistent methods of analysis. Substantial collaboration and cooperation are highly encouraged.

Shipboard sampling will be restricted to acquiring ephemeral data types and to limited low-resolution sampling (e.g., for stratigraphic purposes [biostratigraphy and magnetostratigraphy], physical properties, and geochemical and microbiological analyses). Shipboard biostratigraphic and paleomagnetostratigraphic sampling will

also be restricted to rapidly produce age models that are critical to the overall objectives of the expedition and to the planning for higher resolution postcruise sampling. Because of the anticipated high sedimentation rates, samples for shipboard foraminifer biostratigraphy will be taken with a defined volume and, if possible, weighed prior to sieving. This information will be used to determine the number of foraminifers per centimeters cubed or gram of sediment, which will be used to guide postcruise sample requests.

Sampling for the majority of individual scientist's personal research will be postponed until a shore-based sampling party implemented between 2 and 4 months after the expedition at the Kochi Core Center (KCC) at Kochi University (Kochi, Japan). The KCC repository houses cores from the Pacific Ocean (west of the western boundary of the Pacific plate), the Indian Ocean (north of 60°), the Kerguelen Plateau, and the Bering Sea.

There may be considerable demand for samples from a limited amount of cored material for some critical intervals at certain sites. Critical intervals may require special handling that includes a higher sampling density, reduced sample size, or continuous core sampling for a set of particular high-priority research objectives. The SAC may require a revision of the approved sampling plan before critical intervals are sampled, and a special sampling plan shall be developed to maximize scientific return and participation and to preserve some material for future studies. The SAC can decide at any stage during the expedition or during the one year moratorium period which recovered intervals should be considered as critical.

All collected data and samples will be protected by a one year postcruise moratorium, during which time data and samples are available only to the Expedition 353 science party and approved shore-based participants. This moratorium will extend one year following the completion of the postcruise sampling party (note, not one year from the end of the time at sea). We anticipate that specific shipboard and shore-based scientific party members may require specific sampling methods. For example, Rhizon sampling may be requested for high-resolution or trace metal clean pore water sampling. Participants are encouraged to specifically identify their needs in their requests.

## References

- Ahmad, S.M., Babu, G.A., Padmakumari, V.M., and Raza, W., 2008. Surface and deep water changes in the northeast Indian Ocean during the last 60 ka inferred from carbon and oxygen isotopes of planktonic and benthic foraminifera. *Paleogeography, Paleoclimatology, Paleoecology*, 262(3–4):182–188. http://dx.doi.org/10.1016/j.palaeo.2008.03.007
- Alizai, A., Hillier, S., Clift, P.D., Giosan, L., Hurst, A., VanLaningham, S., and Macklin, M., 2012. Clay mineral variations in Holocene terrestrial sediments from the Indus Basin. *Quaternary Research*, 77(3):368–381. http://dx.doi.org/10.1016/j.yqres.2012.01.008
- Altabet, M.A., Higginson, M.J., and Murray, D.W., 2002. The effect of millennial-scale changes in Arabian Sea denitrification on atmospheric CO<sub>2</sub>. *Nature*, 415(6868):159–162. http://dx.doi.org/10.1038/415159a
- Amakawa, H., Alibo, D.S., and Nozaki, Y., 2000. Nd isotopic composition and REE pattern in the surface waters of the eastern Indian Ocean and its adjacent seas. *Geochimica et Cosmochimica Acta*, 64(10):1715–1727. http://dx.doi.org/10.1016/S0016-7037(00)00333-1
- An, Z., Clemens, S.C., Shen, J., Qiang, X., Jin, Z., Sun, Y., Prell, W.L., Luo, J., Wang, S., Xu, H., Cai, Y., Zhou, W., Liu, X., Liu, W., Shi, Z., Yan, L., Xiao, X., Chang, H., Wu, F., Ai, L., and Lu, F., 2011. Glacial–interglacial Indian summer monsoon dynamics. *Science*, 333(6043):719–723. http://dx.doi.org/10.1126/science.1203752
- Anand, P., Kroon, D., Singh, A.D., Ganeshram, R.S., Ganssen, G., and Elderfield, H., 2008. Coupled sea surface temperature–seawater δ<sup>18</sup>O reconstructions in the Arabian Sea at the millennial scale for the last 35 ka. *Paleoceanography*, 23(4):PA4207. http://dx.doi.org/10.1029/2007PA001564
- Antonov, J.I., Seidov, D., Boyer, T.P., Locarnini, R.A., Mishonov, A.V., Garcia, H.E., Baranova, O.K., Zweng, M.M., and Johnson, D.R., 2010. World Ocean Atlas 2009 (Vol. 2): Salinity. *In* Levitus, S. (Ed.), *NOAA Atlas NESDIS 69:* Washington D.C. (U.S. Government Printing Office). <a href="ftp://ftp.nodc.noaa.gov/pub/WOA09/DOC/woa09\_vol2\_text\_figures.pdf">ftp://ftp.nodc.noaa.gov/pub/WOA09/DOC/woa09\_vol2\_text\_figures.pdf</a>
- Bahr, A., Nürnberg, D., Schönfeld, J., and Garbe-Schönberg, D., 2011. Hydrological variability in Florida Straits during marine isotope Stage 5 cold events. *Paleoceanography*, 26(2):PA2214. http://dx.doi.org/10.1029/2010PA002015
- Billups, K., Channell, J.E.T., and Zachos, J., 2002. Late Oligocene to early Miocene geochronology and paleoceanography from the subantarctic South Atlantic. *Paleoceanography*, 17(1):1–11. http://dx.doi.org/10.1029/2000PA000568
- Bollmann, J., and Herrle, J.O., 2007. Morphological variation of *Emiliania huxleyi* and sea surface salinity. *Earth and Planetary Science Letters*, 255(3–4):273–288. http://dx.doi.org/10.1016/j.epsl.2006.12.029
- Bosilovich, M.G., and Schubert, S.D., 2002. Water vapor tracers as diagnostics of the regional hydrologic cycle. *Journal of Hydrometeorology*, 3(2):149–165. http://dx.doi.org/10.1175/1525-7541(2002)003<0149:WVTADO>2.0.CO;2
- Burton, K.W., and Vance, D., 2000. Glacial–interglacial variations in the neodymium isotope composition of seawater in the Bay of Bengal recorded by planktonic foraminifera. *Earth and Planetary Science Letters*, 176(3–4):425–441. http://dx.doi.org/10.1016/S0012-821X(00)00011-X
- Caballero-Gill, R.P., Clemens, S.C., and Prell, W.L., 2012. Direct correlation of Chinese spele-othem  $\delta^{18}O$  and South China Sea planktonic  $\delta^{18}O$ : transferring a speleothem chronology to the benthic marine chronology. *Paleoceanography*, 27(2):PA2203. http://dx.doi.org/10.1029/2011PA002268

- Cai, Y., An, Z., Cheng, H., Edwards, R.L., Kelly, M.J., Liu, W., Wang, X., and Shen, C.-C., 2006. High-resolution absolute-dated Indian Monsoon record between 53 and 36 ka from Xiaobailong Cave, southwestern China. *Geology*, 34(8):621–624. http://dx.doi.org/10.1130/G22567.1
- Caley, T., Malaizé, B., Bassinot, F., Clemens, S.C., Caillon, N., Linda, R., Charlier, K., and Rebaubier, H., 2011a. The monsoon imprint during the "atypical" MIS 13 as seen through north and equatorial Indian Ocean records. *Quaternary Research*, 76(2):285–293. http://dx.doi.org/10.1016/j.yqres.2011.07.001
- Caley, T., Malaizé, B., Revel, M., Ducassou, E., Wainer, K., Ibrahim, M., Shoeaib, D., Migeon, S., and Marieu, V., 2011b. Orbital timing of the Indian, East Asian and African boreal monsoons and the concept of a "global monsoon." *Quaternary Science Reviews*, 30(25–26):3705–3715. http://dx.doi.org/10.1016/j.quascirev.2011.09.015
- Caley, T., Malaizé, B., Zaragosi, S., Rossignol, L., Bourget, J., Eynaud, F., Martinez, P., Giraudeau, J., Charlier, K., and Ellouz-Zimmermann, N., 2011c. New Arabian Sea records help decipher orbital timing of Indo-Asian monsoon. *Earth and Planetary Science Letters*, 308(3–4):433–444. http://dx.doi.org/10.1016/j.epsl.2011.06.019
- Cane, M.A., and Molnar, P., 2001. Closing of the Indonesian Seaway as a precursor to East African aridification around 3–4 million years ago. *Nature*, 411(6834):157–162. http://dx.doi.org/10.1038/35075500
- Carroll, J., Falkner, K.K., Brown, E.T., and Moore, W.S., 1993. The role of the Ganges-Brahma-putra mixing zone in supplying barium and <sup>226</sup>Ra to the Bay of Bengal. *Geochimica et Cosmochimica Acta*, 57(13):2981–2990. http://dx.doi.org/10.1016/0016-7037(93)90287-7
- Cerling, T.E., Harris, J.M., MacFadden, B.J., Leakey, M.G., Quade, J., Eisenmann, V., and Ehleringer, J.R., 1997. Global vegetation change through the Miocene/Pliocene boundary. *Nature*, 389(6647):153–158. http://dx.doi.org/10.1038/38229
- Cheng, H., Edwards, R.L., Broecker, W.S., Denton, G.H., Kong, X., Wang, Y., Zhang, R., and Wang, X., 2009. Ice age terminations. *Science*, 326(5950):248–252. http://dx.doi.org/10.1126/science.1177840
- Clemens, S., Prell, W., Murray, D., Shimmield, G., and Weedon, G., 1991. Forcing mechanisms of the Indian Ocean monsoon. *Nature*, 353(6346):720–725. http://dx.doi.org/10.1038/353720a0
- Clemens, S.C., 2005. Millennial-band climate spectrum resolved and linked to centennial-scale solar cycles. *Quaternary Science Reviews*, 24(5–6):521–531. http://dx.doi.org/10.1016/j.quascirev.2004.10.015
- Clemens, S.C., Murray, D.W., and Prell, W.L., 1996. Nonstationary phase of the Plio-Pleistocene Asian monsoon. *Science*, 274(5289):943–948. http://dx.doi.org/10.1126/science.274.5289.943
- Clemens, S.C., and Prell, W.L., 2003. A 350,000 year summer-monsoon multi-proxy stack from the Owen Ridge, northern Arabian Sea. *Marine Geology*, 201(1–3):35–51. http://dx.doi.org/10.1016/S0025-3227(03)00207-X
- Clemens, S.C., and Prell, W.L., 2007. The timing of orbital-scale Indian monsoon changes. *Quaternary Science Reviews*, 26(3–4):275–278. http://dx.doi.org/10.1016/j.quascirev.2006.11.010
- Clemens, S.C., Prell, W.L., and Sun, Y., 2010. Orbital-scale timing and mechanisms driving late Pleistocene Indo-Asian summer monsoons: reinterpreting cave speleothem  $\delta^{18}$ O. *Paleoceanography*, 25(4):PA4207. http://dx.doi.org/10.1029/2010PA001926

- Clemens, S.C., Prell, W.L., Sun, Y., Liu, Z., and Chen, G., 2008. Southern hemisphere forcing of Pliocene  $\delta^{18}O$  and the evolution of Indo-Asian monsoons. *Paleoceanography*, 23(4):PA4210. http://dx.doi.org/10.1029/2008PA001638
- Clift, P.D., and Plumb, R.A., 2008. *The Asian Monsoon: Causes, History and Effects:* Cambridge (Cambridge University Press). http://dx.doi.org/10.1017/CBO9780511535833
- Clift, P.D., Hodges, K.V., Heslop, D., Hannigan, R., Long, H.V., and Calves, G., 2008. Correlation of Himalayan exhumation rates and Asian monsoon intensity. *Nature Geoscience*, 1(12):875–880. http://dx.doi.org/10.1038/ngeo351
- Colin, C., Turpin, L., Bertaux, J., Desprairies, A., and Kissel, C., 1999. Erosional history of the Himalayan and Burman ranges during the last two glacial–interglacial cycles. *Earth and Planetary Science Letters*, 171(4):647–660. http://dx.doi.org/10.1016/S0012-821X(99)00184-3
- Colin, C., Turpin, L., Blamart, D., Frank, N., Kissel, C., and Duchamp, S., 2006. Evolution of weathering patterns in the Indo-Burman Ranges over the last 280 kyr: effects of sediment provenance on <sup>87</sup>Sr/<sup>86</sup>Sr ratios tracer. *Geochemistry, Geophysics, Geosystems*, 7(3):Q03007. http://dx.doi.org/10.1029/2005GC000962
- Cullen, J.L., 1981. Microfossil evidence for changing salinity patterns in the Bay of Bengal over the last 20,000 years. *Palaeogeography, Palaeoclimatology, Palaecology,* 35:315–356. http://dx.doi.org/10.1016/0031-0182(81)90101-2
- Cullen, J.L., and Prell, W.L., 1984. Planktonic foraminifera of the northern Indian Ocean: distribution and preservation in surface sediments. *Marine Micropaleontology*, 9(1):1–52. http://dx.doi.org/10.1016/0377-8398(84)90022-7
- Curray, J.R., 1991. Possible greenschist metamorphism at the base of a 22-km sedimentary section, Bay of Bengal. *Geology*, 19(11):1097–1100. http://dx.doi.org/10.1130/0091-7613(1991)019<1097:PGMATB>2.3.CO;2
- Curray, J.R., 2005. Tectonics and history of the Andaman Sea region. *Journal of Asian Earth Sciences*, 25(1):187–232. http://dx.doi.org/10.1016/j.jseaes.2004.09.001
- Dekens, P.S., Ravelo, A.C., McCarthy, M.D., and Edwards, C.A., 2008. A 5 million year comparison of Mg/Ca and alkenone paleothermometers. *Geochemistry, Geophysics, Geosystems*, 9(10):Q10001. http://dx.doi.org/10.1029/2007GC001931
- Delaygue, G., Bard, E., Rollion, C., Jouzel, J., Stiévenard, M., Duplessy, J.C., and Ganssen, G., 2001. Oxygen isotope/salinity relationship in the northern Indian Ocean. *Journal of Geophysical Research: Oceans*, 106(C3):4565–4574. http://dx.doi.org/10.1029/1999JC000061
- Dettman, D.L., Kohn, M.J., Quade, J., Ryerson, F.J., Ojha, T.P., and Hamidullah, S., 2001. Seasonal stable isotope evidence for a strong Asian monsoon throughout the past 10.7 m.y. *Geology*, 29(1):31–34. http://dx.doi.org/10.1130/0091-7613(2001)029<0031:SSIEFA>2.0.CO;2
- Dickens, G.R., and Owen, R.M., 1999. The latest Miocene–early Pliocene biogenic bloom: a revised Indian Ocean perspective. *Marine Geology*, 161(1):75–91. http://dx.doi.org/10.1016/S0025-3227(99)00057-2
- Ding, Y., and Chan, J.C.L., 2005. The East Asian summer monsoon: an overview. *Meteorology and Atmospheric Physics*, 89(1–4):117–142. http://dx.doi.org/10.1007/s00703-005-0125-z
- Ding, Y., Li, C., and Liu, Y., 2004. Overview of the South China Sea monsoon experiment. *Advances in Atmospheric Sciences*, 21(3):343–360. http://dx.doi.org/10.1007/BF02915563
- Elderfield, H., and Ganssen, G., 2000. Past temperature and  $\delta^{18}$ O of surface ocean waters inferred from foraminiferal Mg/Ca ratios. *Nature*, 405(6785):442–445. http://dx.doi.org/10.1038/35013033

- Emile-Geay, J., Cane, M.A., Naik, N., Seager, R., Clement, A.C., and van Geen, A., 2003. Warren revisited: atmospheric freshwater fluxes and "why is no deep water formed in the North Pacific?" *Journal of Geophysics Research: Oceans*, 108(C6):3178. http://dx.doi.org/10.1029/2001JC001058
- Farrell, J.W., Raffi, I., Janecek, T.R., Murray, D.W., Levitan, M., Dadey, K.A., Emeis, K.-C., Lyle, M., Flores, J.-A., and Hovan, S., 1995. Late Neogene sedimentation patterns in the eastern equatorial Pacific Ocean. *In Pisias*, N.G., Mayer, L.A., Janecek, T.R., Palmer-Julson, A., and van Andel, T.H. (Eds.), *Proceedings of the Ocean Drilling Program, Scientific Results*, 138: College Station, TX (Ocean Drilling Program), 717–756. http://dx.doi.org/10.2973/odp.proc.sr.138.143.1995
- Feakins, S.J., deMenocal, P.B., and Eglinton, T.I., 2005. Biomarker records of late Neogene changes in northeast African vegetation. *Geology*, 33(12):977–980. http://dx.doi.org/10.1130/G21814.1
- Federov, L.V., Ravich, M.G., and Hofmann, J., 1982. Geologic comparison of southeastern peninsular India and Sri Lanka with a part of East Antarctica (Enderby Land, MacRobertson Land, and Princess Elizabeth Land). *In* Craddock, C. (Ed.), *Antarctic Geoscience:* Madison, Wisconsin (University of Wisconsin Press), 73–78.
- Frank, M., Whiteley, N., van de Flierdt, T., Reynolds, B.C., and O'Nions, K., 2006. Nd and Pb isotope evolution of deep water masses in the eastern Indian Ocean during the past 33 Myr. *Chemical Geology*, 226(3–4):264–279. http://dx.doi.org/10.1016/j.chemgeo.2005.09.024
- Frerichs, W.E., 1971. Planktonic foraminifera in the sediments of the Andaman Sea. *Journal of Foraminiferal Research*, 1(1):1–14. http://dx.doi.org/10.2113/gsjfr.1.1.1
- Giosan, L., Flood, R.D., Grützner, J., and Mudie, P., 2002. Paleoceanographic significance of sediment color on western North Atlantic drifts: II. Late Pliocene–Pleistocene sedimentation. *Marine Geology*, 189(1–2):43–61. http://dx.doi.org/10.1016/S0025-3227(02)00322-5
- Goswami, V., Singh, S.K., Bhushan, R., and Rai, V.K., 2012. Temporal variations in <sup>87</sup>Sr/<sup>86</sup>Sr and ε<sub>Nd</sub> in sediments of the southeastern Arabian Sea: impact of monsoon and surface water circulation. *Geochemistry, Geophysics, Geosystems,* 13(1):Q01001. http://dx.doi.org/10.1029/2011GC003802
- Gourlan, A.T., Meynadier, L., and Allègre, C.J., 2008. Tectonically driven changes in the Indian Ocean circulation over the last 25 Ma: neodymium isotope evidence. *Earth and Planetary Science Letters*, 267(1–2):353–364. http://dx.doi.org/10.1016/j.epsl.2007.11.054
- Gourlan, A.T., Meynadier, L., Allègre, C.J., Tapponnier, P., Birck, J.-L., and Joron, J.-L., 2010. Northern Hemisphere climate control of the Bengali rivers discharge during the past 4 Ma. *Quaternary Science Reviews*, 29(19–20):2484–2498. http://dx.doi.org/10.1016/j.quascirev.2010.05.003
- Govil, P., and Naidu, P.D., 2011. Variations of Indian monsoon precipitation during the last 32 kyr reflected in the surface hydrography of the Western Bay of Bengal. *Quaternary Science Reviews*, 30(27–28):3871–3879. http://dx.doi.org/10.1016/j.quascirev.2011.10.004
- Govin, A., Holzwarth, U., Heslop, D., Keeling, L.F., Zabel, M., Mulitza, S., Collins, J.A., and Chiessi, C.M., 2012. Distribution of major elements in Atlantic surface sediments (36°N–49°S): imprint of terrigenous input and continental weathering. *Geochemistry, Geophysics, Geosystems*, 13(1). http://dx.doi.org/10.1029/2011GC003785
- Guo, Z.T., Ruddiman, W.F., Hao, Q.Z., Wu, H.B., Qiao, Y.S., Zhu, R.X., Peng, S.Z., Wei, J.J., Yuan, B.Y., and Liu, T.S., 2002. Onset of Asian desertification by 22 Myr ago inferred from loess deposits in China. *Nature*, 416(6877):159–163. http://dx.doi.org/10.1038/416159a

- Gupta, A.K., Singh, R.K., Joseph, S., and Thomas, E., 2004. Indian Ocean high-productivity event (10–8 Ma): linked to global cooling or to the initiation of the Indian monsoons? *Geology*, 32(9):753–756. http://dx.doi.org/10.1130/G20662.1
- Gupta, A.K., Singh, R.K., and Verma, S., 2013. Deep-sea palaeoceanographic evolution of the eastern Indian Ocean during the late Oligocene–Pleistocene: species diversity trends in benthic foraminifera. *Current Science*, 104(7):904–910. http://www.current-science.ac.in/Volumes/104/07/0904.pdf
- Gupta, A.K., and Thomas, E., 2003. Initiation of Northern Hemisphere glaciation and strengthening of the northeast Indian monsoon: Ocean Drilling Program Site 758, eastern equatorial Indian Ocean. *Geology*, 31(1):47–50. http://dx.doi.org/10.1130/0091-7613(2003)031<0047:IONHGA>2.0.CO;2
- Guptha, M.V.S., Curry, W.B., Ittekkot, V., and Muralinath, A.S., 1997. Seasonal variation in the flux of planktonic foraminifera: sediment trap results from the Bay of Bengal, northern Indian Ocean. *Journal of Foraminiferal Research*, 27(1):5–19. http://dx.doi.org/10.2113/gsjfr.27.1.5
- Haarmann, T., Hathorne, E.C., Mohtadi, M., Groeneveld, J., Kölling, M., and Bickert, T., 2011. Mg/Ca ratios of single planktonic foraminifer shells and the potential to reconstruct the thermal seasonality of the water column. *Paleoceanography*, 26(3):PA3218. http://dx.doi.org/10.1029/2010PA002091
- Hall, J.M., and Chan, L.-H., 2004. Ba/Ca in *Neogloboquadrina pachyderma* as an indicator of deglacial meltwater discharge into the western Arctic Ocean. *Paleoceanography*, 19(1):PA1017. http://dx.doi.org/10.1029/2003PA000910
- Hall, R., 2002. Cenozoic geological and plate tectonic evolution of SE Asia and the SW Pacific: computer-based reconstructions, model and animations. *Journal of Asian Earth Sciences*, 20(4):353–431. http://dx.doi.org/10.1016/S1367-9120(01)00069-4
- Hall, R., Cottam, M.A., and Wilson, M.E.J., 2011. The SE Asian gateway: history and tectonics of the Australia–Asia collision. *Special Publication—Geological Society of London*, 355(1):1–6. http://dx.doi.org/10.1144/SP355.1
- Hastenrath, S., and Greischar, L., 1993. The monsoonal heat budget of the hydrosphere atmosphere system in the Indian Ocean sector. *Journal of Geophysical Research: Oceans*, 98(C4):6869–6881. http://dx.doi.org/10.1029/92JC02956
- Holbourn, A., Kuhnt, W., Clemens, S., Prell, W., and Andersen, N., 2013. Middle to late Miocene stepwise climate cooling: evidence from a high-resolution deep water isotope curve spanning 8 million years. *Paleoceanography*, 28(4):688–699. http://dx.doi.org/10.1002/2013PA002538
- Holbourn, A., Kuhnt, W., Regenberg, M., Schulz, M., Mix, A., and Andersen, N., 2010. Does Antarctic glaciation force migration of the tropical rain belt? *Geology*, 38(9):783–786. http://dx.doi.org/10.1130/G31043.1
- Holbourn, A., Kuhnt, W., Schulz, M., Flores, J.-A., and Andersen, N., 2007. Orbitally-paced climate evolution during the middle Miocene "Monterey" carbon-isotope excursion. *Earth and Planetary Science Letters*, 261(3–4):534–550. http://dx.doi.org/10.1016/j.epsl.2007.07.026
- Hönisch, B., Allen, K.A., Russell, A.D., Eggins, S.M., Bijma, J., Spero, H.J., Lea, D.W., and Yu, J., 2011. Planktic foraminifers as recorders of seawater Ba/Ca. *Marine Micropaleontology*, 79(1–2):52–57. http://dx.doi.org/10.1016/j.marmicro.2011.01.003
- Hou, J., D'Andrea, W.J., and Huang, Y., 2008. Can sedimentary leaf waxes record *D/H* ratios of continental precipitation? Field, model, and experimental assessments. *Geochimica et Cosmochimica Acta*, 72(14):3503–3517. http://dx.doi.org/10.1016/j.gca.2008.04.030

- Hou, J., Huang, Y., Oswald, W.W., Foster, D.R., and Shuman, B., 2007a. Centennial-scale compound-specific hydrogen isotope record of Pleistocene–Holocene climate transition from southern New England. *Geophysical Research Letters*, 34(19):L19706. http://dx.doi.org/10.1029/2007GL030303
- Hou, J., D'Andrea, W.J., MacDonald, D., and Huang, Y., 2007b. Hydrogen isotopic variability in leaf waxes among terrestrial and aquatic plants around Blood Pond, Massachusetts (USA). Organic Geochemistry, 38(6):977–984. http://dx.doi.org/10.1016/j.orggeochem.2006.12.009
- Hovan, S., and Rea, D.K., 1992. The Cenozoic record of continental mineral deposition on Broken and Ninetyeast Ridges, Indian Ocean: southern African aridity and sediment delivery from the Himalayas. *Paleoceanography*, 7(6):833–860. http://dx.doi.org/10.1029/92PA02176
- Huang, Y., Clemens, S.C., Liu, W., Wang, Y., and Prell, W.L., 2007. Large-scale hydrological change drove the late Miocene C<sub>4</sub> plant expansion in the Himalayan foreland and Arabian Peninsula. *Geology*, 35(6):531–534. http://dx.doi.org/10.1130/G23666A.1
- Huang, Y.S., Shuman, B., Wang, Y., and Webb, T., III, 2002. Hydrogen isotope ratios of palmitic acid in lacustrine sediments record late Quaternary climate variations. *Geology*, 30(12):1103–1106. http://dx.doi.org/10.1130/0091-7613(2002)030<1103:HIROPA>2.0.CO;2
- Jacob, J., Huang, Y., Disnar, J.-R., Sifeddine, A., Boussafir, M., Albuquerque, A.L.S., and Turcq, B., 2007. Paleohydrological changes during the last deglaciation in northern Brazil. *Quaternary Science Reviews*, 26(7–8):1004–1015. http://dx.doi.org/10.1016/j.quascirev.2006.12.004
- Jensen, T.G., 2001. Arabian Sea and Bay of Bengal exchange of salt and tracers in an ocean model. *Geophysical Research Letters*, 28(20):3967–3970. http://dx.doi.org/10.1029/2001GL013422
- Jensen, T.G., 2003. Cross-equatorial pathways of salt and tracers from the northern Indian Ocean: modeling results. *Deep Sea Research, Part II*, 50(12–13):2111–2127. http://dx.doi.org/10.1016/S0967-0645(03)00048-1
- Khider, D., Stott, L.D., Emile-Geay, J., Thunell, R., and Hammond, D.E., 2011. Assessing El Niño Southern Oscillation variability during the past millennium. *Paleoceanography*, 26(3):PA3222. http://dx.doi.org/10.1029/2011PA002139
- Kroon, D., Steens, T., and Troelstra, S.R., 1991. Onset of monsoonal related upwelling in the western Arabian Sea as revealed by planktonic foraminifers. *In* Prell, W.L., Niitsuma, N., et al., *Proceedings of the Ocean Drilling Program, Scientific Results*, 117: College Station, TX (Ocean Drilling Program), 257–263. http://dx.doi.org/10.2973/odp.proc.sr.117.126.1991
- Kudrass, H.R., Hofmann, A., Doose, H., Emeis, K., and Erlenkeuser, H., 2001. Modulation and amplification of climatic changes in the Northern Hemisphere by the Indian summer monsoon during the past 80 k.y. *Geology*, 29(1):63–66. http://dx.doi.org/10.1130/0091-7613(2001)029<0063:MAAOCC>2.0.CO;2
- Kuhnt, W., Holbourn, A., Hall, R., Zuvela, M. and Käse, R., 2004. Neogene history of the Indonesian throughflow. *In Clift, P., Wang, P., Kuhnt, W., and Hayes, D. (Eds.), Continent-Ocean Interactions within East Asian Marginal Seas*. Geophysical Monograph, 149:299–320. http://dx.doi.org/10.1029/149GM16
- Kumar, S.P., Muraleedharan, P.M., Prasad, T.G., Gauns, M., Ramaiah, N., de Souza, S.N., Sardesai, S., and Madhupratap, M., 2002. Why is the Bay of Bengal less productive during summer monsoon compared to the Arabian Sea? *Geophysical Research Letters*, 29(24):2235. http://dx.doi.org/10.1029/2002GL016013

- Lea, D.W., Pak, D.K., and Spero, H.J., 2000. Climate impact of late Quaternary equatorial Pacific sea surface temperature variations. *Science*, 289(5485):1719–1724. http://dx.doi.org/10.1126/science.289.5485.1719
- LeGrande, A.N., and Schmidt, G.A., 2010. Water isotopologues as a quantitative paleosalinity proxy. *Paleoceanography*, 26(3):PA3225. http://dx.doi.org/10.1029/2010PA002043
- Lisiecki, L.E., and Raymo, M.E., 2005. A Pliocene–Pleistocene stack of 57 globally distributed benthic  $\delta^{18}O$  records. *Paleoceanography*, 20(1):PA1003. http://dx.doi.org/10.1029/2004PA001071
- Lisiecki, L.E., and Raymo, M.E., 2007. Plio–Pleistocene climate evolution: trends and transitions in glacial cycle dynamics. *Quaternary Science Reviews*, 26(1–2):56–69. http://dx.doi.org/10.1016/j.quascirev.2006.09.005
- Liu, W., and Huang, Y., 2005. Compound specific *D/H* ratios and molecular distributions of higher plant leaf waxes as novel paleoenvironmental indicators in the Chinese Loess Plateau. *Organic Geochemistry*, 36(6):851–860. http://dx.doi.org/10.1016/j.orggeochem.2005.01.006
- Liu, W.T., and Tang, W., 2004. Oceanic influence on the precipitation in India and China as observed by TRMM and QuikSCAT [paper presented at 2nd TRMM International Science Conference, Nara, Japan, 6–10 September 2004]. http://airsea-www.jpl.nasa.gov/publication/paper/Liu-Tang-2004-trmm.pdf
- Liu, W.T., and Tang, W., 2005. Estimating moisture transport over oceans using space-based observations. *Journal of Geophysical Research: Atmospheres*, 110(D10):D10101. http://dx.doi.org/10.1029/2004JD005300
- Liu, W.T., Zhang, A., and Bishop, J.K.B., 1994. Evaporation and solar irradiance as regulators of sea surface temperature in annual and interannual changes. *Journal of Geophysical Research: Oceans*, 99(C6):12623–12637. http://dx.doi.org/10.1029/94JC00604
- Liu, X., Liu, Z., Kutzbach, J.E., Clemens, S.C., and Prell, W.L., 2006. Hemispheric insolation forcing of the Indian Ocean and Asian Monsoon: local versus remote impacts. *Journal of Climate*, 19(23):6195–6208. http://dx.doi.org/10.1175/JCLI3965.1
- Liu, Z., Colin, C., Huang, W., Le, K.P., Tong, S., Chen, Z., and Trentesaux, A., 2007. Climatic and tectonic controls on weathering in south China and Indochina Peninsula: clay mineralogical and geochemical investigations from the Pearl, Red, and Mekong drainage basins. *Geochemistry, Geophysics, Geosystems*, 8(5):Q05005. http://dx.doi.org/10.1029/2006GC001490
- Locarnini, R.A., Mishonov, A.V., Antonov, J.I., Boyer, T.P., Garcia, H.E., Baranova, O.K., Zweng, M.M., and Johnson, D.R., 2010. World Ocean Atlas 2009 (Vol. 1): Temperature. *In* Levitus S. (Ed.), *NOAA Atlas NESDIS 68:* Washington D.C. (U.S. Government Printing Office). ftp://ftp.nodc.noaa.gov/pub/WOA09/DOC/woa09\_vol1\_text\_figures.pdf
- Loschnigg, J., and Webster, P.J., 2000. A coupled ocean–atmosphere system of SST modulation for the Indian Ocean. *Journal of Climate*, 13(19):3342–3360. http://dx.doi.org/10.1175/1520-0442(2000)013<3342:ACOASO>2.0.CO;2
- Mantyla, A.W., and Reid, J.L., 1995. On the origins of deep and bottom waters of the Indian Ocean. *Journal of Geophysical Research: Oceans*, 100(C2):2417–2439. http://dx.doi.org/10.1029/94JC02564
- Mazumdar, A., Peketi, A., Joao, H.M., Dewangan, P., and Ramprasad, T., 2014. Pore-water chemistry of sediment cores off Mahanadi Basin, Bay of Bengal: possible link to deep seated methane hydrate deposit. *Marine and Petroleum Geology*, 49:162–175. http://dx.doi.org/10.1016/j.marpetgeo.2013.10.011

- Mertens, K.N., Ribeiro, S., Bouimetarhan, I., Caner, H., Nebout, N.C., Dale, B., De Vernal, A., Ellegaard, M., Filipova, M., Godhe, A., Goubert, E., Grøsfjeld, K., Holzwarth, U., Kotthoff, U., Leroy, S.A.G., Londeix, L., Marret, F., Matsuoka, K., Mudie, P.J., Naudts, L., Peña-Manjarrez, J.L., Persson, A., Popescu, S.-M., Pospelova, V., Sangiorgi, F., van der Meer, M.T.J., Vink, A., Zonneveld, K.A.F., Vercauteren, D., Vlassenbroeck, J., and Louwye, S., 2009. Process length variation in cysts of a dinoflagellate, *Lingulodinium machaerophorum*, in surface sediments: investigating its potential as salinity proxy. *Marine Micropaleontology*, 70(1–2):54–69. http://dx.doi.org/10.1016/j.marmicro.2008.10.004
- Molnar, P., 2005. Mio–Pliocene growth of the Tibetan Plateau and evolution of East Asian climate. *Palaeontologia Electronica*, 8(1):1–23. http://palaeo-electronica.org/2005\_1/molnar2/molnar2.pdf
- Molnar, P., Boos, W.R., and Battisti, D.S., 2010. Orographic controls on climate and paleoclimate of Asia: thermal and mechanical roles for the Tibetan Plateau. *Annual Review of Earth and Planetary Sciences*, 38(1):77–102. http://dx.doi.org/10.1146/annurev-earth-040809-152456
- Moore, W.S., 1997. High fluxes of radium and barium from the mouth of the Ganges-Brahmaputra River during low river discharge suggest a large groundwater source. *Earth and Planetary Science Letters*, 150(1–2):141–150. http://dx.doi.org/10.1016/S0012-821X(97)00083-6
- Mulitza, S., Prange, M., Stuut, J.-B., Zabel, M., von Dobeneck, T., Itambi, A.C., Nizou, J., Schulz, M., and Wefer, G., 2008. Sahel megadroughts triggered by glacial slowdowns of Atlantic meridional overturning. *Paleoceanography*, 23(4):PA4206. http://dx.doi.org/10.1029/2008PA001637
- Nicholls, R.J., Wong, P.P., Burkett, V., Codignotto, J., Hay, J., McLean, R., Ragoonaden, S., and Woodroffe, C.D., 2007. Coastal systems and low-lying areas. *In* Parry, M.L., Canziani, O.F., Palutikof, J.P., van der Linden, P.J., and Hanson, C.E. (Eds.), *Climate Change 2007: Impacts, Adaptation and Vulnerability. Contribution of Working Group II to the Fourth Assessment Report of the Intergovernmental Panel on Climate Change:* Cambridge (Cambridge University Press), 315–356. <a href="https://www.ipcc.ch/pdf/assessment-report/ar4/wg2/ar4-wg2-chapter6.pdf">https://www.ipcc.ch/pdf/assessment-report/ar4/wg2/ar4-wg2-chapter6.pdf</a>
- Nürnberg, D., Bijma, J., and Hemleben, C., 1996. Assessing the reliability of magnesium in foraminiferal calcite as a proxy for water mass temperatures. *Geochimica et Cosmochimica Acta*, 60(5):803–814. http://dx.doi.org/10.1016/0016-7037(95)00446-7
- Osborne, A.H., Vance, D., Rohling, E.J., Barton, N., Rogerson, M., and Fello, N., 2008. A humid corridor across the Sahara for the migration of early modern humans out of Africa 120,000 years ago. *Proceedings of the National Academy of Sciences of the United States of America*, 105(43):16444–16447. http://dx.doi.org/10.1073/pnas.0804472105
- Padmakumari, V.M., Ahmad, S.M., Dayal, A.M., Rajan, R.S., and Gopalan, K., 2006. Seawater neodymium isotopic composition in the northeast Indian Ocean during the LGM to Holocene: response to glacial and monsoonal weathering in Himalaya-Tibet. *Journal of the Geological Society of India*, 68:425–432. http://www.geosocindia.org/Special%20Issue/Monsoon/pp425-432.pdf
- Pagani, M., Pedentchouk, N., Huber, M., Sluijs, A., Schouten, S., Brinkhuis, H., Sinninghe Damsté, J.S., Dickens, G.R., and Expedition 302 Scientists, 2006. Arctic hydrology during global warming at the Palaeocene/Eocene Thermal Maximum. *Nature*, 443(7103):671–675. http://dx.doi.org/10.1038/nature05043
- Park, S.-C., Sohn, B.-J., and Wang, B., 2007. Satellite assessment of divergent water vapor transport from NCEP, ERA40, and JRA25 reanalyses over the Asian summer monsoon

- region. Journal of the Meteorological Society of Japan, 85(5):615–632. http://dx.doi.org/10.2151/jmsj.85.615
- Ponton, C., Giosan, L., Eglinton, T.I., Fuller, D.Q., Johnson, J.E., Kumar, P., and Collett, T.S., 2012. Holocene aridification of India. *Geophysical Research Letters*, 39(3):L3407. http://dx.doi.org/10.1029/2011GL050722
- Powell, C.McA., Roots, S.R., and Veevers, J.J., 1988. Pre-breakup continental extension in East Gondwanaland and the early opening of the eastern Indian Ocean. *Tectonophysics*, 155(1–4):261–283. http://dx.doi.org/10.1016/0040-1951(88)90269-7
- Prell, W.L., Murray, D.W., Clemens, S.C., and Anderson, D.M., 1992. Evolution and variability of the Indian Ocean summer monsoon: evidence from the western Arabian Sea drilling program. *In Duncan, R.A.* (Ed.), *The Indian Ocean: A Synthesis of Results from the Ocean Drilling Program.* American Geophysical Union, 70:447–469.
- Quade, J., and Cerling, T.E., 1995. Expansion of C<sub>4</sub> grasses in the late Miocene of northern Pakistan: evidence from stable isotopes in paleosols. *Palaeogeography, Palaeoclimatology, Palaeoecology,* 115(1–4):91–116. http://dx.doi.org/10.1016/0031-0182(94)00108-K
- Rahaman, W., Singh, S.K., Sinha, R., and Tandon, S.K., 2009. Climate control on erosion distribution over the Himalaya during the past ~100 ka. *Geology*, 37(6):559–562. http://dx.doi.org/10.1130/G25425A.1
- Randall, D.A., Wood, R.A., Bony, S., Colman, R., Fichefet, T., Fyfe, J., Kattsov, V., Pitman, A., Shukla, J., Srinivasan, J., Stouffer, R.J., Sumi, A., and Taylor, K.E., 2007. Climate models and their evaluation. *In* Solomon, S., Qin, D., Manning, M., Chen, Z., Marquis, M., Averyt, K.B., Tingor, M., and Miller, H.L. (Eds.), *Climate Change 2007: The Physical Science Basis. Contribution of Working Group I to the Fourth Assessment Report of the Intergovernmental Panel on Climate Change:* Cambridge (Cambridge University Press), 589–662. http://www.ipcc.ch/pdf/assessment-report/ar4/wg1/ar4-wg1-chapter8.pdf
- Rao, Z., Zhu, Z., Jia, G., Henderson, A.C.G., Xue, Q., and Wang, S., 2009. Compound specific δD values of long chain *n*-alkanes derived from terrestrial higher plants are indicative of the δD of meteoric waters: evidence from surface soils in eastern China. *Organic Geochemistry*, 40(8):922–930. http://dx.doi.org/10.1016/j.orggeochem.2009.04.011
- Rashid, H., England, E., Thompson, L., and Polyak, L., 2010. Late glacial to Holocene Indian summer monsoon variability based upon sediment records taken from the Bay of Bengal. *Terrestrial, Atmospheric and Oceanic Sciences*, 22(2):215–228. http://dx.doi.org/10.3319/TAO.2010.09.17.02(TibXS)
- Rashid, H., Flower, B.P., Poore, R.Z., and Quinn, T.M., 2007. A ~25 ka Indian Ocean monsoon variability record from the Andaman Sea. *Quaternary Science Reviews*, 26(19–21):2586–2597. http://dx.doi.org/10.1016/j.quascirev.2007.07.002
- Rodriguez, M., Chamot-Rooke, N., Huchon, P., Fournier, M., and Delescluse, M., 2014. The Owen Ridge uplift in the Arabian Sea: implications for the sedimentary record of Indian monsoon in late Miocene. *Earth and Planetary Science Letters*, 394:1–12. http://dx.doi.org/10.1016/j.epsl.2014.03.011
- Royer, J.-Y., Peirce, J.W., and Weissel, J.K., 1991. Tectonic constraints on the hotspot formation of the Ninetyeast Ridge. *In* Weissel, J., Peirce, J., Taylor, E., Alt, J., et al., *Proceedings of the Ocean Drilling Program, Scientific Results*, 121: College Station, TX (Ocean Drilling Program), 763–776. http://dx.doi.org/10.2973/odp.proc.sr.121.122.1991
- Ruddiman, W.F., 2006. What is the timing of orbital-scale monsoon changes? *Quaternary Science Reviews*, 25(7–8):657–658. http://dx.doi.org/10.1016/j.quascirev.2006.02.004
- Ryan, W.B.F., Carbotte, S.M., Coplan, J.O., O'Hara, S., Melkonian, A., Arko, R., Weissel, R.A., Ferrini, V., Goodwillie, A., Nitsche, F., Bonczkowski, J., and Zemsky, R., 2009. Global

- multi-resolution topography synthesis. *Geochemistry, Geophysics, Geosystems,* 10(3):Q03014. http://dx.doi.org/10.1029/2008GC002332
- Sachse, D., Radke, J., and Gleixner, G., 2004. Hydrogen isotope ratios of recent lacustrine sedimentary n-alkanes record modern climate variability. *Geochimica et Cosmochimica Acta*, 68(23):4877–4889. http://dx.doi.org/10.1016/j.gca.2004.06.004
- Sager, W.W., Paul, C.F., Krishna, K.S., Pringle, M., Eisin, A.E., Frey, F.A., Gopala Rao, D., and Levchenko, O., 2010. Large fault fabric of the Ninetyeast Ridge implies near-spreading ridge formation. *Geophysical Research Letters*, 37(17):L17304. http://dx.doi.org/10.1029/2010GL044347
- Sauer, P.E., Eglinton, T.I., Hayes, J.M., Schimmelmann, A., and Sessions, A.L., 2001. Compound-specific D/H ratios of lipid biomarkers from sediments as a proxy for environmental and climatic conditions. *Geochimica et Cosmochimica Acta*, 65(2):213–222. http://dx.doi.org/10.1016/S0016-7037(00)00520-2
- Schefuß, E., Kuhlmann, H., Mollenhauer, G., Prange, M., and Pätzold, J., 2011. Forcing of wet phases in southeast Africa over the past 17,000 years. *Nature*, 480(7378):509–512. http://dx.doi.org/10.1038/nature10685
- Schlitzer, R., 2000. Electronic atlas of WOCE hydrographic and tracer data now available. *Eos, Transactions American Geophysical Union*, 81(5):45. http://dx.doi.org/10.1029/00EO00028
- Schmittner, A., Galbraith, E.D., Hostetler, S.W., Pedersen, T.F., and Zhang, R., 2007. Large fluctuations of dissolved oxygen in the Indian and Pacific oceans during Dansgaard–Oeschger oscillations caused by variations of North Atlantic Deep Water subduction. *Paleoceanography*, 22(3):PA3207. http://dx.doi.org/10.1029/2006PA001384
- Schott, F.A., and McCreary, J.P., Jr., 2001. The monsoon circulation of the Indian Ocean. *Progress in Oceanography*, 51(1):1–123. http://dx.doi.org/10.1016/S0079-6611(01)00083-0
- Schott, F.A., Xie, S.-P., and McCreary, J.P., Jr., 2009. Indian Ocean circulation and climate variability. *Reviews of Geophysics*, 47(1):RG1002. http://dx.doi.org/10.1029/2007RG000245
- Schouten, S., Ossebaar, J., Schreiber, K., Kienhuis, M.V.M., Langer, G., Benthien, A., and Bijma, J., 2006. The effect of temperature, salinity and growth rate on the stable hydrogen isotopic composition of long chain alkenones produced by *Emiliania huxleyi* and *Gephyrocapsa oceanica*. *Biogeosciences*, 3(1):113–119. http://dx.doi.org/10.5194/bg-3-113-2006
- Schulz, H., von Rad, U., and Erlenkeuser, H., 1998. Correlation between Arabian Sea and Greenland climate oscillations of the past 110,000 years. *Nature*, 393(6680):54–57. http://dx.doi.org/10.1038/31750
- Scotese, C.R., Gahagan, L.M., and Larson, R.L., 1988. Plate tectonic reconstructions of the Cretaceous and Cenozoic ocean basins. *Tectonophysics*, 155(1–4):27–48. http://dx.doi.org/10.1016/0040-1951(88)90259-4
- Shuman, B., Huang, Y., Newby, P., and Wang, Y., 2006. Compound-specific isotopic analyses track changes in seasonal precipitation regimes in the northeastern United States at ca 8200 cal yr BP. *Quaternary Science Reviews*, 25(21–22):2992–3002. http://dx.doi.org/10.1016/j.quascirev.2006.02.021
- Simmonds, I., Bi, D., and Hope, P., 1999. Atmospheric water vapor flux and its association with rainfall over China in summer. *Journal of Climate*, 12(5):1353–1367. http://dx.doi.org/10.1175/1520-0442(1999)012<1353:AWVFAI>2.0.CO;2

- Singh, A., Jani, R.A., and Ramesh, R., 2010. Spatiotemporal variations of the  $\delta^{18}$ O–salinity relation in the northern Indian Ocean. *Deep Sea Research, Part I*, 57(11):1422–1431. http://dx.doi.org/10.1016/j.dsr.2010.08.002
- Singh, A.D., Jung, S.J.A., Darling, K., Ganeshram, R., Ivanochko, T., and Kroon, D., 2011. Productivity collapses in the Arabian Sea during glacial cold phases. *Paleoceanography*, 26(3):PA3210. http://dx.doi.org/10.1029/2009PA001923
- Singh, R.K., and Gupta, A.K., 2005. Systematic decline in benthic foraminiferal species diversity linked to productivity increases over the last 26 Ma in the Indian Ocean. *Journal of Foraminiferal Research*, 35(3):219–227. http://dx.doi.org/10.2113/35.3.219
- Singh, S.C., Moeremans, R., McArdle, J., and Johansen, K., 2013. Seismic images of the sliver strike-slip fault and back thrust in the Andaman-Nicobar region. *Journal of Geophysical Research: Solid Earth*, 118(10):5208–5224. http://dx.doi.org/10.1002/jgrb.50378
- Sluijs, A., Schouten, S., Pagani, M., Woltering, M., Brinkhuis, H., Sinninghe Damsté, J.S., Dickens, G.R., Huber, M., Reichart, G.-J., Stein, R., Matthiessen, J., Lourens, L.J., Pedentchouk, N., Backman, J., Moran, K., and the Expedition 302 Scientists, 2006. Subtropical Arctic Ocean temperatures during the Palaeocene/Eocene Thermal Maximum. *Nature*, 441(7093):610–613. http://dx.doi.org/10.1038/nature04668
- Sprovieri, M., d'Alcalà, M.R., Manta, D.S., Bellanca, A., Neri, R., Lirer, F., Taberner, C., Pueyo, J.J., and Sammartino, S., 2008. Ba/Ca evolution in water masses of the Mediterranean late Neogene. *Paleoceanography*, 23(3):PA3205. http://dx.doi.org/10.1029/2007PA001469
- Sridhar, P.N., Ali, M.M., Vethamony, P., Babu, M.T., Ramana, I.V., and Jayakumar, S., 2008. Seasonal occurrence of unique sediment plume in the Bay of Bengal. *Eos, Transactions American Geophysical Union*, 89(3):22–23. http://dx.doi.org/10.1029/2008E0030002
- Steinke, S., Groeneveld, J., Johnstone, H., and Rendle-Bühring, R., 2010. East Asian summer monsoon weakening after 7.5 Ma: evidence from combined planktonic foraminifera Mg/Ca and δ<sup>18</sup>O (ODP Site 1146; northern South China Sea). *Palaeogeography, Palaeoclimatology, Palaeoecology,* 289(1–4):33–43. http://dx.doi.org/10.1016/j.palaeo.2010.02.007
- Stoll, H.M., Vance, D., and Arevalos, A., 2007. Records of the Nd isotope composition of seawater from the Bay of Bengal: implications for the impact of Northern Hemisphere cooling on ITCZ movement. *Earth and Planetary Science Letters*, 255(1–2):213–228. http://dx.doi.org/10.1016/j.epsl.2006.12.016
- Subrahmanyam, V., Subrahmanyam, A.S., Murty, G.P.S., and Murthy, K.S.R., 2008. Morphology and tectonics of Mahanadi Basin, northeastern continental margin of India from geophysical studies. *Marine Geology*, 253(1–2):63–72. http://dx.doi.org/10.1016/j.margeo.2008.04.007
- Sun, X., and Wang, P., 2005. How old is the Asian monsoon system?—Palaeobotanical records from China. *Palaeogeography, Palaeoclimatology, Palaeoecology*, 222(3–4):181–222. http://dx.doi.org/10.1016/j.palaeo.2005.03.005
- Sun, Y., Clemens, S.C., Morrill, C., Lin, X., Wang, X., and An, Z., 2011. Influence of Atlantic meridional overturning circulation on the East Asian winter monsoon. *Nature Geoscience*, 5(1):46–49. http://dx.doi.org/10.1038/ngeo1326
- Thomas, D.J., Bralower, T.J., and Jones, C.E., 2003. Neodymium isotopic reconstruction of late Paleocene–early Eocene thermohaline circulation. *Earth and Planetary Science Letters*, 209(3–4):309–322. http://dx.doi.org/10.1016/S0012-821X(03)00096-7
- Tierney, J.E., Russell, J.M., Huang, Y., Sinninghe Damsté, J.S., Hopmans, E.C., and Cohen, A.S., 2008. Northern Hemisphere controls on tropical southeast African climate during the past 60,000 years. *Science*, 322(5899):252–255. http://dx.doi.org/10.1126/science.1160485

- Tomczak, M., and Godfrey, J.S., 2003. *Regional Oceanography: An Introduction* (2nd ed.): Delhi (Daya Publishing House).
- Tripathy, G.R., Singh, S.K., Bhushan, R., and Ramaswamy, V., 2011. Sr–Nd isotope composition of the Bay of Bengal sediments: impact of climate on erosion in the Himalaya. *Geochemical Journal*, 45(3):175–186. http://dx.doi.org/10.2343/geochemj.1.0112
- Varkey, M.J., Murty, V.S.N., and Suryanarayana, A., 1996. Physical oceanography of the Bay of Bengal and Andaman Sea. *Oceanography and Marine Biology*, 34:1–70. http://drs.nio.org/drs/handle/2264/2276
- Vasiliev, I., Reichart, G.-J., and Krijgsman, W., 2013. Impact of the Messinian Salinity Crisis on Black Sea hydrology—insights from hydrogen isotopes analysis on biomarkers. *Earth and Planetary Science Letters*, 362:272–282. http://dx.doi.org/10.1016/j.epsl.2012.11.038
- Wajsowicz, R.C., and Schopf, P.S., 2001. Oceanic influences on the seasonal cycle in evaporation over the Indian Ocean. *Journal of Climate*, 14(6):1199–1226. http://dx.doi.org/10.1175/1520-0442(2001)014<1199:OIOTSC>2.0.CO;2
- Wan, S., Li, A., Clift, P.D., and Jiang, H., 2006. Development of the East Asian summer monsoon: evidence from the sediment record in the South China Sea since 8.5 Ma. *Palaeogeography, Palaeoclimatology, Palaeoecology,* 241(1):139–159. http://dx.doi.org/10.1016/j.palaeo.2006.06.013
- Wan, S., Li, A., Clift, P.D., and Stuut, J.-B.W., 2007. Development of the East Asian monsoon: mineralogical and sedimentologic records in the northern South China Sea since 20 Ma. *Palaeogeography, Palaeoclimatology, Palaeoecology,* 254(3–4):561–582. http://dx.doi.org/10.1016/j.palaeo.2007.07.009
- Wan, S., Kürschner, W.M., Clift, P.D., Li, A., and Li, T., 2009. Extreme weathering/erosion during the Miocene Climatic Optimum: evidence from sediment record in the South China Sea. *Geophysical Research Letters*, 36(19):L19706. http://dx.doi.org/10.1029/2009GL040279
- Wang, P., Clemens, S., Beaufort, L., Braconnot, P., Ganssen, G., Jian, Z., Kershaw, P., and Sarnthein, M., 2005. Evolution and variability of the Asian monsoon system: state of the art and outstanding issues. *Quaternary Science Review*, 24(5–6):595–629. http://dx.doi.org/10.1016/j.quascirev.2004.10.002
- Wang, Y.J., Cheng, H., Edwards, R.L., An, Z.S., Wu, J.Y., Shen, C.-C., and Dorale, J.A., 2001. A high-resolution absolute-dated late Pleistocene monsoon record from Hulu Cave, China. *Science*, 294(5580):2345–2348. http://dx.doi.org/10.1126/science.1064618
- Wang, Y., Cheng, H., Edwards, R.L., Kong, X., Shao, X., Chen, S., Wu, J., Jiang, X., Wang, X., and An, Z., 2008. Millennial- and orbital-scale changes in the East Asian monsoon over the past 224,000 years. *Nature*, 451(7182):1090–1093. http://dx.doi.org/10.1038/nature06692
- Webster, P.J., 1987a. The elementary monsoon. *In* Fein, J.S., and Stephens, P.L. (Eds.), *Monsoons:* New York (Wiley), 3–32.
- Webster, P.J., 1987b. The variable and interactive monsoon. *In* Fein, J.S., and Stephens, P.L. (Eds.), *Monsoons:* New York (Wiley), 269–330.
- Webster, P.J., 1994. The role of hydrological processes in ocean-atmosphere interactions. *Reviews of Geophysics*, 32(4):427–476. http://dx.doi.org/10.1029/94RG01873
- Webster, P.J., Magaña, V.O., Palmer, T.N., Tomas, R.A., Shukla, J., Yanai, M., and Yasunari, T., 1998. Monsoons: processes, predictability, and the prospects for prediction. *Journal of Geophysical Research: Oceans*, 103(C7):14451–14510. http://dx.doi.org/10.1029/97JC02719

- Weldeab, S., Lea, D.W., Schneider, R.R., and Andersen, N., 2007a. Centennial scale climate instabilities in a wet early Holocene West African monsoon. *Geophysical Research Letters*, 34(24):L24702. http://dx.doi.org/10.1029/2007GL031898
- Weldeab, S., Lea, D.W., Schneider, R.R., and Andersen, N., 2007b. 155,000 years of West African monsoon and ocean thermal evolution. *Science*, 316(5829):1303–1307. http://dx.doi.org/10.1126/science.1140461
- Wyrtki, K., 1971. Oceanographic Atlas of the International Ocean Expedition. National Science Foundation.
- Xie, P., and Arkin, P.A., 1997. Global precipitation: a 17-year monthly analysis based on gauge observations, satellite estimates, and numerical model outputs. *Bulletin of the American Meteorological Society*, 78(11):2539–2558. http://dx.doi.org/10.1175/1520-0477(1997)078<2539:GPAYMA>2.0.CO;2
- Xu, J., Kuhnt, W., Holbourn, A., Andersen, N., and Bartoli, G., 2006. Changes in the vertical profile of the Indonesian Throughflow during Termination II: evidence from the Timor Sea. *Paleoceanography*, 21(4):PA4202. http://dx.doi.org/10.1029/2006PA001278
- Yancheva, G., Nowaczyk, N.R., Mingram, J., Dulski, P., Schettler, G., Negendank, J.F.W., Liu, J., Sigman, D.M., Peterson, L.C., and Haug, G.H., 2007. Influence of the intertropical convergence zone on the East Asian monsoon. *Nature*, 445(7123):74–77. http://dx.doi.org/10.1038/nature05431
- You, Y., and Tomczak, M., 1993. Thermocline circulation and ventilation in the Indian Ocean derived from water mass analysis. *Deep Sea Research, Part I,* 40(1):13–56. http://dx.doi.org/10.1016/0967-0637(93)90052-5
- Zachos, J., Pagani, M., Sloan, L., Thomas, E., and Billups, K., 2001. Trends, rhythms, and aberrations in global climate 65 Ma to present. *Science*, 292(5517):686–693. http://dx.doi.org/10.1126/science.1059412
- Zachos, J.C., Flower, B.P., and Paul, H., 1997. Orbitally paced climate oscillations across the Oligocene/Miocene boundary. *Nature*, 388(6642):567–570. http://dx.doi.org/10.1038/41528
- Zhu, Y., and Newell, R.E., 1998. A proposed algorithm for moisture fluxes from atmospheric rivers. *Monthly Weather Review*, 126(3):725–735. http://dx.doi.org/10.1175/1520-0493(1998)126<0725:APAFMF>2.0.CO;2
- Ziegler, M., Lourens, L.J., Tuenter, E., Hilgen, F., Reichart, G.-J., and Weber, N., 2010. Precession phasing offset between Indian summer monsoon and Arabian Sea productivity linked to changes in Atlantic overturning circulation. *Paleoceanography*, 25(3):PA3213. http://dx.doi.org/10.1029/2009PA001884

## **Expedition 353 Scientific Prospectus**

**Table T1.** Operations and time estimates for Expedition 353 primary sites.

		Seafloor						
Site	Location	depth (mbrf)	Operations descript	ion		Transit (days)	Drilling coring (days)	log (days
	Singapore		Begin expediti	on	5.0	Port call days		
			Transit ~16 nmi to W1 (	@ 6.0 kt		0.1		
			Transit ~2 nmi to W2 @	6.0 kt		0.0		
			Transit ~9 nmi to W3 @	6.0 kt		0.1		
			Transit ~151 nmi to W4 (	2 10.5 kt		0.6		
			Transit ~705 nmi to AA-4	@ 10.5 kt		2.8		
AA-4B EPSP to 422 mbsf	10°38.03′N 93°0.00′E	1102	Hole A - APC/XCB core to 422 mbsf Hole B - APC/XCB core to 422 mbsf Hole C - APC/XCB core to 422 mbsf	Subtotal days on site:	6.8	0 0 0	2.8 1.9 2.2	0.0 0.0 0.0
			Transit ~9 nmi to AA-2B (	@ 10.5 kt		0.0		
AA-2B EPSP to 738 mbsf	10°47.41′N 93°0.00′E	1380	Hole A - APC/XCB core to 738 mbsf Hole B - APC/XCB core to 738 mbsf; combo/FMS-sonic	wireline log-triple Subtotal days on site:	10.3	0	4.7 4.6	0 1
			Transit ~652 nmi to BB-7	@ 10.5 kt		2.5		
BB-7 EPSP to 184 mbsf	19°5.01′N 85°44.09′E	1436	Hole A - APC/XCB core to 184 mbsf Hole B - APC/XCB core to 184 mbsf Hole C - APC/XCB core to 184 mbsf	Subtotal days on site:	3.1	0 0 0	1.4 0.8 0.9	0 0 0
			Transit ~97 nmi to BB-5 (	2 10.5 kt		0.4		
BB-5 EPSP to 680 mbsf	17°44.72′N 84°47.25′E	2506	Hole A - APC/XCB core to 680 mbsf Hole B - APC/XCB core to 680 mbsf; combo/FMS-sonic	wireline log-triple Subtotal days on site:	11.4	0	5.2 5.1	0 1.0
			Transit ~89 nmi to BB-2B	@ 10.5 kt		0.4		
BB-2B EPSP to 184 mbsf	18°59.82′N 85°37.29′E	1189	Hole A - APC/XCB core to 184 mbsf Hole B - APC/XCB core to 184 mbsf Hole C - APC/XCB core to 184 mbsf	Subtotal days on site:	2.6	0 0 0	1.1 0.7 0.9	0 0 0
			Transit ~862 nmi to N90E-2	C @ 10.5 kt		3.5		
N90E-2C Pending EPSP approval	5°23.0041′N 90°21.7099′E	2974	Hole A - APC/XCB core to 350 mbsf Hole B - APC/XCB core to 350 mbsf Hole C - APC/XCB core to 350 mbsf combo/FMS-sonic	wireline log-triple Subtotal days on site:	8	0 0 0	2.6 2.1 2.5	0 0 0.8
			Transit ~317 nmi to W6 @	*		1.3		
			Transit ~459 nmi to W7 (	҈ 10.5 kt		1.9		
			Transit ~149 nmi to W8 (	҈ 10.5 kt		0.6		
			Transit ~10 nmi to W9 @	10.5 kt		0.0		
			Transit ~3 nmi to W10 @	10.5 kt		0.0		
			Transit ~16 nmi to Singapor	re @ 10.5 kt		0.1		
	Singapore		End expedition			14.1	39.3	2.9
		Port call: total on site:	5.0			al operating days: Total expedition:		

LWD = logging while drilling, MWD = measurement while drilling. EPSP = Environmental Protection and Safety Panel. APC = advanced piston corer, XCB = extended core barrel, FMS = Formation MicroScanner.

Table T2. Operations and time estimates for Expedition 353 alternate sites.

Site	Location	Seafloor depth (mbrf)	Operations description		Drilling coring (days)	LWD/MWD log (days)
AA-1 EPSP to 544 mbsf	10°49.34′N 93°6.73′E	1556	Hole A - APC/XCB core to 544 mbsf Hole B - APC/XCB core to 544 mbsf Hole C - APC/XCB core to 544 mbsf; wireline log-triple combo/FMS-sonic Subtotal days on site	: 10.1	3.3 2.8 3.2	0 0 0.8
AA-3 EPSP to 471 mbsf	10°23.44′N 93°16.69′E	2636	Hole A - APC/XCB core to 471 mbsf Hole B - APC/XCB core to 471 mbsf; wireline log-triple combo/FMS-sonic Subtotal days on site	: 7.5	3.4 3.3	0 0.8
AA-5 EPSP to 603 mbsf	10°43.47′N 93°5.33′E	1491	Hole A - APC/XCB core to 603 mbsf Hole B - APC/XCB core to 603 mbsf; wireline log-triple combo/FMS-sonic Subtotal days on site	: 8.1	3.7 3.6	0 0.9
BB-1B EPSP to 222 mbsf	18°56.11′N 85°41.98′E	1678	Hole A - APC/XCB core to 222 mbsf Hole B - APC/XCB core to 222 mbsf Hole C - APC/XCB core to 222 mbsf Subtotal days on site	: 3.6	1.4 1 1.2	0 0 0
BB-4 EPSP to 172 mbsf	19°1.47′N 85°42.88′E	1618	Hole A - APC/XCB core to 172 mbsf Hole B - APC/XCB core to 172 mbsf Hole C - APC/XCB core to 172 mbsf Subtotal days on site	: 3	1.4 0.7 0.9	0 0 0
BB-6 EPSP to 624 mbsf	18°2.21′N 85°9.74′E	2411	Hole A - APC/XCB core to 624 mbsf Hole B - APC/XCB core to 624 mbsf; wireline log-triple combo/FMS-sonic Subtotal days on site	: 9.6	4.4 4.3	0 0.9
BB-8B EPSP to 206 mbsf	18°55.32′N 85°45.87′E	1837	Hole A - APC/XCB core to 206 mbsf Hole B - APC/XCB core to 206 mbsf Hole C - APC/XCB core to 206 mbsf Subtotal days on site	: 3.4	1.4 0.9 1.2	0 0 0

LWD = logging while drilling, MWD = measurement while drilling. EPSP = Environmental Protection and Safety Panel. APC = advanced piston corer, XCB = extended core barrel, FMS = Formation MicroScanner.

**Table T3.** Summary of site information for Expedition 353.

Expedition 353 primary sites					
Site		Latitude	Longitude	Water depth (m)	Target depth (mbsf)
AA-4B	Andaman Sea	10°38.03071′N	93°00.0036366′E	1091	422
AA-2B	Andaman Sea	10°47.40586′N	93°00.0000'E	1369	738
BB-7	Mahanadi Basin	19°5.01′N	85°44.09′E	1425	184
BB-5	Mahanadi Basin	17°44.72183′N	84°47.2513332′E	2495	680
BB-2B	Mahanadi Basin	18°5981534′N	85°37.29411405′E	1178	184
N90E-2C	Southern Bay of Bengal	5°23.0041′N	90°21.7099′E	2963	350
		Alternate site	es		
Site		Latitude	Longitude	Water depth (m)	Target depth (mbsf)
Site	Andaman Sea	Latitude 10°49.33639′N	Longitude 93°6.7339482′E		
	Andaman Sea Andaman Sea			(m) ·	(mbsf)
AA-1	7 11 1 da 11 da 1	10°49.33639′N	93°6.7339482′E	(m) 1545	(mbsf) 544
AA-1 AA-3	Andaman Sea	10°49.33639′N 10°23.43684′N	93°6.7339482′E 93°16.6901004′E	(m) 1545 2625	(mbsf) 544 471
AA-1 AA-3 AA-5	Andaman Sea Andaman Sea	10°49.33639′N 10°23.43684′N 10°43.46856′N	93°6.7339482′E 93°16.6901004′E 93°5.32998′E	(m) 1545 2625 1480	(mbsf) 544 471 603
AA-1 AA-3 AA-5 BB-1B	Andaman Sea Andaman Sea Mahanadi Basin	10°49.33639′N 10°23.43684′N 10°43.46856′N 18°56.10636′N	93°6.7339482′E 93°16.6901004′E 93°5.32998′E 85°41.9823′E	(m) 1545 2625 1480 1667	(mbsf) 544 471 603 222

**Figure F1.** A. Location of Expedition 353 primary and alternate sites and anticipated recovery for site locations in the Andaman Sea (AA), Mahanadi Basin, Bay of Bengal (BB), and N90E-2C (redrill ODP Site 758). Map was generated using the Generic Mapping Tools (GMT 4.5.8; **gmt.soest.hawaii.edu/**) and the bathymetric GEBCO\_08 Grid (version 20100927; **www.gebco.net/**). (Continued on next three pages.)

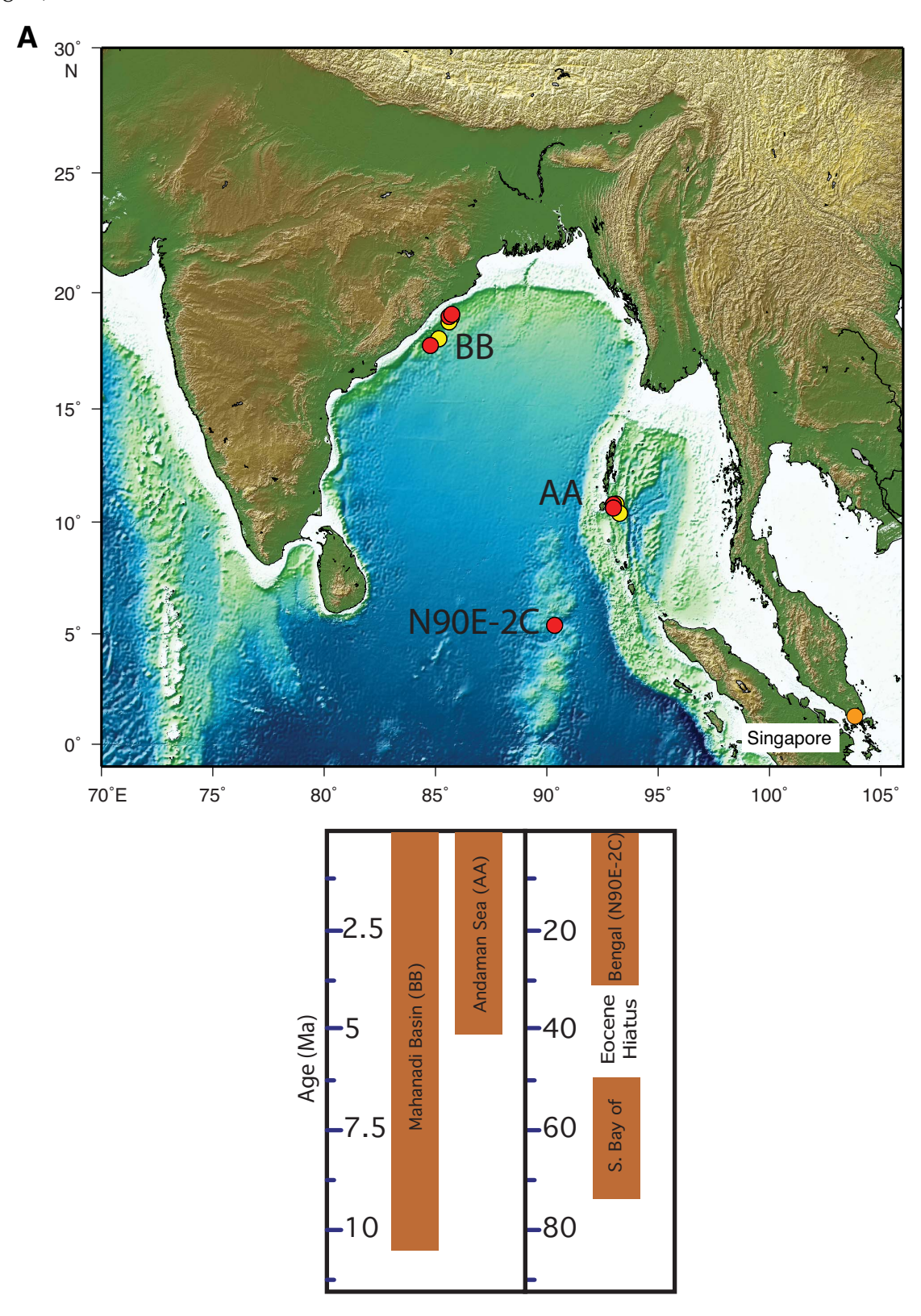


**Figure F1 (continued). B.** Location of Andaman Sea sites. Map was generated using the Generic Mapping Tools (GMT 4.5.8; **gmt.soest.hawaii.edu**/) and the bathymetric GEBCO\_08 Grid (version 20100927; **www.gebco.net**/). (Continued on next page.)

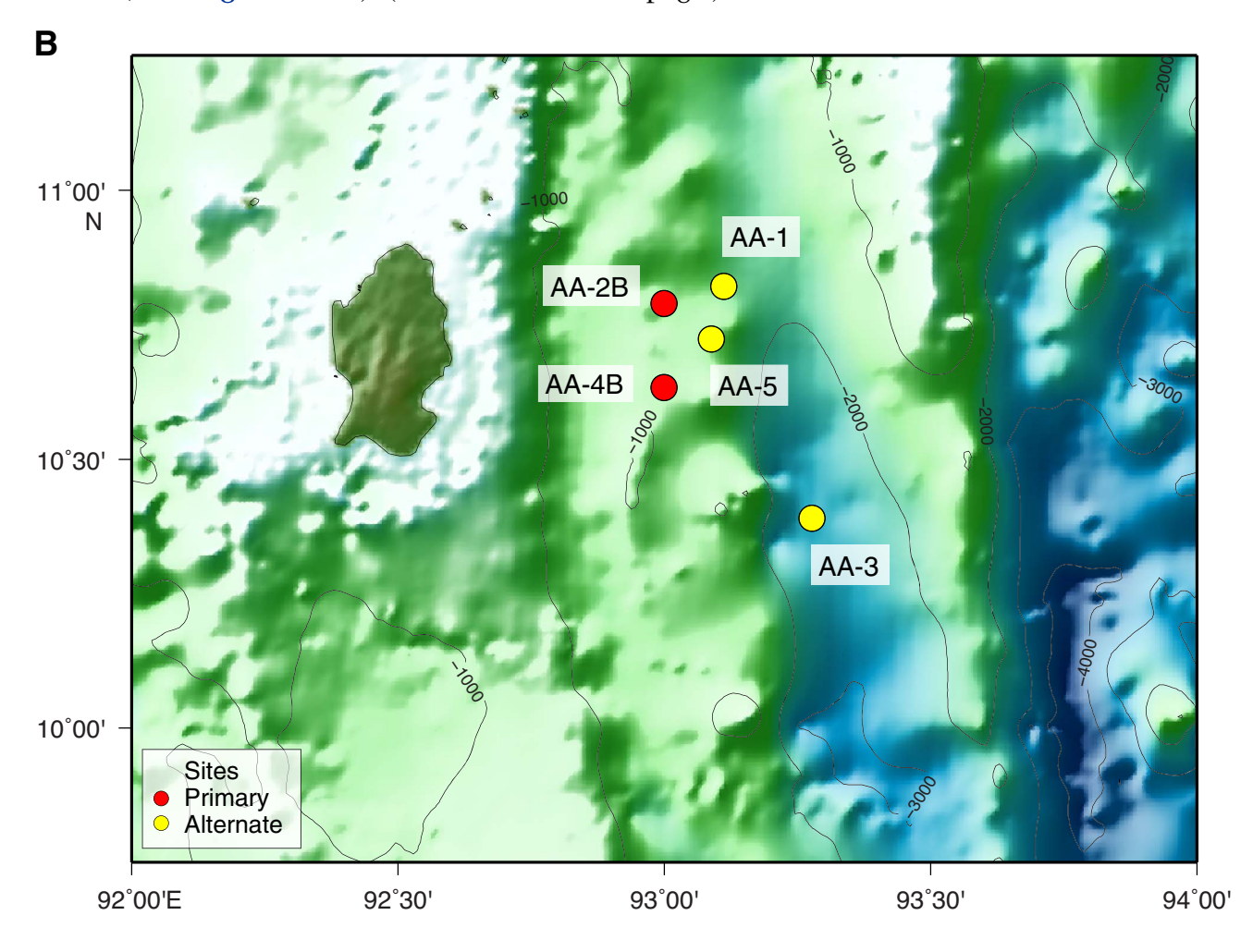


**Figure F1 (continued).** C. Location of the Mahanadi Basin sites. Map was generated using the Generic Mapping Tools (GMT 4.5.8; **gmt.soest.hawaii.edu**/) and the bathymetric GEBCO\_08 Grid (version 20100927; **www.gebco.net**/). (Continued on next page.)

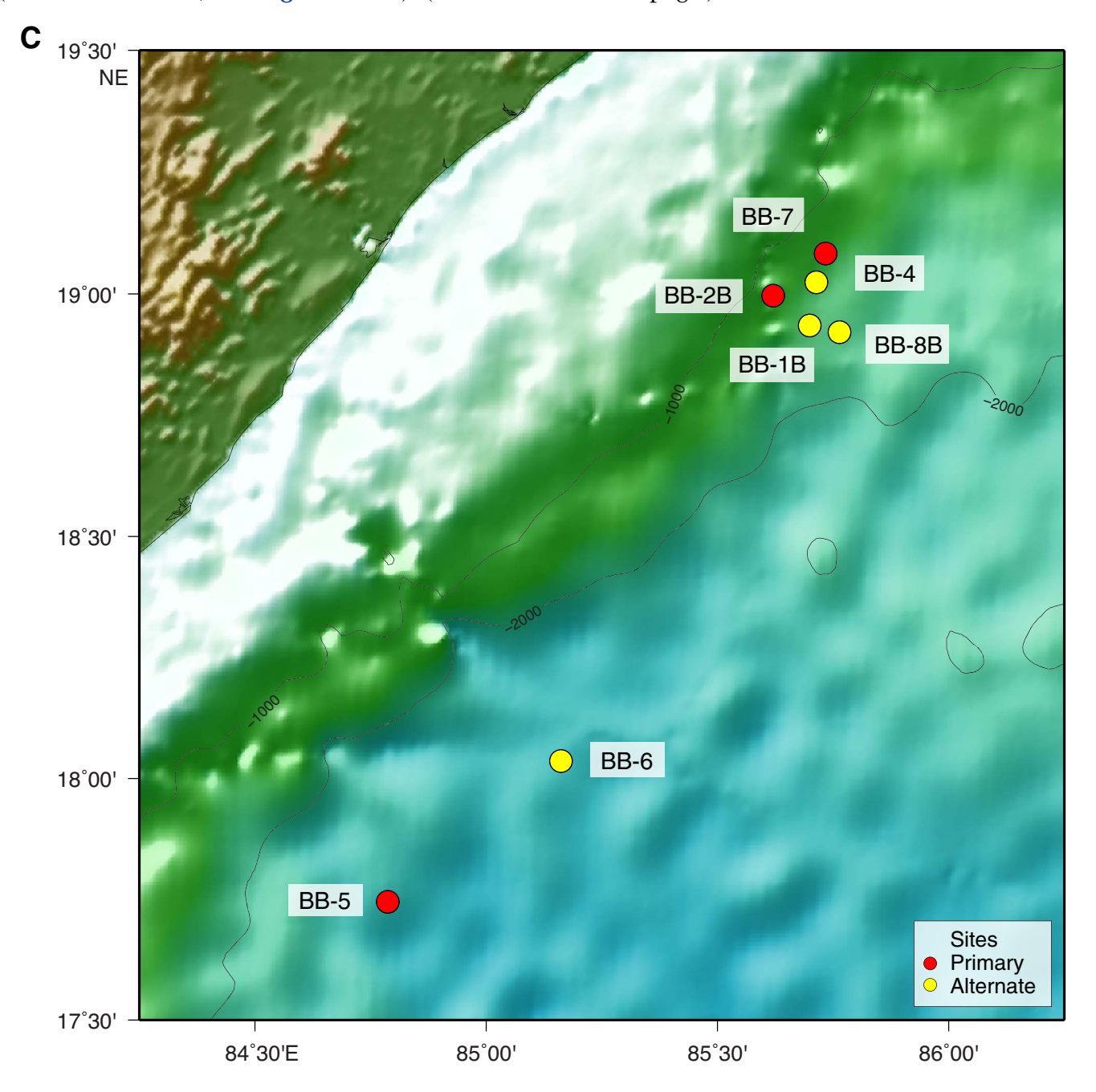


**Figure F1 (continued). D.** Detailed bathymetry showing proposed site locations and existing National Gas Hydrate Program (NGHP) well locations. Bathymetric map after Mazumdar et al. (2014).

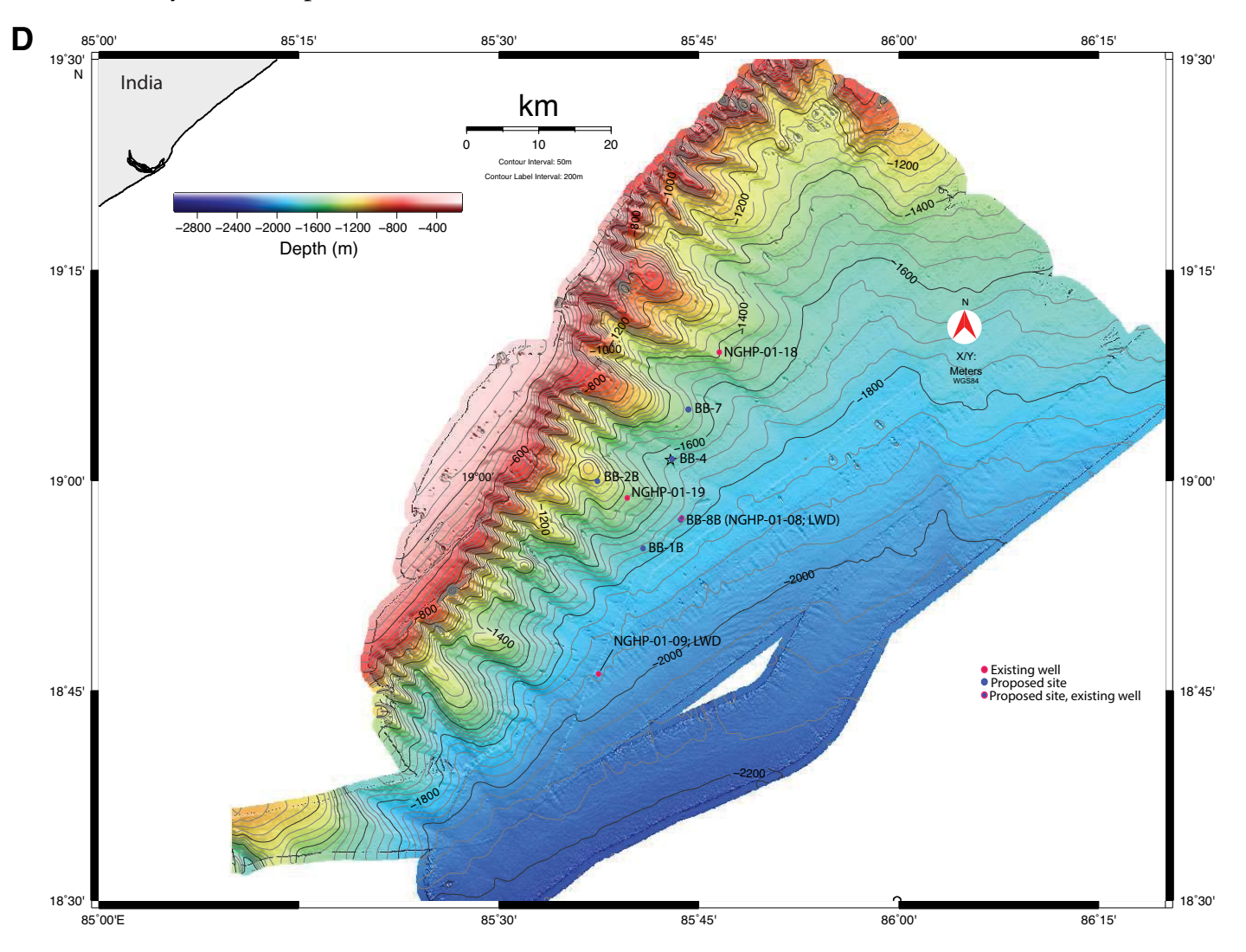


**Figure F2.** Climatological (**A**) July–August and (**B**) January–February mean precipitation rates (shading in mm/day) and 925 hPa wind vectors (arrows). Precipitation and wind climatology are derived from CMAP (Xie and Arkin, 1997) (1979–2000) and NCEP/NCAR reanalysis (1951–2000), respectively.

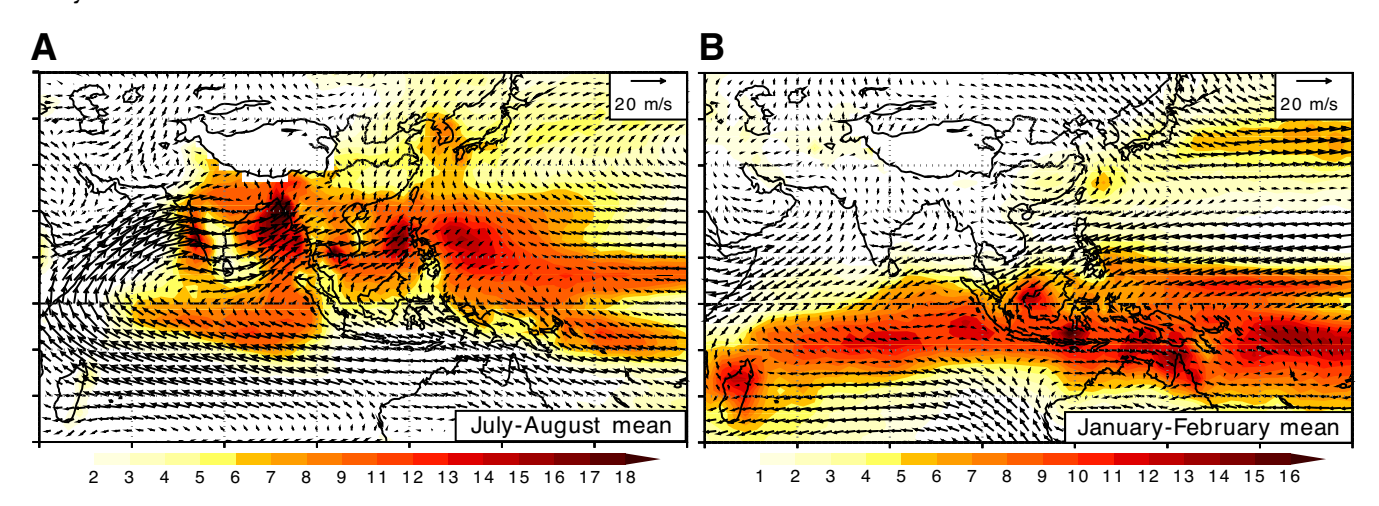


**Figure F3.** World Ocean Atlas Monthly Mean Salinity for 1955–2006 (Antonov et al., 2010). Proposed site locations in the Andaman Sea (AA), Mahanadi Basin, Bay of Bengal (BB), and N90E-2C (redrill ODP Site 758) are shown.

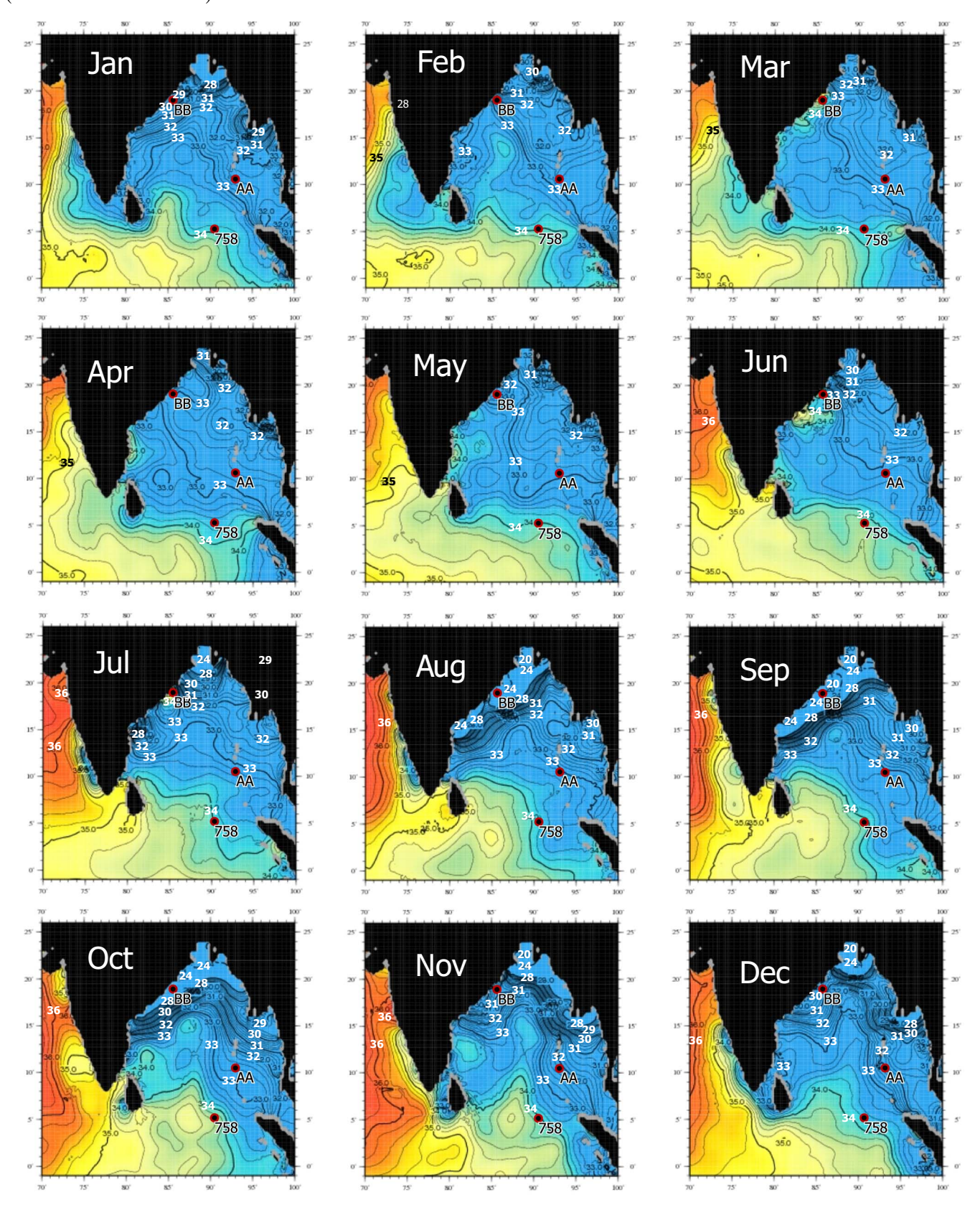


**Figure F4.** Ten-day National Oceanic and Atmospheric Administration HYSPLIT backtracks (2007–2011). Green indicates rain-bearing air trajectories. Rain-bearing trajectories over India are dominated by summer season (southwest) winds, whereas both winter (northerly) and summer (southerly) air masses carry precipitation to the monsoonal region of southeast China. This is consistent with World Meteorological Organization rainfall records indicating that JJA rainfall accounts for 50% of the total annual rainfall in this region. The Bay of Bengal location better isolates the summer season dynamics.

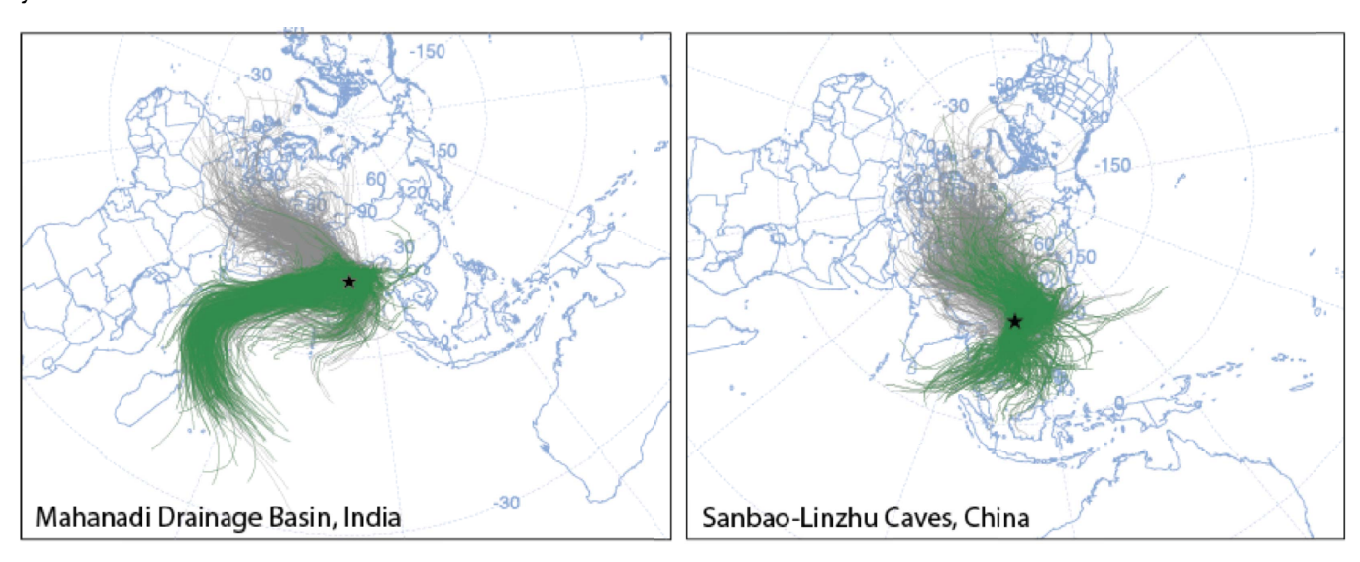
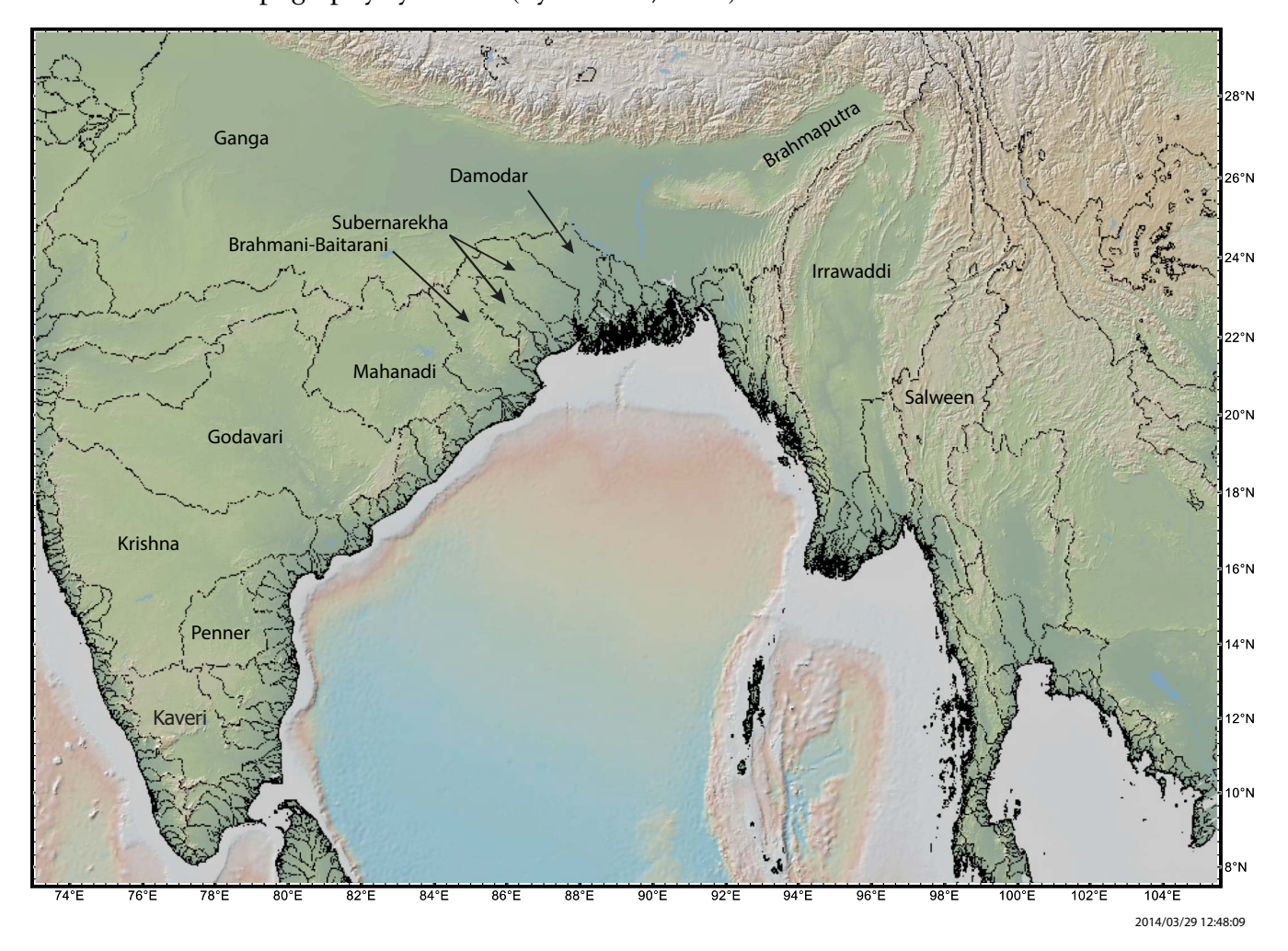
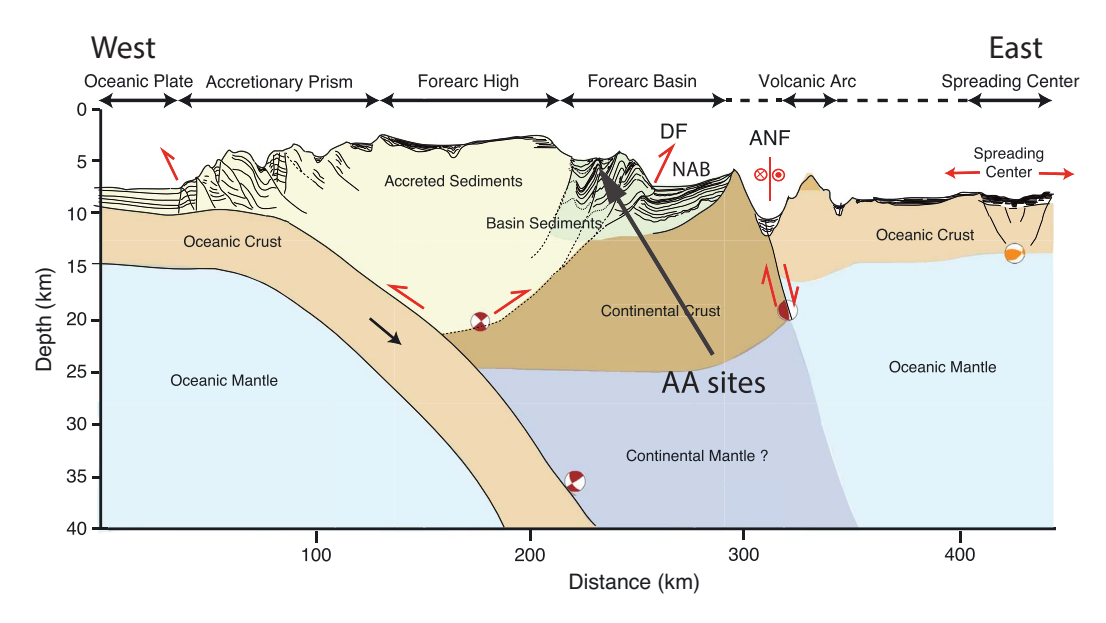


**Figure F5.** Main river basins draining into the Bay of Bengal and Andaman Sea. Map was generated using GeoMapApp, (www.geomapapp.org/) using topography and bathymetry from the Global multiResolution Topography synthesis (Ryan et al., 2009).

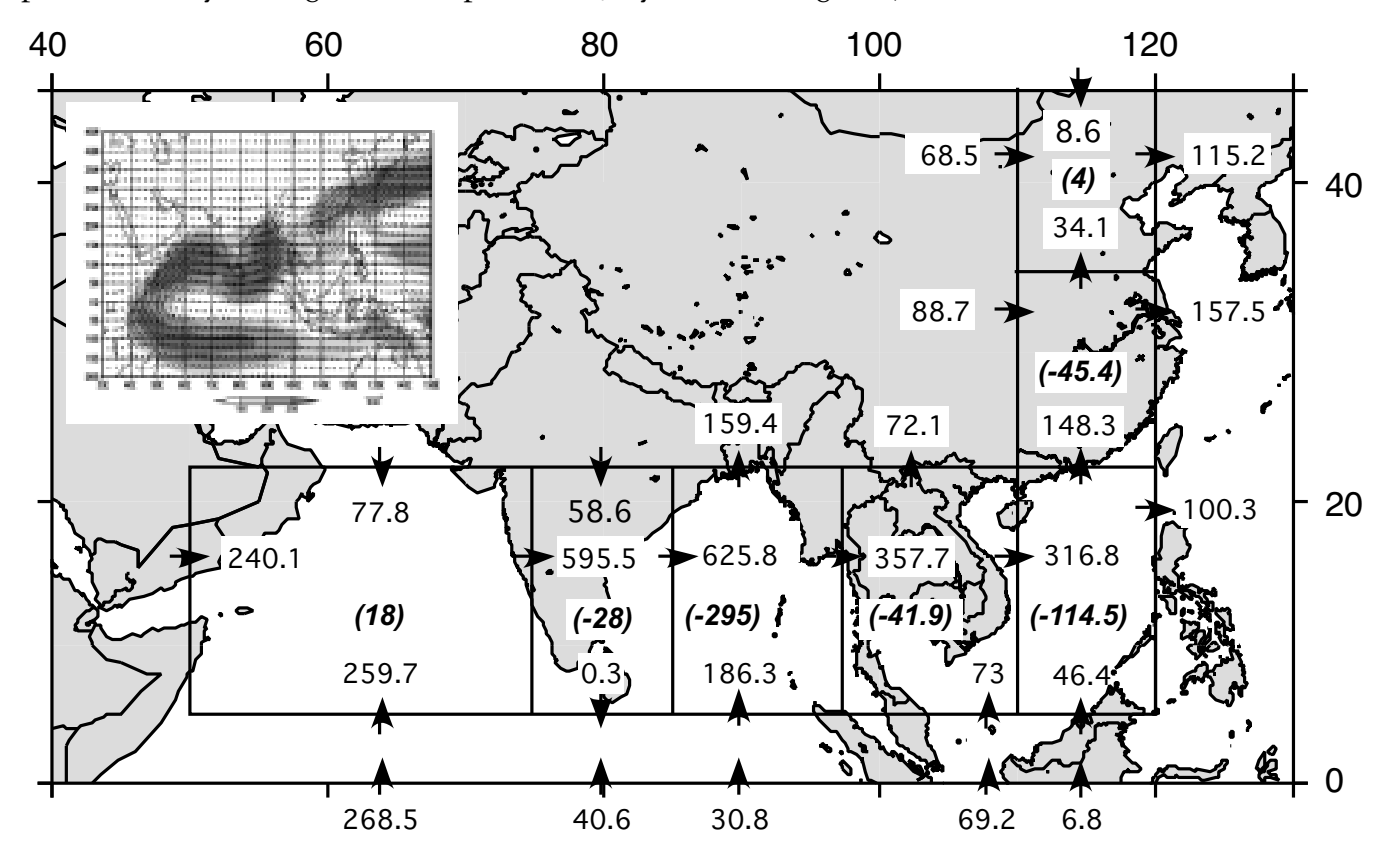


46

Figure F6. Summary sketch after Singh et al. (2013) showing the subduction zone through the backarc basin to  $\sim$ 40 km depth. DF = Diligent Fault, NAB = Nicobar Andaman Basin, ANF = Andaman-Nicobar Fault.



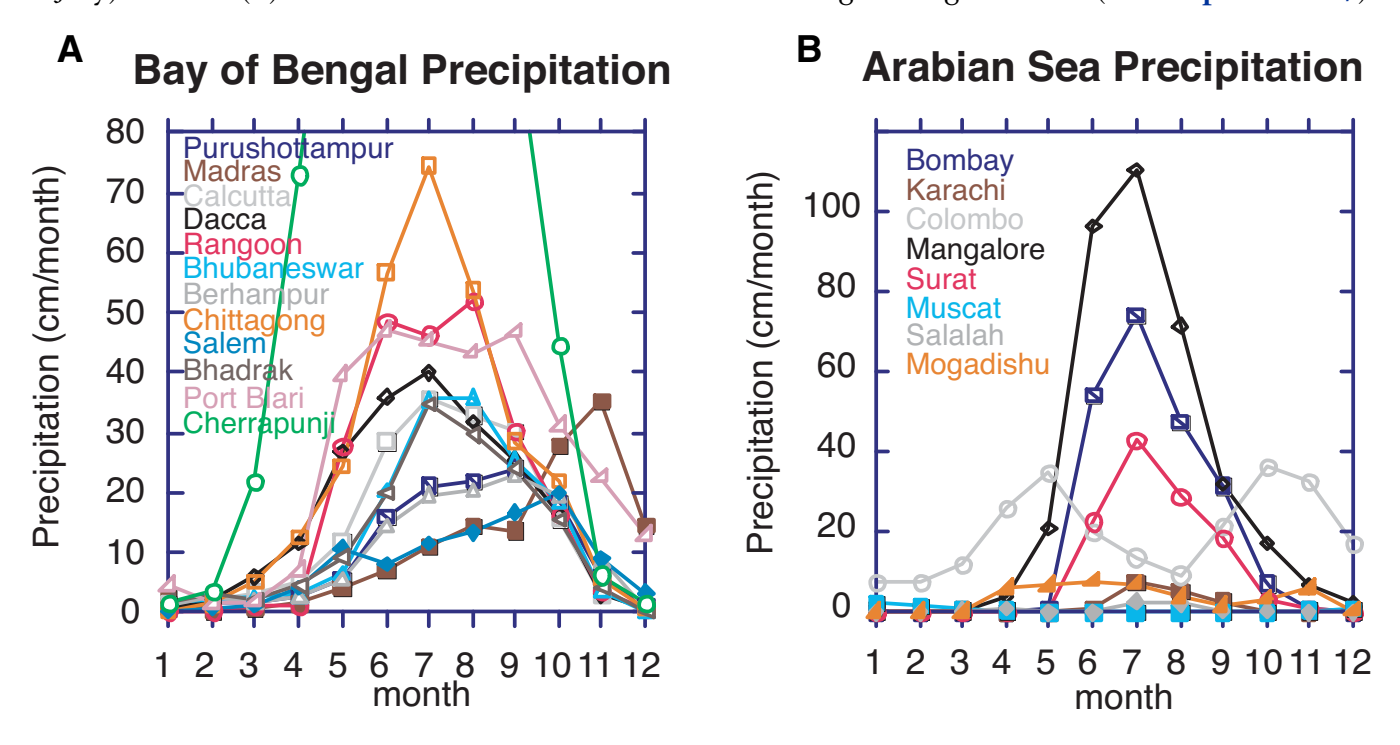
**Figure F7.** Summer monsoon moisture budget and transport path (inset) after Ding et al. (2004). Moisture budget averaged for 1990–1999 (June, July, and August; units are  $10^6$  kg/s). The southern Indian Ocean is the dominant moisture (latent heat) source. The Bay of Bengal, Indochina, the South China Sea, and China are all moisture sinks. No significant Pacific moisture source is indicated. Summer monsoon moisture transport patterns (inset) averaged for 1990–1999 (the 5th pentad of May through the 2nd pentad of July; units are kg/m/s).



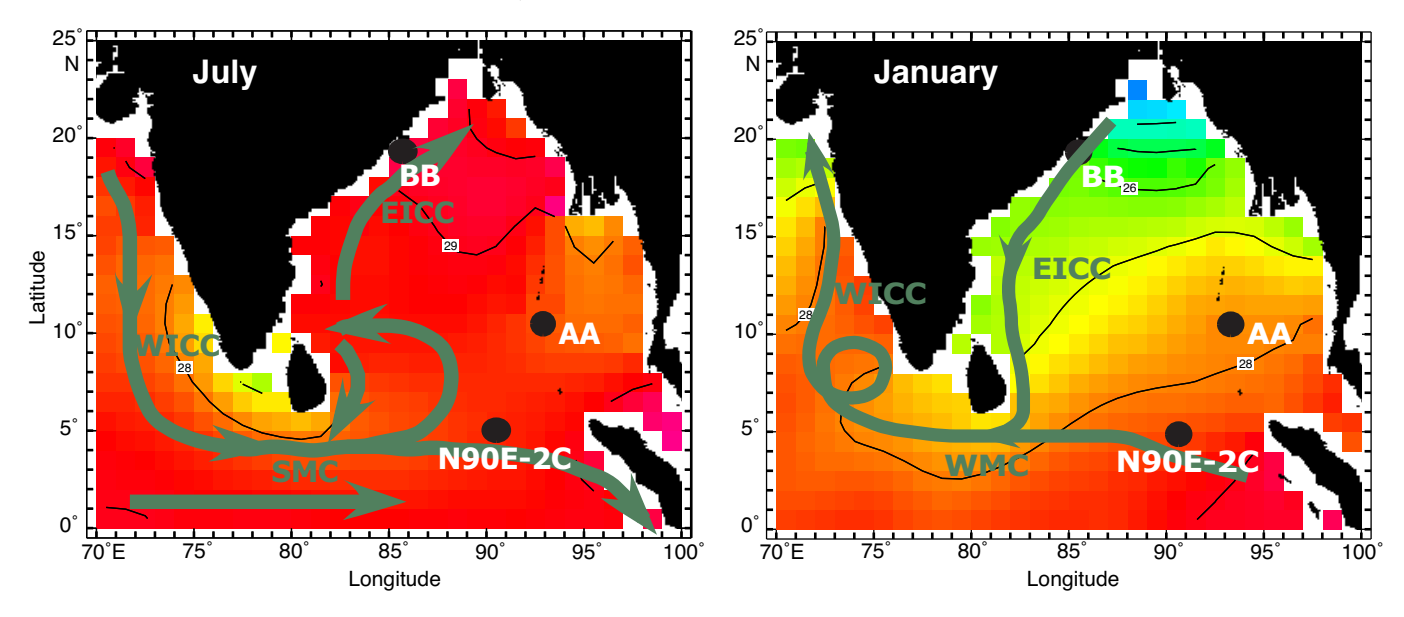
**Figure F8.** Major rivers on the Indian subcontinent. Location base map from **worldmap.har-vard.edu/maps/new/**.



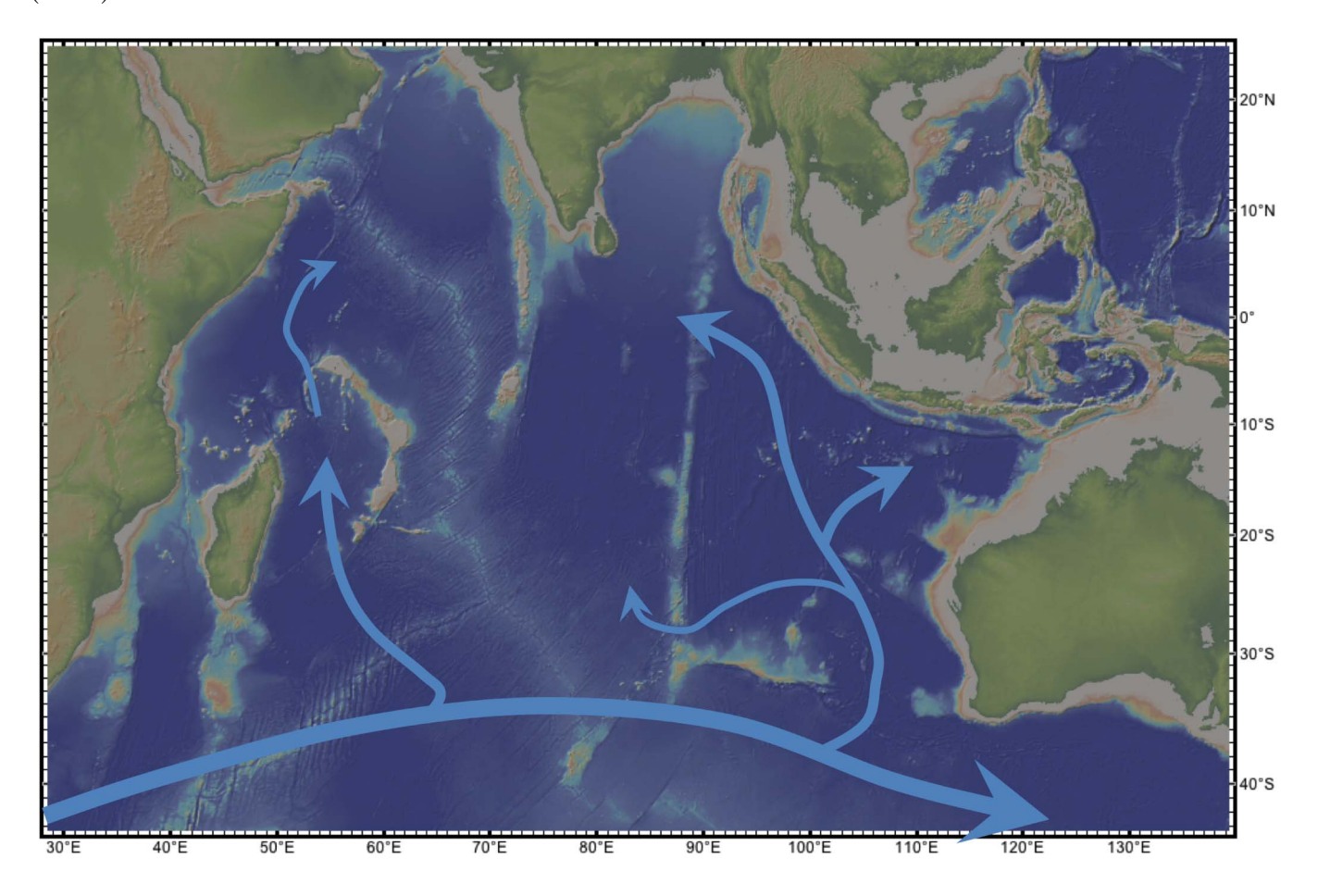
**Figure F9.** Monthly precipitation data for 1948–2011 (as available) for locations with drainage into the (A) Bay of Bengal (Cherrapunji precipitation is off scale, reaching a maximum of 277 cm/month in July) and the (B) Arabian Sea. Data from World Meteorological Organization (climexp.knmi.nl/).



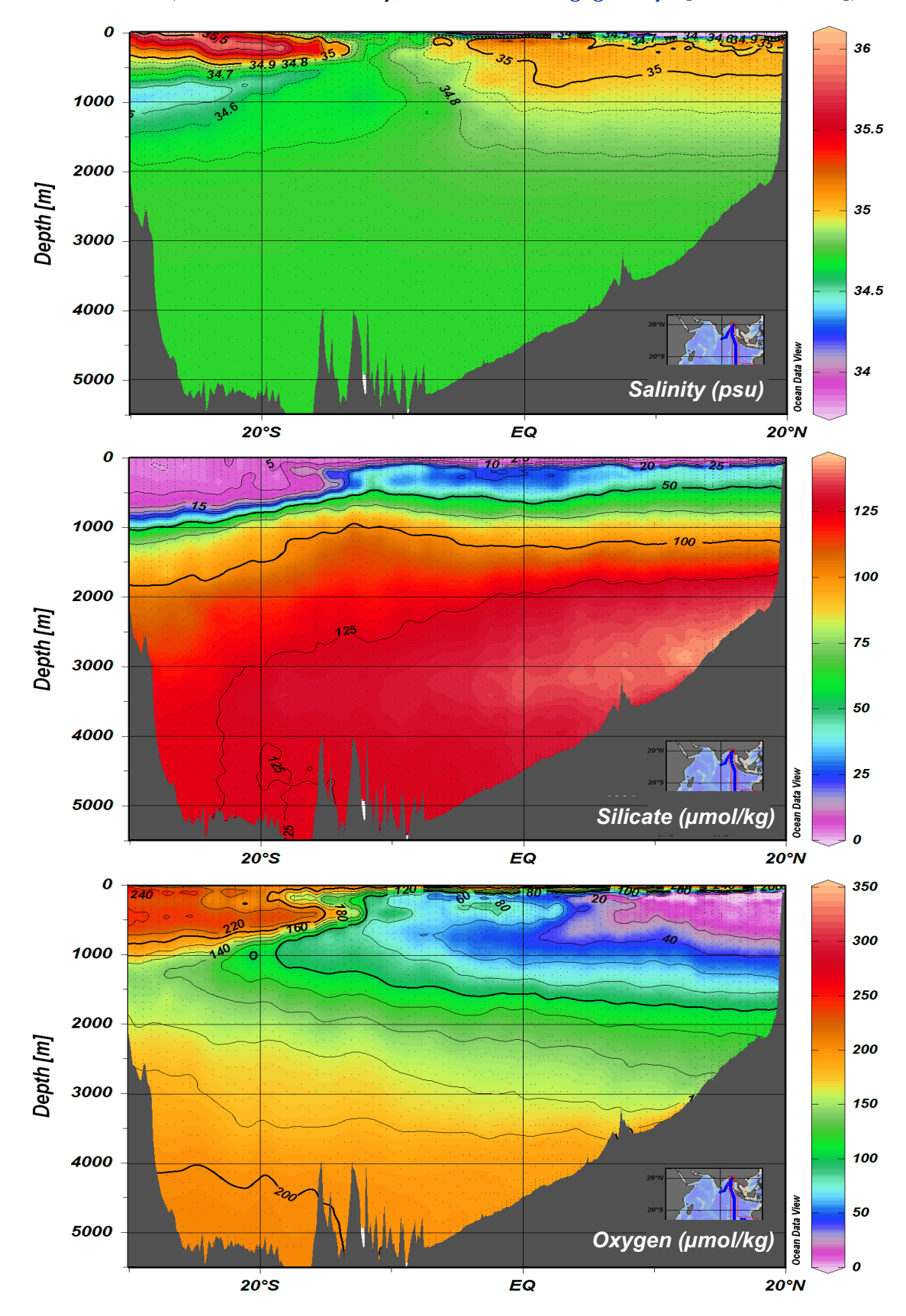
**Figure F10.** World Ocean Atlas Monthly Mean Temperature (°C) for 1955–2006 (Locarini et al., 2010). Summer and winter monsoon current systems follow Schott and McCreary (2001). Proposed site locations in the Andaman Sea (AA), Mahanadi Basin, Bay of Bengal (BB), and N90E-2C (redrill ODP Site 758) are shown. EICC = East Indian Coastal Current, WICC = West Indian Coastal Current, SMC = Southwest Monsoon Current, WMC = Winter Monsoon Current.



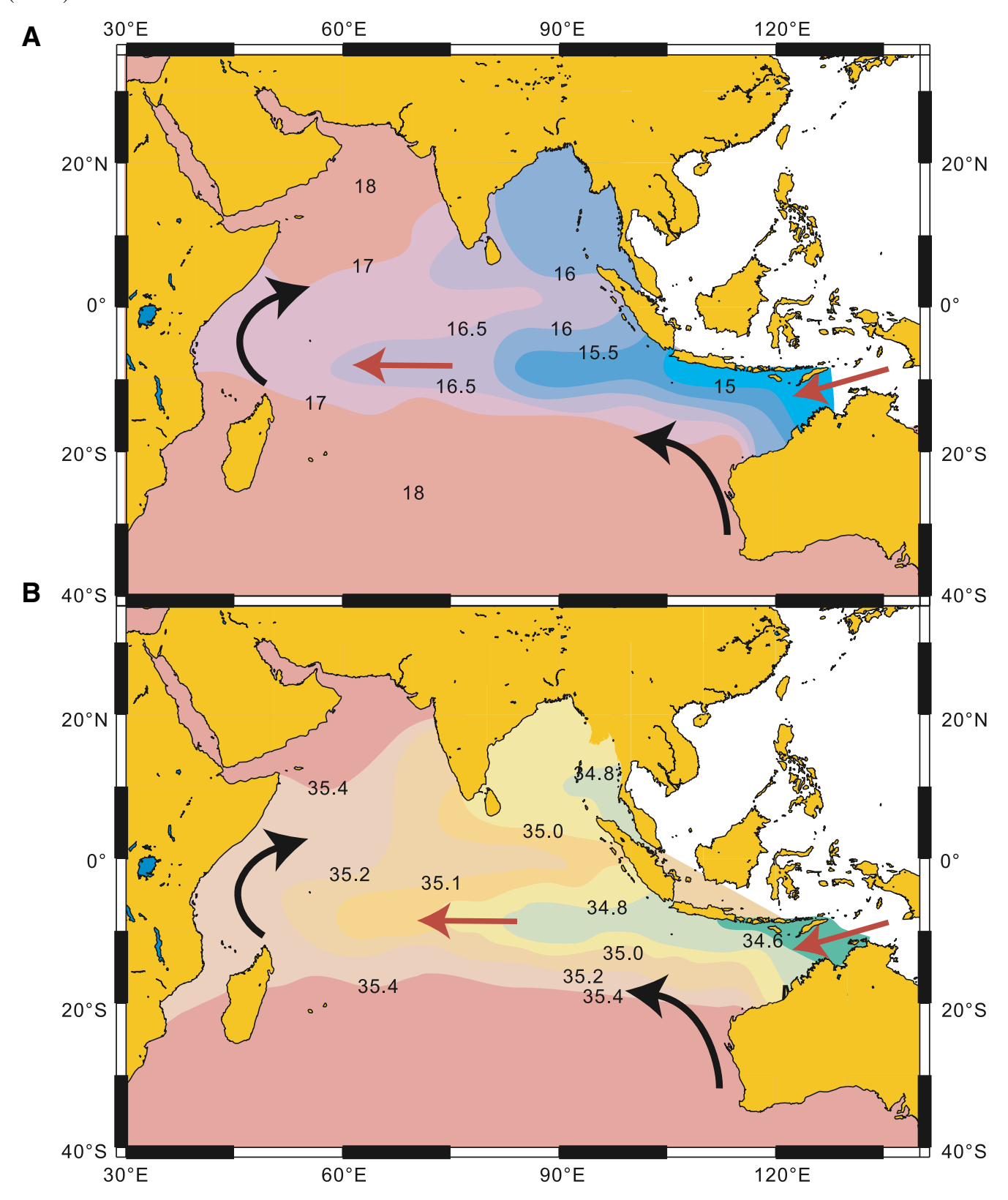
**Figure F11.** Indian Ocean deep and bottom water circulation (from Frank et al., 2006). Blue arrows represent the deep and bottom water flow patterns in the Indian Ocean. After Mantyla and Reid (1995).



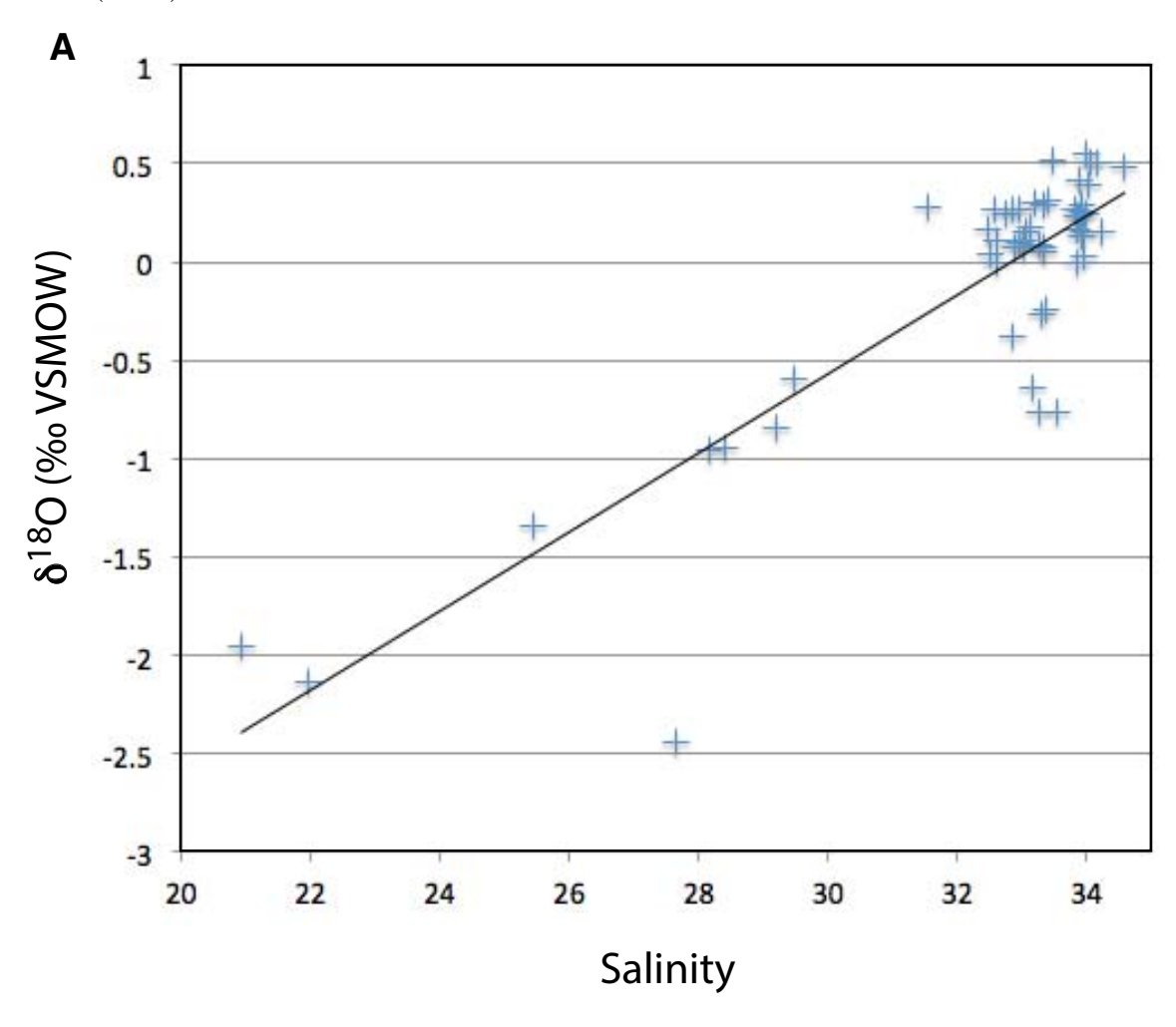
**Figure F12.** Salinity, silicate, and oxygen from eastern Indian Ocean WOCE meridional Transect I09, eastern Indian Ocean (from eWOCE Gallery, www.ewoce.org/gallery/ [Schlitzer, 2000]).



**Figure F13.** Mean (A) temperature (°C) and (B) salinity (psu) in the upper thermocline on isopycnal Surface 25.7, located in the depth range 150–200 m (after You and Tomczak, 1993). Arrows indicate movement of Indian Central Water (black) and Indonesian Throughflow Water (red). From Xu et al. (2006).



**Figure F14.**  $\delta^{18}$ O-salinity relationships for the Bay of Bengal after (A) Singh et al. (2010) and (B) Delaygue et al. (2001).



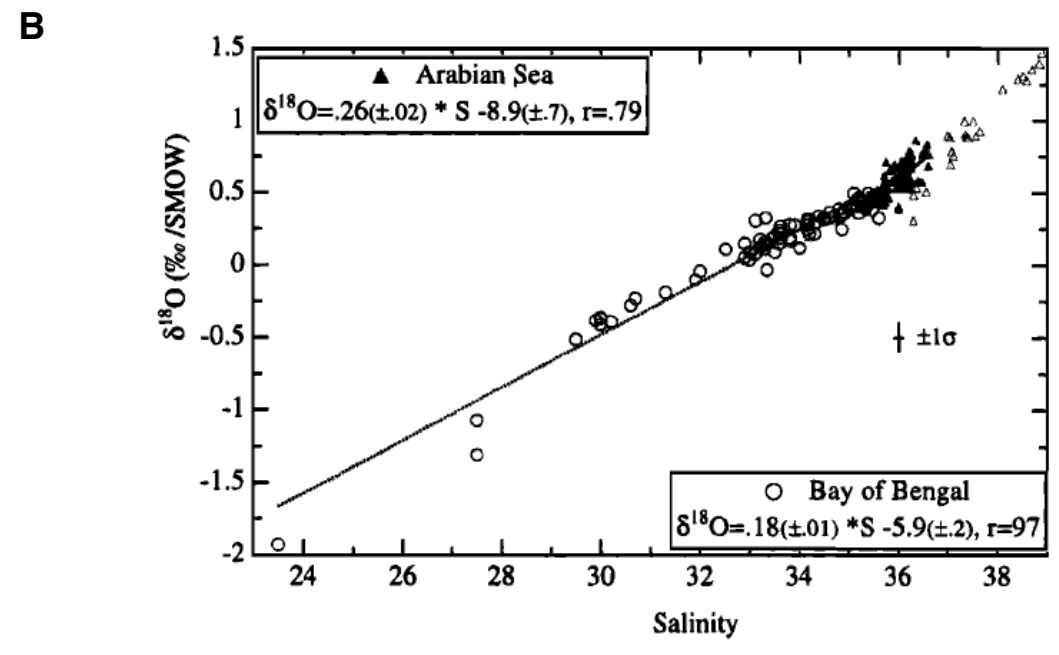
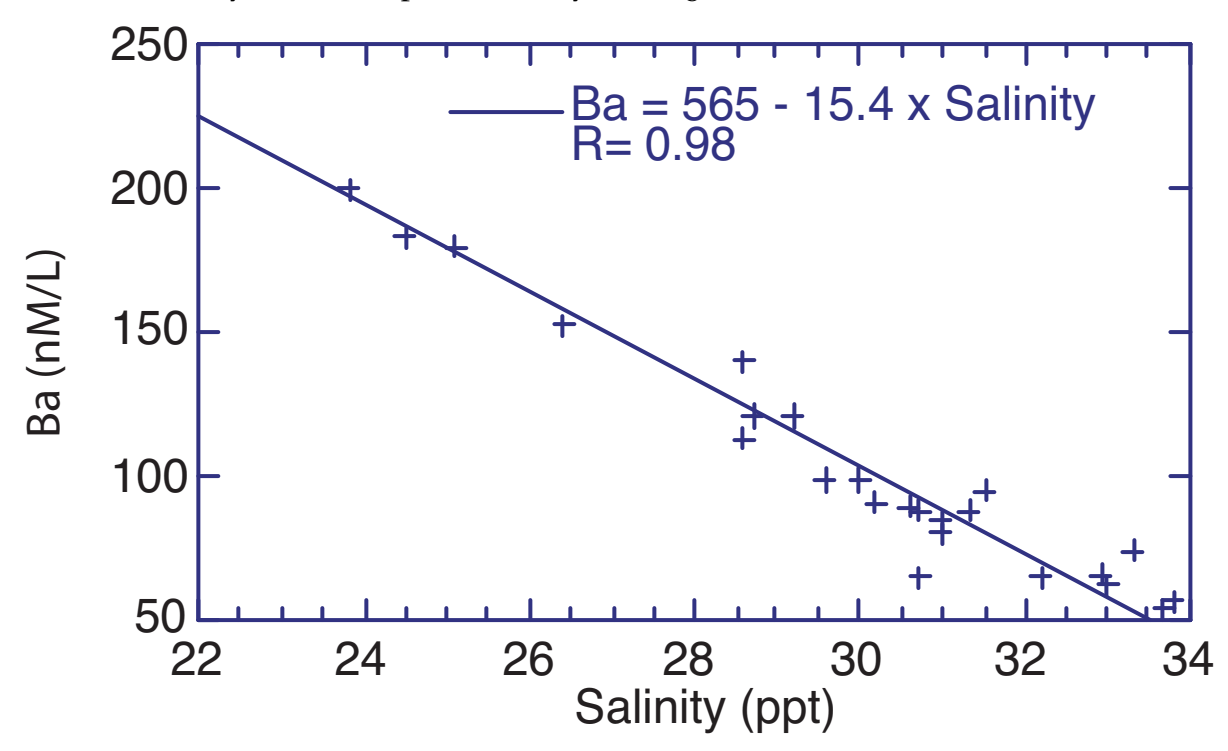


Figure F15. Ba-salinity relationships for the Bay of Bengal after Carroll et al. (1993).



## **Site summaries**

## Site AA-2B

Priority:	Primary
Position:	10°47.4059′N, 93°00.0000′E
Water depth (m):	1369
Target drilling depth (mbsf):	738
Approved maximum penetration (mbsf):	738
Survey coverage (track map; seismic profile):	Lines AN-01-26A and AN-01-25A (site map Fig. F1B, seismic lines Fig. AF2)
Objective(s):	<ol> <li>High-resolution reconstruction of oceanic monsoonal paleoclimate and runoff from the Irrawaddy/Salween drainage basins since the Miocene, eastern Bay of Bengal.</li> <li>High-resolution reconstruction of oceanic circulation at intermediate depths in the Andaman Sea since the Miocene.</li> </ol>
Drilling program:	Holes A, B: APC core to refusal/XCB core to 738 mbsf
Logging program and downhole measurements program:	Hole A: APCT-3 temperature measurements and FlexIT orientation Hole B: FlexIT orientation, wireline logging using the triple combo and FMS- sonic
Nature of rock anticipated:	Nannofossil and foraminifer oozes, volcanic ashes

## Site AA-4B

Priority:	Primary
Position:	10°38.0307′N, 93°00.0036′E
Water depth (m):	1091
Target drilling depth (mbsf):	422
Approved maximum penetration (mbsf):	422
Survey coverage (track map; seismic profile):	Lines AN-01-26A and AN-99-17A (site map Fig. F1B, seismic lines Fig. AF3)
Objective(s):	<ol> <li>High-resolution reconstruction of oceanic monsoonal paleoclimate and runoff from the Irrawaddy/Salween drainage basins since the Miocene, eastern Bay of Bengal.</li> <li>High-resolution reconstruction of oceanic circulation at intermediate depths in the Andaman Sea since the Miocene.</li> </ol>
Drilling program:	Holes A, B, C: APC core to refusal/XCB core to 422 mbsf
Logging program and downhole measurements program:	Hole A: APCT-3 temperature measurements and FlexIT orientation Hole B: FlexIT orientation Hole C: FlexIT orientation
Nature of rock anticipated:	Nannofossil and foraminifer oozes, volcanic ashes

## Site AA-1

Priority:	Alternate
Position:	10°49.3364′N, 93°6.7339′E
Water depth (m):	1545
Target drilling depth (mbsf):	544
Approved maximum penetration (mbsf):	544
Survey coverage (track map; seismic profile):	Line AN-01-34A (site map Fig. <b>F1B</b> , seismic lines Fig. <b>AF4</b> )
Objective(s):	<ol> <li>High-resolution reconstruction of oceanic monsoonal paleoclimate and runoff from the Irrawaddy/Salween drainage basins since the Miocene, eastern Bay of Bengal.</li> <li>High-resolution reconstruction of oceanic circulation at intermediate depths in the Andaman Sea since the Miocene.</li> </ol>
Drilling program:	Holes A, B, C: APC core to refusal/XCB core to 544 mbsf
Logging program and downhole measurements program:	Hole A: APCT-3 temperature measurements and FlexIT orientation Hole B: FlexIT orientation Hole C: FlexIT orientation, wireline logging using the triple combo and FMS- sonic
Nature of rock anticipated:	Nannofossil and foraminifer oozes, volcanic ashes

## Site AA-3

Priority:	Alternate
Position:	10°23.4368′N, 93°16.6901′E
Water depth (m):	2625
Target drilling depth (mbsf):	471
Approved maximum penetration (mbsf):	471
Survey coverage (track map; seismic profile):	Lines AN-01-26A and AN-01-25A (site map Fig. F1B, seismic lines Fig. AF5)
Objective(s):	<ol> <li>High-resolution reconstruction of oceanic monsoonal paleoclimate and runoff from the Irrawaddy/Salween drainage basins since the Miocene, eastern Bay of Bengal.</li> <li>High-resolution reconstruction of oceanic circulation at intermediate depths in the Andaman Sea since the Miocene.</li> </ol>
Drilling program:	Holes A, B: APC core to refusal/XCB core to 471 mbsf
Logging program and downhole measurements program:	Hole A: APCT-3 temperature measurements and FlexIT orientation Hole B: FlexIT orientation, wireline logging using the triple combo and FMS-sonic
Nature of rock anticipated:	Nannofossil and foraminifer oozes, volcanic ashes

## Site AA-5

Priority:	Alternate
Position:	10°43.4686′N, 93°5.3300′E
Water depth (m):	1480
Target drilling depth (mbsf):	603
Approved maximum penetration (mbsf):	603
Survey coverage (track map; seismic profile):	Lines AN-01-32A and AN-99-15A (site map Fig. F1B, seismic lines Fig. AF6)
Objective(s):	<ol> <li>High-resolution reconstruction of oceanic monsoonal paleoclimate and runoff from the Irrawaddy/Salween drainage basins since the Miocene, eastern Bay of Bengal.</li> <li>High-resolution reconstruction of oceanic circulation at intermediate depths in the Andaman Sea since the Miocene.</li> </ol>
Drilling program:	Holes A, B: APC core to refusal/XCB core to 603 mbsf
Logging program and downhole measurements program:	Hole A: APCT-3 temperature measurements and FlexIT orientation Hole B: FlexIT orientation, wireline logging using the triple combo and FMS- sonic
Nature of rock anticipated:	Nannofossil and foraminifer oozes, volcanic ashes

## Site BB-7

Priority:	Primary
Position:	19°5.0100′N, 85°44.0923′E
Water depth (m):	1425
Target drilling depth (mbsf):	184
Approved maximum penetration (mbsf):	184
Survey coverage (track map; seismic profile):	Lines L1500-1900-Tr2774-T0-2800 and L1737-Tr2400-3400-T0-2800 (site map Fig. F1C, seismic lines Fig. AF7, bathymetric map Fig. F1D)
Objective(s):	<ol> <li>High-resolution reconstruction of oceanic monsoonal paleoclimate in the Bay of Bengal during the Pleistocene.</li> <li>High-resolution reconstruction of oceanic circulation at intermediate depths in the Bay of Bengal during the Pleistocene.</li> </ol>
Drilling program:	Holes A, B, C: APC core to refusal/XCB core to 184 mbsf
Logging program and downhole measurements program:	Hole A: APCT-3 temperature measurements and FlexIT orientation Holes B, C: FlexIT orientation
Nature of rock anticipated:	Biogenic clay and oozes; clays subordinate

## Site BB-5

Priority:	Primary
Position:	17°44.7218′N, 84°47.2513′E
Water depth (m):	2495
Target drilling depth (mbsf):	680
Approved maximum penetration (mbsf):	680
Survey coverage (track map; seismic profile):	Not yet available
Objective(s):	<ol> <li>High-resolution reconstruction of oceanic monsoonal paleoclimate in the Bay of Bengal during the Pleistocene.</li> <li>High-resolution reconstruction of oceanic circulation at intermediate depths in the Bay of Bengal during the Pleistocene.</li> </ol>
Drilling program:	Holes A, B: APC core to refusal/XCB core to 680 mbsf
Logging program and downhole measurements program:	Hole A: APCT-3 temperature measurements and FlexIT orientation Hole B: FlexIT orientation and wireline logging using the triple combo and FMS-sonic
Nature of rock anticipated:	Biogenic clays and oozes, clays subordinate

## Site BB-2B

Priority:	Primary
Position:	18°59.8153′N, 85°37.2941′E
Water depth (m):	1178
Target drilling depth (mbsf):	184
Approved maximum penetration (mbsf):	184
Survey coverage (track map; seismic profile):	Lines L2200-2400-Tr2707-T0-2500 and L2348-Tr2350-3400-T0-2600 (site map Fig. F1C, seismic lines Fig. AF8, bathymetric map Fig F1D)
Objective(s):	<ol> <li>High-resolution reconstruction of oceanic monsoonal paleoclimate in the Bay of Bengal during the Pleistocene.</li> <li>High-resolution reconstruction of oceanic circulation at intermediate depths in the Bay of Bengal during the Pleistocene.</li> </ol>
Drilling program:	Holes A, B, C: APC core to refusal/XCB core to 184 mbsf
Logging program and downhole measurements program:	Hole A: APCT-3 temperature measurements and FlexIT orientation Holes B, C: FlexIT orientation
Nature of rock anticipated:	Biogenic clays and oozes, clays subordinate

## Site BB-1B

Priority:	Alternate
Position:	18°56.1064′N, 85°41.9823′E
Water depth (m):	1667
Target drilling depth (mbsf):	222
Approved maximum penetration (mbsf):	222
Survey coverage (track map; seismic profile):	Lines L2200-2700-Tr3554-T0-2900 and L2403-Tr3200-3900-T0-2900 (site map Fig. <b>F1C</b> , seismic lines Fig. <b>AF9</b> , bathymetric map Fig <b>F1D</b> )
Objective(s):	<ol> <li>High-resolution reconstruction of oceanic monsoonal paleoclimate and runoff from the Mahanadi drainage basins since the Pliocene, northern Bay of Bengal.</li> <li>High-resolution reconstruction of oceanic circulation at intermediate depths in the Bay of Bengal since the Pleistocene.</li> </ol>
Drilling program:	Holes A, B, C: APC core to refusal/XCB core to 222 mbsf
Logging program and downhole measurements program:	Hole A: APCT-3 temperature measurements and FlexIT orientation Holes B, C: FlexIT orientation
Nature of rock anticipated:	Biogenic clays and oozes, clays subordinate

## Site BB-4

Priority:	Alternate
Position:	19°1.4682′N, 85°42.8782′E
Water depth (m):	1607
Target drilling depth (mbsf):	172
Approved maximum penetration (mbsf):	172
Survey coverage (track map; seismic profile):	Not yet available
Objective(s):	<ol> <li>High-resolution reconstruction of oceanic monsoonal paleoclimate in the Bay of Bengal during the Pleistocene.</li> <li>High-resolution reconstruction of oceanic circulation at intermediate depths in the Bay of Bengal during the Pleistocene.</li> </ol>
Drilling program:	Holes A, B, C: APC core to refusal/XCB core to 172 mbsf
Logging program and downhole measurements program:	Hole A: APCT-3 temperature measurements and FlexIT orientation Holes B, C: FlexIT orientation
Nature of rock anticipated:	Biogenic clays and oozes, clays subordinate

## Site BB-6

Priority:	Alternate
Position:	18°2.2147′N, 85°9.7384′E
Water depth (m):	2400
Target drilling depth (mbsf):	624
Approved maximum penetration (mbsf):	624
Survey coverage (track map; seismic profile):	Not yet available
Objective(s):	<ol> <li>High-resolution reconstruction of oceanic monsoonal paleoclimate in the Bay of Bengal during the Pleistocene.</li> <li>High-resolution reconstruction of oceanic circulation at intermediate depths in the Bay of Bengal during the Pleistocene.</li> </ol>
Drilling program:	Holes A, B: APC core to refusal/XCB core to 624 mbsf
Logging program and downhole measurements program:	Hole A: APCT-3 temperature measurements and FlexIT orientation Hole B: FlexIT orientation, wireline logging using the triple combo and FMS- sonic
Nature of rock anticipated:	Biogenic clays and oozes, clays subordinate

## Site BB-8B

Priority:	Alternate
Position:	18°55.3193′N, 85°45.8676′E
Water depth (m):	1826
Target drilling depth (mbsf):	206
Approved maximum penetration (mbsf):	206
Survey coverage (track map; seismic profile):	Lines trace355 and line2148 (site map Fig. F1C, seismic lines Fig. AF10, bathymetric map Fig. F1D)
Objective(s):	<ol> <li>High-resolution reconstruction of oceanic monsoonal paleoclimate in the Bay of Bengal during the Pleistocene.</li> <li>High-resolution reconstruction of oceanic circulation at intermediate depths in the Bay of Bengal during the Pleistocene.</li> </ol>
Drilling program:	Holes A, B, C: APC core to refusal/XCB core to 206 mbsf
Logging program and downhole measurements program:	Hole A: APCT-3 temperature measurements and FlexIT orientation Holes B, C: FlexIT orientation
Nature of rock anticipated:	Biogenic clays and oozes, clays subordinate

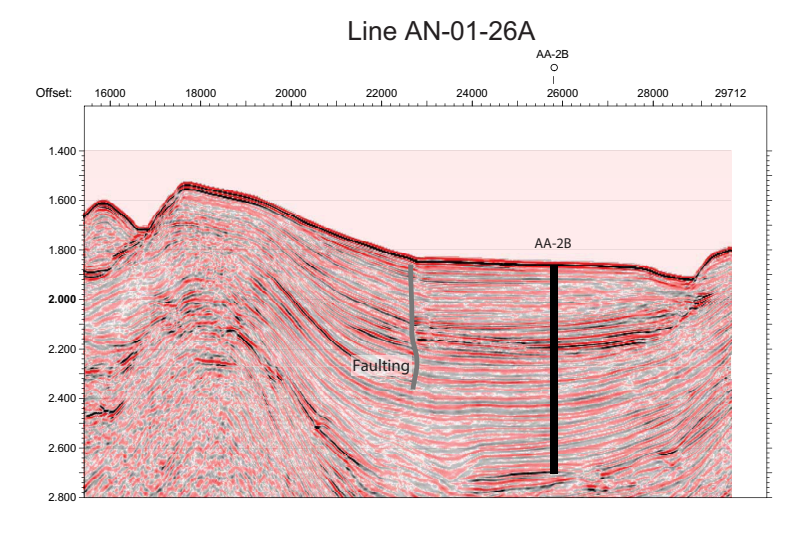
## Site N90E-2C

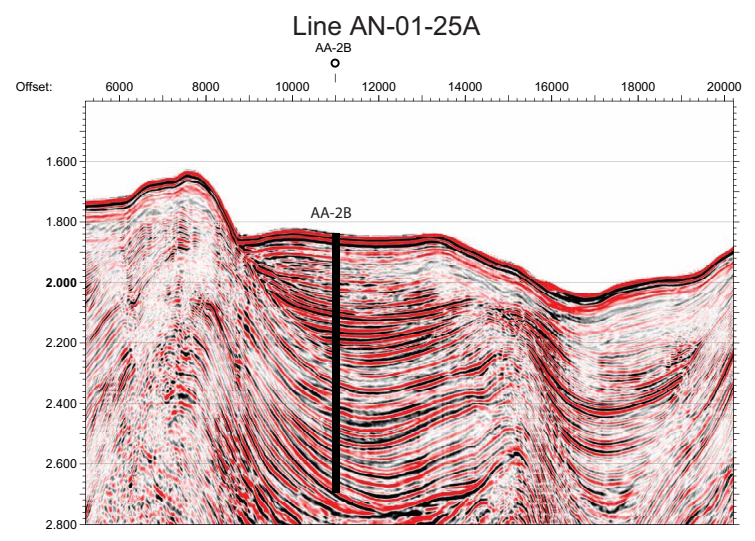
Priority:	Primary
Position:	5°23.0041′N, 90°21.7099′E
Water depth (m):	2963
Target drilling depth (mbsf):	350
Approved maximum penetration (mbsf):	Pending EPSP approval
Survey coverage (track map; seismic profile):	Line ar55.0881.knox06rr and ar55.0885.knox06rr (site map Fig. F1A, seismic lines Fig. AF11)
Objective(s):	<ol> <li>Reconstruction of oceanic monsoonal paleoclimate in the southern Bay of Bengal during the Paleocene and Oligocene to present.</li> <li>Reconstruction of oceanic monsoonal circulation at intermediate depths in the southern Bay of Bengal during the Paleocene and Oligocene to present.</li> </ol>
Drilling program:	Holes A, B, C: APC core to refusal/XCB core to 350 mbsf
Logging program and downhole measurements program:	Hole A: APCT-3 temperature measurements and FlexIT orientation Hole B: FlexIT orientation Hole C: FlexIT orientation, wireline logging with triple combo and FMS-sonic
Nature of rock anticipated:	<ul> <li>Unit 1 (0–96 mbsf): nannofossil ooze with foraminifers and clay and clayey nannofossil ooze with foraminifers; nannofossil ooze with clay, foraminifers, and micrite</li> <li>Unit 2 (96–350 mbsf): nannofossil chalk and calcareous nannofossil chalk; calcareous chalk with nannofossils, foraminifers, and clay</li> </ul>

Figure AF1. Planned transit path of the R/V JOIDES Resolution during Expedition 353.

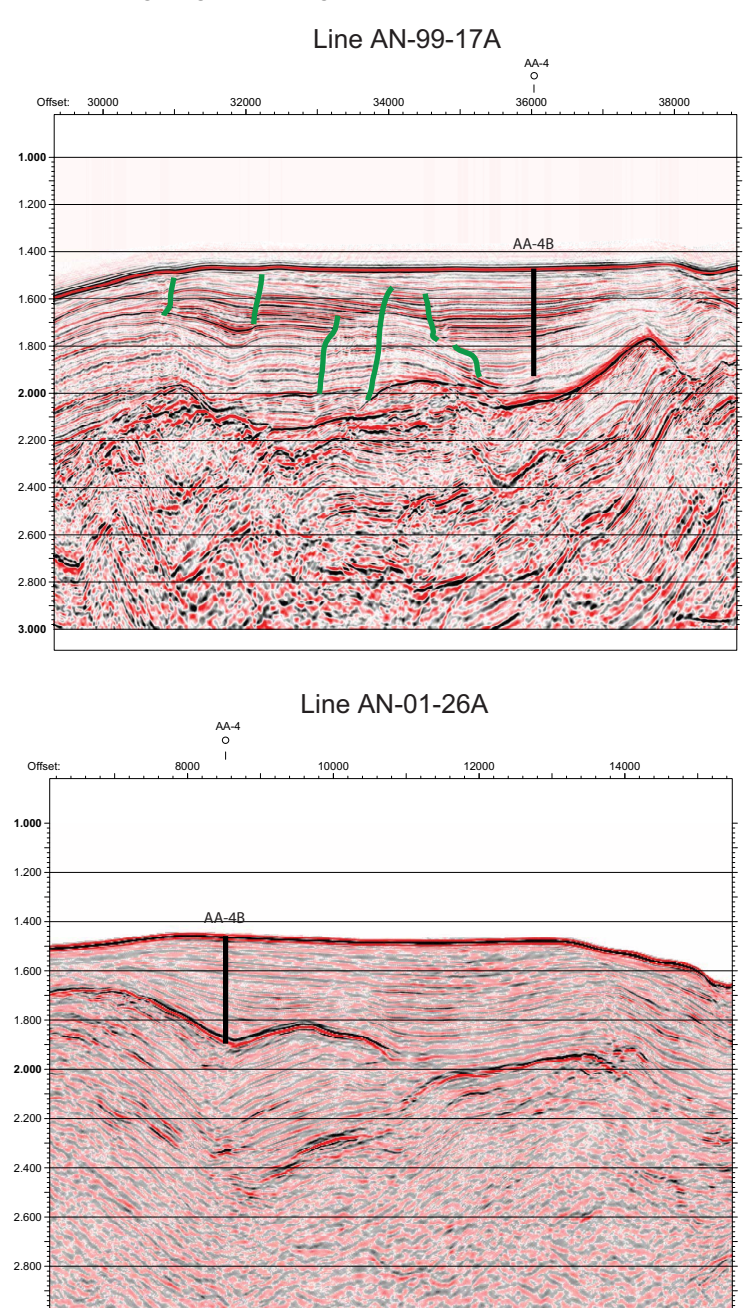


Figure AF2. Seismic crossing Lines AN-01-26A and AN-01-25A with the location of proposed primary Site AA-2B.





**Figure AF3.** Seismic crossing Lines AN-99-17A and AN-01-26A with the location of proposed primary Site AA-4B. Faults are highlighted in green.



**Figure AF4.** Seismic profile Line AN-01-34A displaying the position of proposed Site AA-1 and the Indian National Gas Hydrate Program (NGHP) Site 01-17. The 5.3 Ma horizon is highlighted in yellow and the bottom-simulating reflector (BSR) is highlighted in blue.

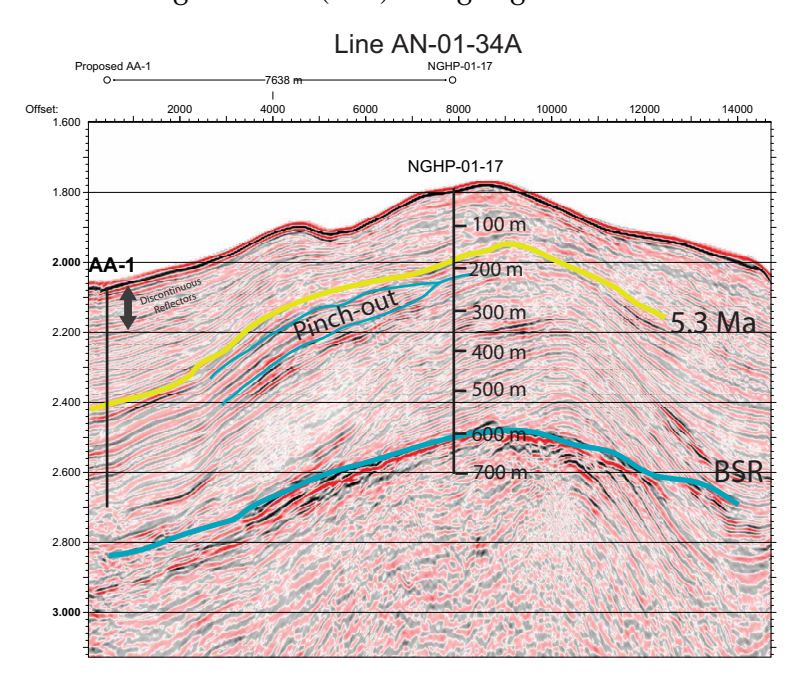
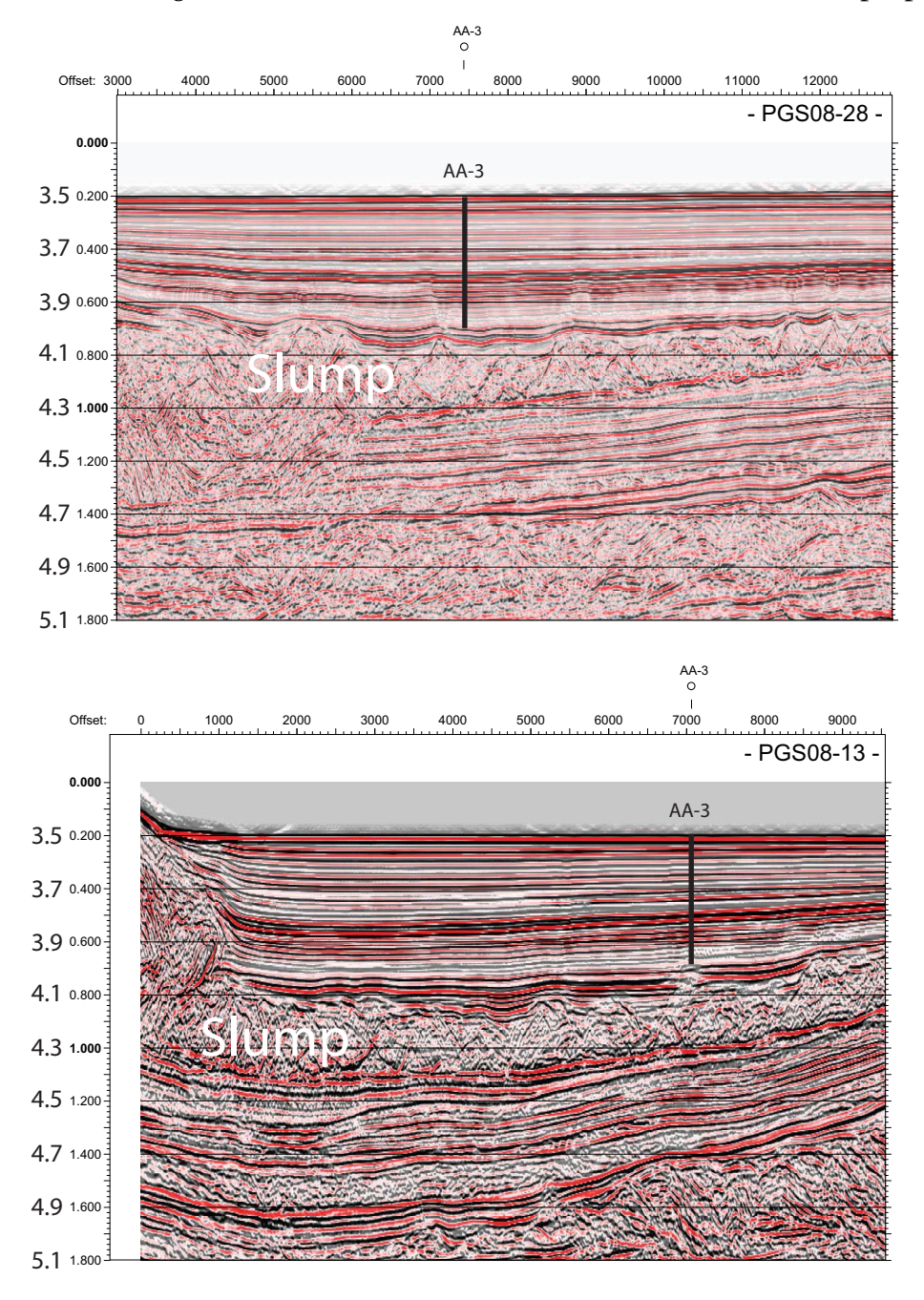
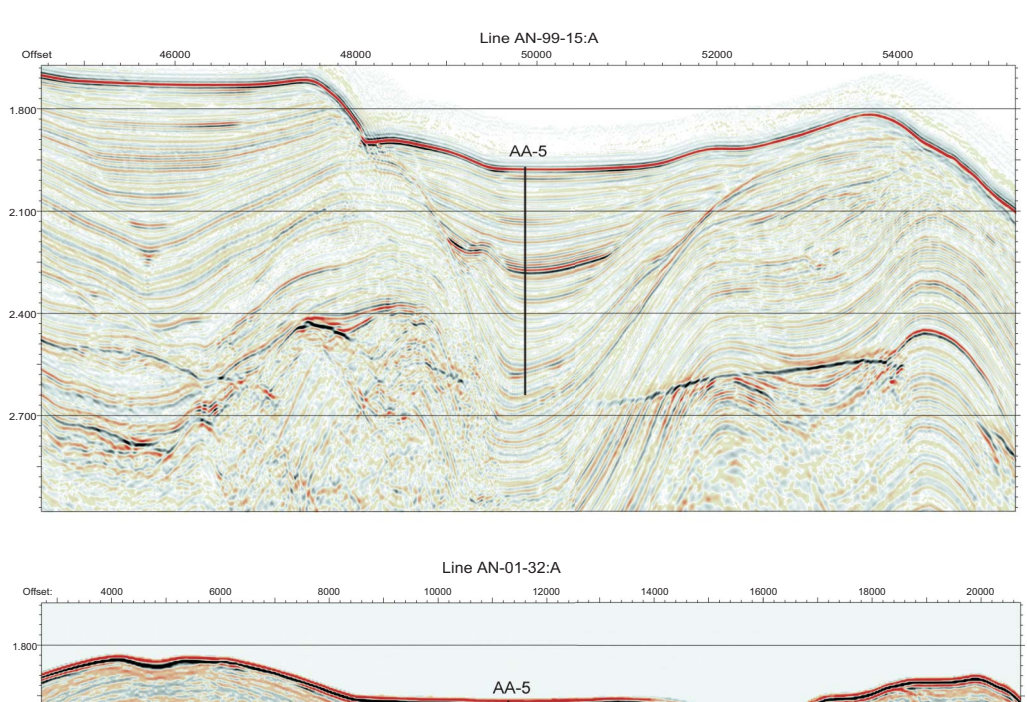
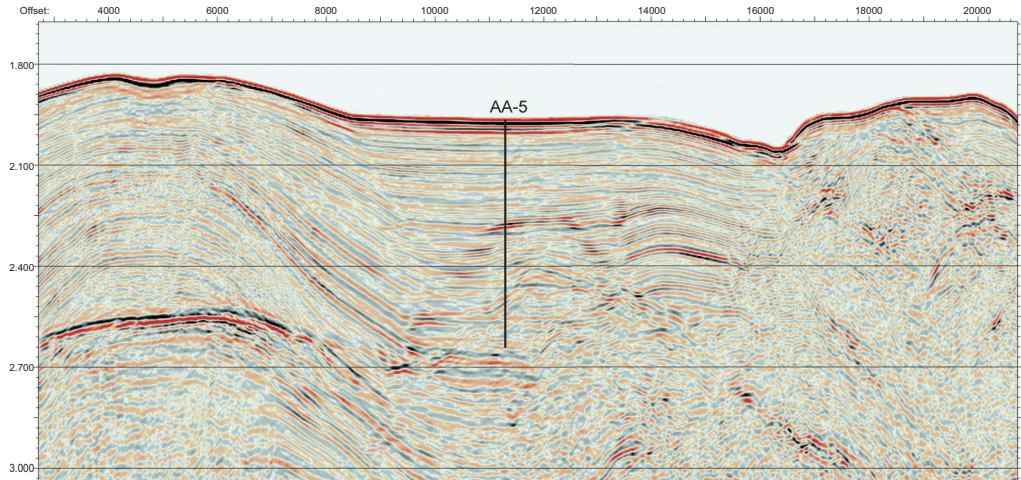


Figure AF5. Seismic crossing Lines PGS08-28 and PGS08-13 with the location of proposed Site AA-3.

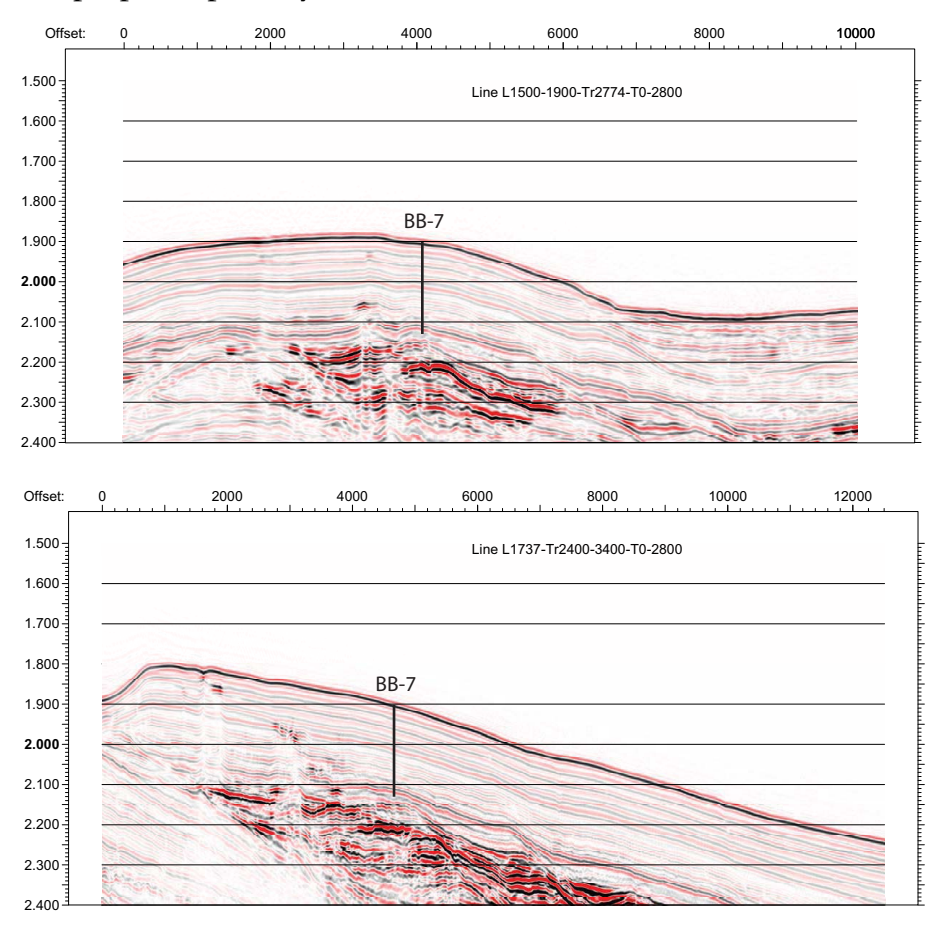


**Figure AF6.** Seismic crossing Lines AN-99-15:A and AN-01-32:A with the location of proposed Site AA-5.

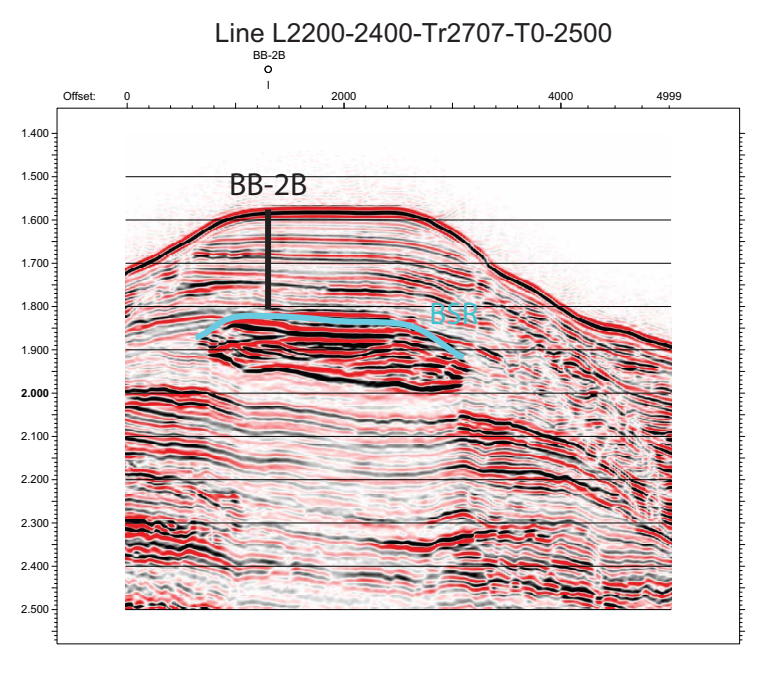


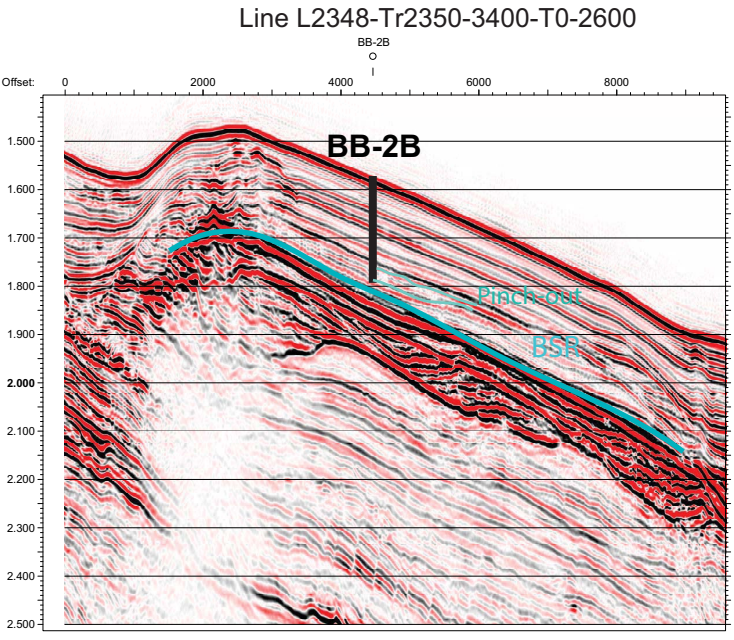


**Figure AF7.** Seismic crossing Lines L1500-1900-Tr2774-T0-2800 and L1737-Tr2400-3400-T0-2800 with the location of proposed primary Site BB-7.

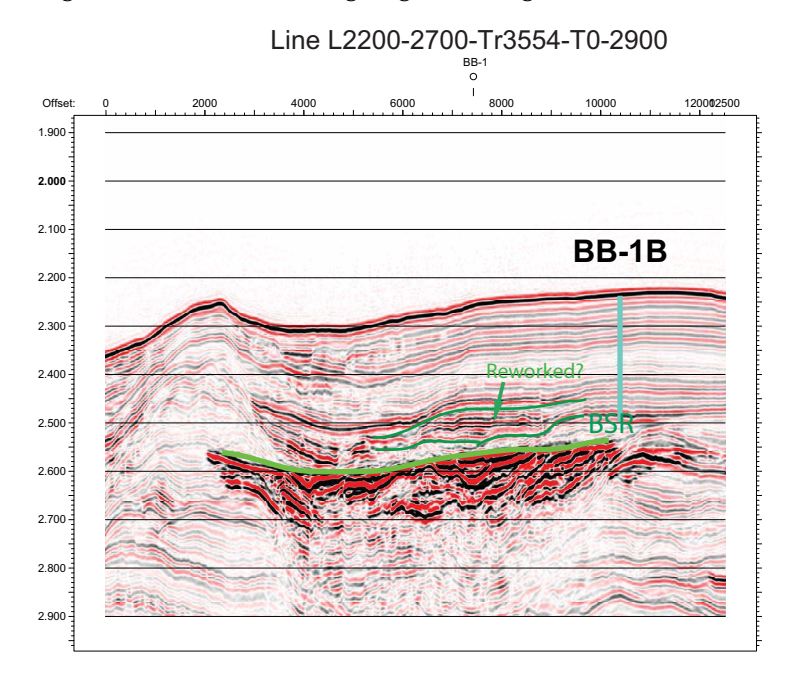


**Figure AF8.** Seismic crossing Lines L2200-2400-Tr2707-T0-2500 and L2348-Tr2350-3400-T0-2600 with the location of proposed primary Site BB-2B. Bottom-simulating reflector (BSR) is highlighted in blue.

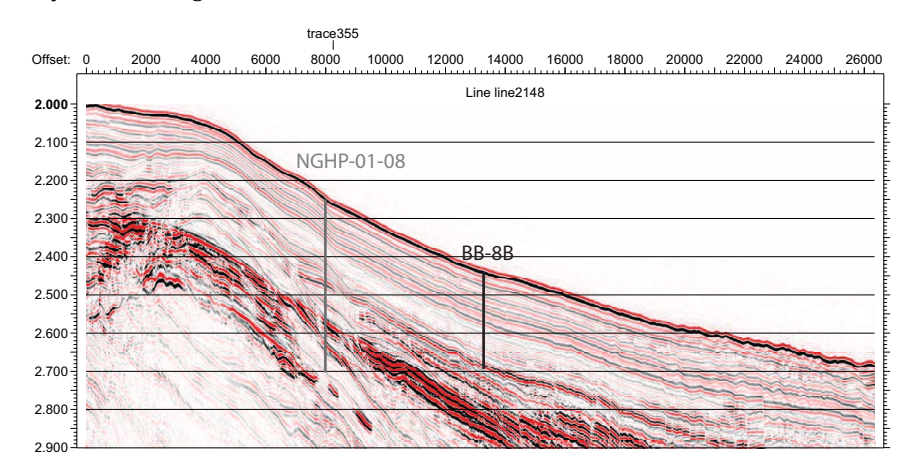




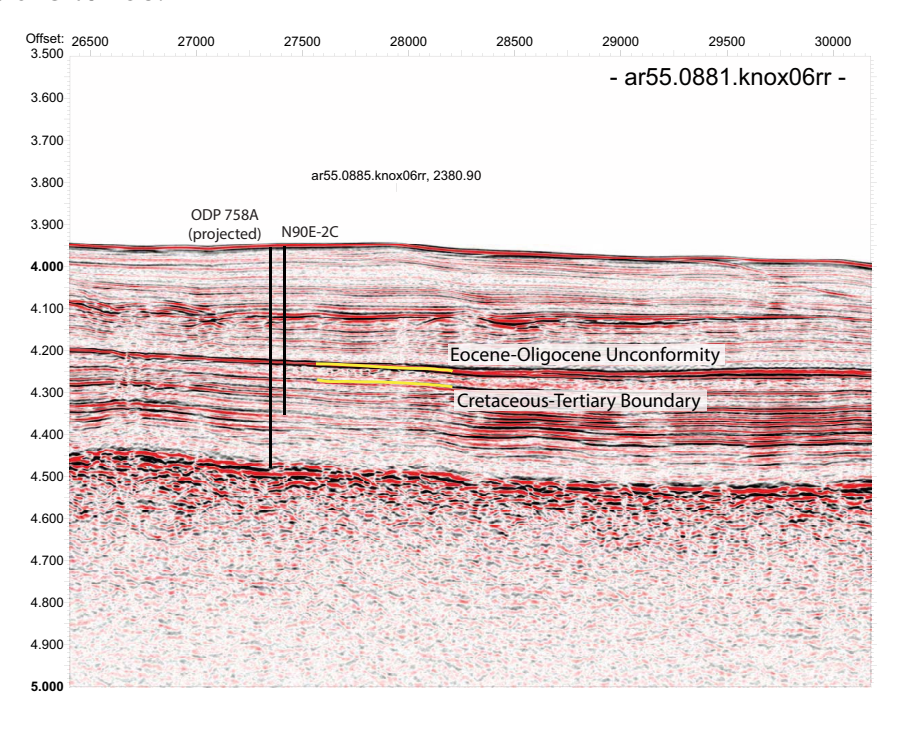
**Figure AF9.** Seismic crossing Line L2200-2700-Tr3554-T0-2900 with the location of proposed Site BB-1B. Bottom-simulating reflector (BSR) is highlighted in green.



**Figure AF10.** Seismic crossing Lines line2148 and trace335 with the location of proposed Site BB-8B and National Gas Hydrate Program (NGHP) Site 01-08.



**Figure AF11.** Seismic crossing Lines ar55.0881.knox06rr and ar55.0885.knox06rr with the location of proposed primary Site N90E-2C and Ocean Drilling Program (ODP) Hole 758A. Site N90E-2C is 800 m northwest of Site 758.



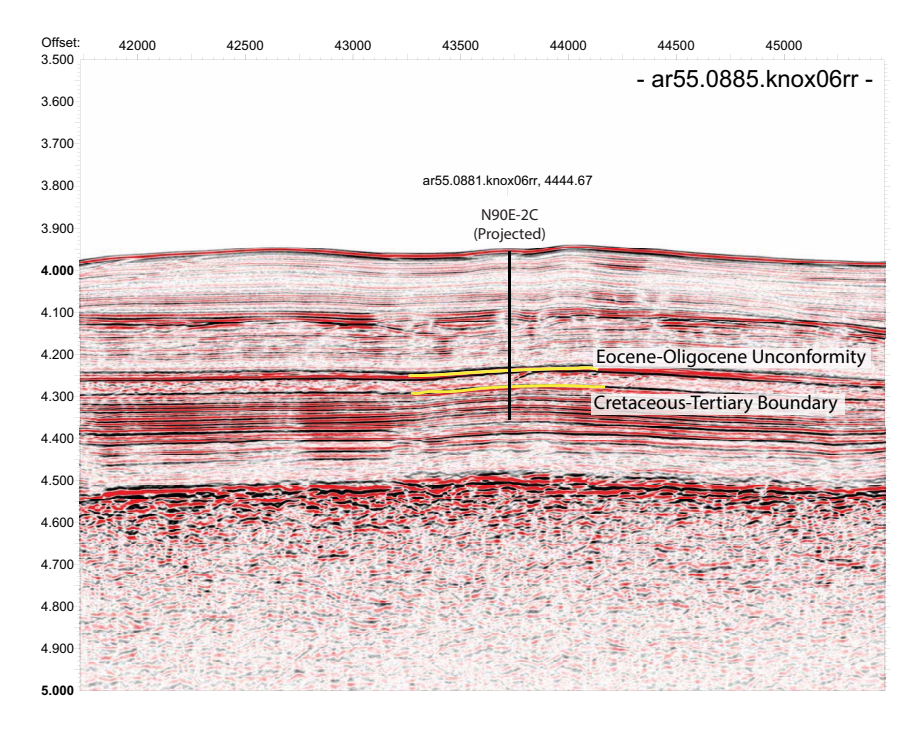
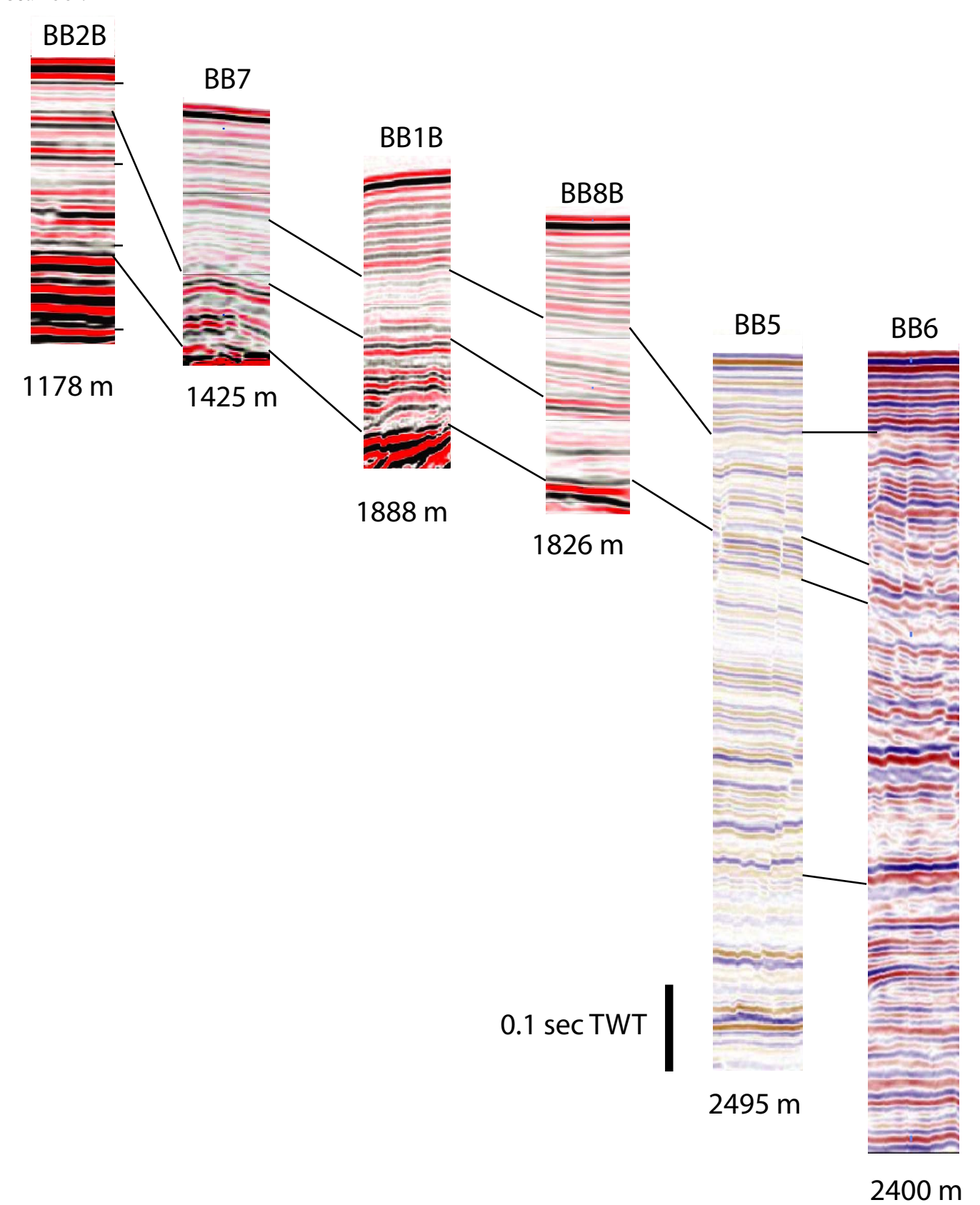


**Figure AF12.** Correlation of seismic records (strike lines close to projected drill sites) in the Mahanadi Basin. Correlation lines are tentative. TWT = two-way traveltime. Depths are in meters below seafloor.



## **Expedition scientists and scientific participants**

The current list of participants for Expedition 353 can be found at **iodp.tamu.edu/** scienceops/precruise/indianmonsoon/participants.html.